View metadata, citation and similar papers at core.ac.uk
brought to you by CORE
provided by CERN Document Server

PHYSICS BEYOND THE STANDARD MODEL AND COLLIDER PHENOMENOLOGY

by

PIYABUT BURIKHAM

A dissertation submitted in partial fulfillment of the requirements for the Degree of

DOCTOR OF PHILOSOPHY

(Physics)

at the

UNIVERSITY OF WISCONSIN-MADISON

2005

Abstract

We briefly review the Standard Model of the particle physics focussing on the gauge hierachy problem and the naturalness problem regarding the stabilization of the light Higgs mass. We list the alternative models which address the hierachy problem in addition to conventional Supersymmetric models and Composite models. They include extra dimensional models and Little Higgs models.

We investigate the production of heavy W_H at the linear e^+e^- collider at high centre-of-mass energies at 3 and 5 TeV using the Littlest Higgs model where the global group is $SU(5)/SO(5)$. In certain region of the parameter space, the heavy boson induced signals could be distinguishable from the Standard Model background.

Based on tree-level open-string scattering amplitudes in the low string-scale scenario, we derive the massless fermion scattering amplitudes. The amplitudes are required to reproduce those of the Standard Model at tree level in the low energy limit. We then obtain four-fermion contact interactions by expanding in inverse powers of the string scale and explore the constraints on the string scale from low energy data. The Chan-Paton factors and the string scale are treated as free parameters. We find that data from the neutral and charged current processes at HERA, Drell-Yan process at the Tevatron, and from LEP-II put lower bounds on the string scale M_S, for typical values of the Chan-Paton factors, in the range $M_S \geq 0.9 - 1.3$ TeV, comparable to Tevatron bounds on Z' and W' masses.

We consider the low-energy stringy corrections to the 4-fermion scattering at the linear e^+e^- collider at the 500-GeV centre-of-mass energy. The signals look similar to the

contributions from the Kaluza-Klein (KK) graviton exchange but could be distinguishable if there is sufficient number of events. Theoretically, the stringy signals contain both spin 1 and 2 corrections while the KK contains only spin 2.

We calculate the tree-level open-string amplitudes for the scattering of four massless particles with diphoton final states. These amplitudes are required to reproduce those of standard model at the tree level in the low energy limit. After low energy stringy corrections, we found that they have similar form to the same processes induced by exchange of the Kaluza-Klein (KK) excitations of graviton in ADD scenario. Using this similarity, we apply constraints on the KK mass scale M_D to the string scale M_S. The results are consistent with constraints from the 4-fermion scattering, about $0.6 - 0.9$ TeV.

We construct tree-level four-particle open-string amplitudes relevant to dilepton and diphoton production at hadron colliders. We expand the amplitudes into string resonance (SR) contributions and compare the total cross-section through the first SR with the Z' search at the Tevatron. We establish a current lower bound based on the CDF Run I results on the string scale to be about $1.1 - 2.1$ TeV, and it can be improved to about $1.5 - 3$ TeV with 2 fb^{-1}. At the LHC, we investigate the properties of signals induced by string resonances in dilepton and diphoton processes. We demonstrate the unique aspects of SR-induced signals distinguishable from other new physics, such as the angular distributions and forward-backward asymmetry. A 95% C.L. lower bound can be reached at the LHC for $M_S > 8.2 - 10$ TeV with an integrated luminosity of 300 fb^{-1}. We emphasize the generic features and profound implications of the amplitude construction.

We discuss the stringy gauge "singlet" interaction induced by stringy dynamics for

scattering of $n > 3$ particles. Existence of this stringy interaction could lead to stringent bound on the string scale in the braneworld scenario when it is subject to experimental constraints on proton decay.

We discuss IR limit of four-fermion scattering amplitudes in braneworld models including intersecting-branes and SUSY $SU(5)$ GUT version of it. With certain compactification where instanton effect is negligible, grand unification condition in D6-D6 intersecting-branes scenario subject to experimental constraint on proton decay provides possibility for upper limit on the string scale, M_S, through relationship between the string coupling, g_s, and the string scale. We discuss how IR divergence is related to number of twisted fields we have to introduce into intersection region and how it can change IR behaviour of tree-level amplitudes in various intersecting-branes models. Using number of twisted fields, we identify some intersecting-branes models whose tree-level amplitudes are purely stringy in nature and automatically proportional to g_s/M_S^2 at low energy. They are consequently suppressed by the string scale. For comparison, we also derive limit on the lower bound of the string scale from experimental constraint on proton decay induced from purely stringy contribution in the coincident-branes model, the limit is about 10^5 TeV.

Dedication

I dedicate this thesis to my father, Term Burikham, and my mother, Pakprim Burikham. My father's version of the translation of Einstein's General Relativity article was by far the most intriguing one I have ever encountered. His way of life gives me inspiration to live the life that I want. And my mother who always insists that I consider the political correctness to be crucial in life eventhough I keep telling her how that is not derivable from the "First Principle".

Acknowledgments

I would like to thank my advisor, Prof. Tao Han, for introducing me to many research topics, educating me and his relentless request for clarity of concepts and statements. I would like to thank Prof. Tohru Eguchi for constantly supporting my desire to pursue the theoretical research in particle physics and cosmology, his letters of recommendation helped me come to this point. I would also like to thank Prof. Vernon Barger, Dieter Zeppenfeld, Gary Shiu, Akikazu Hashimoto, Martin Olsson, Duncan Carlsmith and Lee Pondrom for terrific physics courses and valuable academic supports. I thank my colleagues for many helps especially Keith Thomas, Terrance Figy, Hye-Sung Lee, Adam Tregre, and Homer Wolfe. I deeply appreciate my family for all of the encouragement and support whenever I needed. I thank my friends and colleagues in Thailand for simply loving physics and enjoying doing it regardless of many disadvantages they have.

Contents

1 Introduction **1**

1.1 The Standard Model (SM) 3

1.1.1 Quark Flavour Mixing in the SM 7

1.1.2 Global Symmetries of the SM 8

2 Models of Physics beyond the Standard Model **11**

2.1 SUSY models 12

2.2 Composite models and strong EW at TeV scale 14

2.3 The extra dimensional models 15

2.4 The Little Higgs models 18

3 Phenomenology of the Littlest Higgs model **20**

3.1 WW_H production at the Linear e^+e^- Collider 22

4 Low-Energy Stringy Corrections to the SM **27**

4.1 Bounds on Four-Fermion Contact Interactions Induced by String Resonances 27

4.1.1 Open String Tree Graph Amplitudes 29

4.1.2 Linking String amplitudes to Contact Interactions 36

4.1.3 Summary and Conclusions 44

4.2 TeV-Scale Stringy Signals at Linear e^+e^- Collider 46

4.3 Similarity between Kaluza-Klein and Open-String Low-Energy Amplitudes 51

4.3.1 Open-string amplitudes for diphoton production processes 52

4.3.2 Comparison between open-string and Kaluza-Klein amplitudes . . 57

4.3.3 Understanding string-KK Similarity in Diphoton production . . . 58

4.3.4 Conclusions 60

5 TeV-Scale String Resonances at Hadron Colliders 62

5.0.5 Construction of open-string amplitudes 65

5.0.6 String Resonances and Partial Waves Expansion 69

5.0.7 Bounds on the String Scale from the Tevatron 73

5.0.8 String Resonances at the LHC 75

5.0.9 Summary and Conclusions 83

5.0.10 Appendix 86

6 Stringy Interaction and Low-Energy Effects in Braneworld Models 93

6.1 Stringy Gauge "Singlet" Interaction 93

6.2 Remarks on Limits on the String Scale in Braneworld Scenario 97

6.2.1 IR-amplitudes in Intersecting-branes Models 99

6.2.2 Classical Contributions to String Amplitudes 106

6.2.3 Limit on lower bound of string scale in bottom-up approach from proton decay 110

6.2.4 Conclusions 111

Chapter 1

Introduction

There are four fundamental interactions that exhibit themselves at the energies we can observe up to date, around 100 GeV. They are electromagnetism, weak, strong and gravitational interactions. The first three interactions can be formulated in terms of quantum gauge theories while the gravity is described successfully only at the classical level, the Einstein's General Relativity Theory. Electromagnetic, strong, and gravitational interactions are transmitted by massless particles, namely photon, gluon and graviton. The weak interaction is transmitted by massive vector bosons, the Z and W. The vector gauge bosons have spin 1 and the graviton has spin 2. The high-energy dependence of the three gauge interactions is proved to be characterized by finite number of parameters including the cut-off scale (i.e. renormalisability in the effective field-theory viewpoint) and the finite quantum predictions are guaranteed.

On the contrary, the "renormalisability" that was proved in the quantum gauge interactions cannot be extended to the spin-2 interaction that gives Einstein theory of gravitation as the classical limit. The failure of quantum gravity to give finite prediction at the quantum level suggests the need for radical changes in the framework of the

quantization scheme. It should be emphasized that this is the problem of the formalism at the most fundamental level. The Grand Unification of the gauge interactions (GUT) will not induce "miracle" to solve the problem of the quantum gravity.

The idea of replacing the point particle with the finite-size object was originated in strong interaction but proved to be the most promising candidate for the finite quantum theory of gravitation as well as the gauge interactions. This is the strongest motivation of why we should consider string theoretic framework as a serious candidate of the fundamental quantum interactions, it provides for the first time, the consistent way to quantize gravity with finite number of degrees of freedom in the unifying picture with the other gauge interactions.

At the less fundamental level even within the quantum gauge theoretic formalism, there exist the phenomenological problems. One is the hierachy problem, namely the enormous mass gap between the electroweak scale (100 GeV) and the UV scale which could be the GUT scale (10^{16} GeV) or the Planck scale (10^{18} GeV). This actually leads to the naturalness/fine-tuning problem of the parameters in the SM in order to suppress the 1-loop contribution to the Higgs mass.

We will start with the brief review of the Standard Model (SM). Then we will discuss the alternative models which address the hierachy/naturalness problem in the Standard Model.

1.1 The Standard Model (SM)

The Gauge Sector

In the context of the renormalizable quantum gauge theoretic formalism, almost all of the essential experimental facts can be explained consistently in the most straight forward way by the following Lagrangian [1, 2],

$$\mathcal{L} = \mathcal{L}_{EW} + \mathcal{L}_{QCD} \tag{1.1}$$

with

$$\mathcal{L}_{EW} = i\bar{\psi}\gamma^{\mu}D_{\mu}\psi - \frac{1}{4}\mathbf{W}^{\mu\nu}\cdot\mathbf{W}_{\mu\nu} - \frac{1}{4}B^{\mu\nu}B_{\mu\nu} + \mathcal{L}_{\Phi} \tag{1.2}$$

$$\mathcal{L}_{\Phi} = |D_{\mu}\Phi|^2 - \mu^2|\Phi|^2 - \lambda|\Phi|^4 + \mathcal{L}_{Yukawa} \tag{1.3}$$

$$\mathcal{L}_{QCD} = i\bar{\psi}_a\gamma^{\mu}D_{\mu}^{ab}\psi_b - \frac{1}{4}G_a^{\mu\nu}G_{\mu\nu}^a \tag{1.4}$$

where

$$\mathbf{W}_{\mu\nu} = \partial_{\mu}\mathbf{W}_{\nu} - \partial_{\nu}\mathbf{W}_{\mu} - g\mathbf{W}_{\mu}\times\mathbf{W}_{\nu} \tag{1.5}$$

$$G_{\mu\nu}^a = \partial_{\mu}G_{\nu}^a - \partial_{\nu}G_{\mu}^a - igf^{abc}G_{\mu b}G_{\nu c} \tag{1.6}$$

$$D_{\mu} = \partial_{\mu} + ig\mathbf{W}_{\mu}\cdot\mathbf{T} + ig'\frac{1}{2}B_{\mu}Y \tag{1.7}$$

$$D_{\mu}^{ab} = \partial_{\mu}\delta^{ab} + ig_s\mathbf{G}_{\mu}\cdot\mathbf{T}_s^{ab}. \tag{1.8}$$

$\mathbf{T}(\mathbf{T}_s)$ are the generators of $SU(2)_L(SU(3)_c)$, the electroweak (EW) and quantum chromodynamics (QCD) gauge group. The flavor indices are suppressed. The color indices are suppressed in the electroweak interaction and expressed as a, b, etc. in the QCD Lagrangian. The fermions are all in the fundamental representation and the gauge bosons

	T	T_3	$\frac{1}{2}Y$	Q
ν_{eL}	$\frac{1}{2}$	$\frac{1}{2}$	$-\frac{1}{2}$	0
e_L	$\frac{1}{2}$	$-\frac{1}{2}$	$-\frac{1}{2}$	-1
u_L	$\frac{1}{2}$	$\frac{1}{2}$	$\frac{1}{6}$	$\frac{2}{3}$
d_L	$\frac{1}{2}$	$-\frac{1}{2}$	$\frac{1}{6}$	$-\frac{1}{3}$
e_R	0	0	-1	-1
u_R	0	0	$\frac{2}{3}$	$\frac{2}{3}$
d_R	0	0	$-\frac{1}{3}$	$-\frac{1}{3}$

Table 1.1: The weak quantum numbers of the first-generation fermions in the Standard Model

are in the adjoint representation of the SM gauge group $SU(3)_c \times SU(2)_L \times U(1)_Y$. While the electroweak eigenstates of the fermions are the mixing of the mass eigenstates, the QCD eigenstates are assumed simply to be the mass eigenstates through the definition of "kinematical masses" which are generated through the vev (vacuum expectation value) of the color-singlet scalar doublets in the conventional SM Higgs mechanism.

The Fermion-Higgs Sector and the EW breaking

The SM fermions have chiral interactions due to the $SU(2)_L \times U(1)_Y$ gauge charges. The chiral leptons (quarks) can be expressed by the weak doublets and singlets as

$$\psi_L^j = \begin{pmatrix} \nu_L^j(u_L^j) \\ \ell_L^j(d_L^j) \end{pmatrix} \tag{1.9}$$

$$\psi_R^j = \nu_R^j(u_R^j) \text{ and } \ell_R^j(d_R^j) \tag{1.10}$$

After the spontaneous symmetry breaking $SU(2)_L \times U(1)_Y \to U(1)_{em}$ with only QED symmetry remained in the vacuum, the masses of fermions are generated by the vev v of the $SU(2)_L$ scalar doublets

$$\Phi = \begin{pmatrix} \phi^+ \\ \phi^0 \end{pmatrix} \tag{1.11}$$

$$= \exp\left(\frac{i\zeta(x)\cdot\mathbf{T}}{v\sqrt{2}}\right)\begin{pmatrix} 0 \\ (v+H(x))/\sqrt{2} \end{pmatrix}, \tag{1.12}$$

through the Yukawa coupling

$$\mathcal{L}_{Yukawa} = -\frac{\sqrt{2}}{v}\left[M_{ij}^d\overline{\psi_R^{di}}\Phi^\dagger\psi_L^j + M_{ij}^u\overline{\psi_R^{ui}}(i\tau_2\Phi^*)^\dagger\psi_L^j\right] + \text{ h.c.} \tag{1.13}$$

where the real field $\zeta_1(x), \zeta_2(x), \zeta_3(x)$ and $H(x)$ have zero vev. $\psi^{u(d)}$ refers to the u(d)-type quark and neutrino (lepton). $M^{u(d)}$ is the mass matrix of u(d)-type quark and neutrino (lepton). The spacetime dependent phase of the scalar fields in Eqn. (1.12) can be absorbed into the redefined fields and the three Goldstone bosons $\zeta_1(x), \zeta_2(x)$, and $\zeta_3(x)$ will appear "eaten" by the three gauge bosons W^+, W^-, and Z through the term $|D_\mu\Phi|^2$. The new EW fields in the unitary gauge after the symmetry breaking are defined by the effective Lagrangian

$$\mathcal{L}_{EW} = \mathcal{L}_{KE} - \frac{m}{v}H\bar{\psi}\psi + \mathcal{L}_{em} + \mathcal{L}_{neutral} + \mathcal{L}_{charged} + \mathcal{L}_{Higgs} \tag{1.14}$$

	T	T_3	$\frac{1}{2}Y$	Q
ϕ^+	$\frac{1}{2}$	$\frac{1}{2}$	$\frac{1}{2}$	1
ϕ^0	$\frac{1}{2}$	$-\frac{1}{2}$	$\frac{1}{2}$	0

Table 1.2: The weak quantum numbers of the complex scalars in the Standard Model

with

$$\mathcal{L}_{em} = -eQ\bar{\psi}\gamma^\mu\psi A_\mu \tag{1.15}$$

$$\mathcal{L}_{neutral} = -\frac{g}{\cos\theta_W}\overline{\psi_\alpha}\gamma^\mu g_\alpha\psi_\alpha Z_\mu \tag{1.16}$$

$$\mathcal{L}_{charged} = -\frac{g}{\sqrt{2}}\overline{\psi_L^i}\gamma^\mu(T^+W_\mu^+ + T^-W_\mu^-)\psi_L^i \tag{1.17}$$

$$\mathcal{L}_{Higgs} = \frac{1}{4}g^2W^+W^-(v+H)^2 + \frac{1}{8}\frac{g^2}{\cos^2\theta_W}ZZ(v+H)^2 - V \tag{1.18}$$

and

$$V = \frac{\mu^2}{2}(v+H)^2 + \frac{\lambda}{4}(v+H)^4, \tag{1.19}$$

where $g_\alpha = T_3 - Q\sin^2\theta_W, -Q\sin^2\theta_W$ for $\alpha = L, R$, and $\tan\theta_W = g'/g$. θ_W is the Weinberg angle, representing the mixing between B and W^3 to form the photon $A = B\cos\theta_W + W^3\sin\theta_W$, and the $Z = -B\sin\theta_W + W^3\cos\theta_W$. $W^\pm = (W^1 \mp iW^2)/\sqrt{2}$ are the charged gauge bosons from the mixing of the original $W^{1,2}$.

In this "unitary gauge" where unitarity is manifest only by the physical fields, the three gauge bosons will therefore become massive with masses given by $M_W = gv/2$ and $M_Z = gg'v/(2e) = M_W/\cos\theta_W$. The single massless gauge boson remaining is identified as photon which couples to fermions with charge $Q = T_3 + Y/2$ and therefore the couplings are related by $1/g^2 + 1/g'^2 = 1/e^2$.

It is important to note that there are two essential processes in deriving the final effective Lagrangian that we call the SM. First we mix W^3 and B with a fixed mixing angle θ_W, the mixing process. Then we break the EW symmetry "spontaneously" by Higgs mechanism to ensure its renormalizability, the symmetry breaking process. The Lagrangian still have all of the original symmetry while the vacuum has only $U(1)_{em}$ at low energy. In most extensions of the SM, e.g. technicolor, Little Higgs or Higgsless models, while the mixing process remains unchanged, the symmetry breaking part gets modified or altered by other means.

1.1.1 Quark Flavour Mixing in the SM

There are three generations of fermions which have exactly the same gauge interactions to the gauge bosons. Each copy has exactly the same gauge charges and the only difference between them is the mass. Generically, the weak eigenstates in Eqn. (1.16, 1.17) are related to the mass eigenstates by the mixing unitary matrices,

$$u^i = U_{iq} q \text{ for } q = u, c, t \tag{1.20}$$

$$d^i = D_{iq'} q' \text{ for } q' = d, s, b \tag{1.21}$$

for both doublets and singlets. It turns out that the interaction involving singlets (right-handed fermions) and the neutral current are in the same form with the mass eigenstates replacing the weak states, no mixing effect is observable. The mixing becomes observable only in the charged current interaction as $V = U_L^\dagger D_L$,

$$\mathcal{L}_{charged} = -\frac{g}{\sqrt{2}} \left(\overline{q_L} \gamma^\mu W_\mu^+ V_{qq'} q'_L + \overline{q'_L} V^*_{q'q} \gamma^\mu W_\mu^- q_L \right). \tag{1.22}$$

Therefore the mixing effectively appears as the mixing of $(d, s, b) \to (d', s', b')$ through the matrix $V_{qq'}$.

1.1.2 Global Symmetries of the SM

The SM has accidental (and thus global) symmetries. Baryon ($U(1)_B$) and lepton ($U(1)_L$) numbers are the most obvious ones, separately conserved in each generation. They are the relic of the original global flavour symmetry $U(3)^5$ broken by the Yukawa coupling. $U(1)_B$ and $U(1)_L$ are anomalous but $U(1)_{B-L}$ is not and thus can be gauged in some extension of the SM [3, 4]. In extension of the SM with Majorana mass term of the neutrino, the sterile (gauge singlet) right-handed neutrino N_R can induce a high mass and provide a natural "seesaw" mechanism to give a very small left-handed neutrino ν_L mass. The Majorana mass term violates the lepton number explicitly and we are left with two Majorana fermions ν_L and N_R per generation.

In the EW breaking Higgs sector, the SM has the "custodial" (global) symmetry $SU(2)_{L+R}$ in the hypercharge-decoupling limit $g' \to 0$. This custodial symmetry is the relic of the approximate (since g' is not exactly zero) global symmetry $SU(2)_L \times SU(2)_R$ before the scalar doublets get the vev. After the symmetry breaking, the three Goldstone bosons are eaten and become the longitudinal components of Z and $W^\pm$. The Z and $W^\pm$ form an $SU(2)_{L+R}$ triplet and therefore $M_Z = M_W$ in the $g' \to 0$ limit. In terms of the parameter $\rho = M_W^2/M_Z^2 \cos^2\theta_W$, the custodial symmetry $SU(2)_{L+R}$ implies that the one-loop radiative correction from the Higgs to the masses of the gauge bosons must be proportional to g'^2, and thus suppressed. In the $\overline{MS}$ scheme, the 1-loop Higgs radiative correction to the ρ parameter is

$$\hat{\rho} \approx 1 - \frac{11 G_F M_Z^2 \sin^2\theta_W}{24\sqrt{2}\pi^2} \ln \frac{m_h^2}{M_Z^2} \tag{1.23}$$

This contribution provides us the estimation of the bound on the Higgs mass from the EW precision measurements of the masses of the gauge bosons. Additionally, the

Parameter	Value	SM value
m_t[GeV]	176.1 ± 7.4	176.9 ± 4.0
M_W[GeV]	80.454 ± 0.059	80.390 ± 0.018
M_Z[GeV]	91.1876 ± 0.0021	91.1874 ± 0.0021
Γ_Z[GeV]	2.4952 ± 0.0023	2.4972 ± 0.0012
Γ(had)[GeV]	1.7444 ± 0.0020	1.7435 ± 0.0011
Γ(inv)[MeV]	499.0 ± 1.5	501.81 ± 0.13
$\Gamma(\ell^+\ell^-)$[MeV]	83.984 ± 0.086	84.024 ± 0.025

Table 1.3: Some important global best fit values of the EW parameters from the precision measurements [15]

similar relation from the heavy fermion loop correction which is the dominant radiative contribution leads to the estimation of the top quark mass from the EW precision data before the discovery of the top quark at the Fermilab.

EW precision measurements show that the value of ρ parameter is very close to 1 [2]. Custodial symmetry is actually proven to be sufficient to produce $\rho = 1$ at the leading order and therefore it is well motivated that any physics responsible for the EW symmetry breaking (conventional Higgs mechanism or new physics models) should possess custodial symmetry in the Higgs sector as an approximate symmetry (become exact when $g' \to 0$).

Some EW parameters best fit values are given in Table 1.3. In the on-shell scheme, the value of $x_W \equiv \sin^2\theta_W = 0.22280 \pm 0.00035$ and $\alpha_s(M_Z) = 0.1213 \pm 0.0018$. The corresponding 95% CL upper limit on the Higgs mass is $M_H < 246$ GeV.

Chapter 2

Models of Physics beyond the Standard Model

The SM is successful in explaining most of the experimental data in particle physics up to date. If we assume the EW sector remains perturbative to energies higher than 1 TeV and beyond, we need the SM Higgs to be light, few hundreds GeV. The light Higgs will restore unitarity of the tree-level scattering involving massive EW gauge bosons at the energy around TeV scale by cancelling the contributions from the eaten Goldstone bosons from the spontaneous symmetry breaking. However, SM cannot explain, in a natural way, the stability of light Higgs mass under rediative corrections from within the SM particle content. The contributions from the one-loop diagrams to the Higgs mass are

$$-\frac{3}{8\pi^2}\lambda_t^2\Lambda^2 \qquad \text{from the top} \tag{2.1}$$

$$\frac{1}{16\pi^2}g^2\Lambda^2 \qquad \text{from the gauge boson} \tag{2.2}$$

$$\frac{1}{16\pi^2}\lambda^2\Lambda^2 \qquad \text{from the Higgs} \tag{2.3}$$

where λ_t is the top Yukawa coupling and Λ is the UV cut-off of the loop integral. For the corrections from these contributions to be less than one-tenth of the tree-level Higgs mass (or the contribution itself to be less than 10 times of the physical Higgs mass), the new physics scale Λ is expected to be around 2 TeV [5].

There are models which address the hierachy/naturalness problem of the SM's parameters. In 4 dimensions, there are supersymmetric extension of the SM, the composite models, the Little Higgs models, etc. Recently there is the class of models with extra dimensions.

2.1 SUSY models

Supersymmetry (SUSY) is the generalized spacetime symmetries of quantum field theory that transforms fermion to boson and vice versa. The basic consequence is that there is the same number of bosons and fermions and that the masses of the fermion-boson superpartners are the same if SUSY is an exact symmetry. Phenomenological facts imply that SUSY must be broken or else we would see the degeneracy of masses of fermions and bosons in the SM. The TeV-scale SUSY could induce the loop contributions to the Higgs mass from the TeV-scale superpartners which have the opposite signs to the ones from the SM. The net quadratic dependence of the cut-off scale of the 1-loop mass corrections will be suppressed and the Higgs mass is stabilized without the need for the fine tuning.

The minimal supersymmetric extension of the SM (MSSM) is the model where there is one superpartner for each SM particle, and TWO hypercharge $Y = \pm 1$ Higgs doublets and their partners. This Higgs structure is the minimal one without anomaly in

the SUSY framework. The requirement of the *analyticity* of the superpotential which generates the Yukawa couplings forces us to have one Higgs supermultiplet for u and d type quarks separately. This requirement does not exist in the SM inwhich we have only one Higgs doublet.

MSSM with the R-parity, $R = (-1)^{3(B-L)+2S}$, provides a way to prevent too-fast proton decay and to give a candidate for cold dark matter (CDM). The SM particles are R-even states and the superpartners are R-odd ones. The lightest supersymmetric particle (LSP) is therefore stable and can be serve as a CDM candidate.

There are 3-4 approaches to break SUSY apart from the conventional spontaneous breaking within MSSM content which has been proved to be very difficult (if not impossible). They are *gravity-mediated, gauge-mediated, anomaly-mediated, and gaugino-mediated* SUSY breaking scenarios. All of these have the "hidden" sector consisting of particles which are singlet (neutral) under the SM gauge groups where the SUSY is broken. The broken SUSY is mediated to the "visible" MSSM sector by various means.

In gravity-mediated scenario, SUSY breaking is mediated to visible sector by gravitational interaction [6, 7]. SUSY will be gauged to be local symmetry and there is the superpartner state of graviton with spin 3/2 called *gravitino*. In gauge-mediate scenario, there is additional "messenger" sector which is charged under the SM groups [8, 9]. The messengers will couple directly with the hidden sector and generate its own broken SUSY spectrum. The breaking then is mediated to the visible MSSM sector by virtual exchange of the messengers.

The braneworld-inspired SUSY breaking scenarios, the anomaly-mediated[10] and gaugino-mediated [11], postulate two branes separately located in the extra dimension. The MSSM particles are more localized to one brane and the SUSY breaking sector is

localized on the other. The messengers in both scenarios are the field propagating in the bulk of the extra dimension. Finally, there is a scenario where SUSY appears broken in 4 dimension by the boundary conditions of the MSSM fields in the 5th dimension [12, 13] (Scherk-Schwarz mechanism [14]).

2.2 Composite models and strong EW at TeV scale

Quarks and leptons could be made of constituents tightly bound together. At low energy, the effects of the compositeness are characterized by higher dimensional operators being suppressed by the inverse powers of the composite scale Λ, the cut-off scale. The effective dominant chiral-invariant Lagrangian is of the contact form between 4 fermions that reads [15]

$$\mathcal{L} = \frac{g^2}{2\Lambda^2}\eta_{\alpha\beta}(\overline{\psi_\alpha}\gamma_\mu\psi_\alpha)(\overline{\psi'_\beta}\gamma^\mu\psi'_\beta), \tag{2.4}$$

where $\alpha, \beta = L, R$, the chirality of the fermion. This kind of interaction is induced by the constituent exchange and thus appears as dimension 6 operator at low energy. We also expect to see excited states of the SM's fermions such as excited electron and quarks.

In the composite model, color triplet and antitriplet constituents can pair up to form a color singlet which we can identify with leptons. In this case, there is the color octet partners of the leptons, and they can interact via the Lagrangian

$$\mathcal{L} = \frac{g_s}{2\Lambda}\left(\bar{\ell}_8^a\sigma^{\mu\nu}F^a_{\mu\nu}\eta_\alpha\ell_\alpha + h.c.\right), \tag{2.5}$$

where a is the color index and g_s is the strong coupling.

In order to resolve the hierachy problem, Λ should be about few TeVs. The current lower bounds on the contact interact [15] from the LEP are actually about 3 TeV. The constraints get much stronger when analyzed as global fit with the low energy atomic parity violation experiment, about few tens of TeV.

2.3 The extra dimensional models

The major scenarios are large extra dimension (ADD [16] scenario), curved extra dimension (RS [17] scenario), and braneworld scenario. There is overlapping between different scenarios such as the branes models with large compactified extra dimensions or with curved extra dimensions. There is also universal extra dimension model (UED) where all of the SM particles have Kaluza-Klein (KK) states and the compactification scale is of a TeV scale [18]. UED can be embedded in the braneworld model where the SM particles are open-string states confined to stack of D4-branes (for 1 extra dimensional UED) wrapping TeV^{-1}-size extra dimension. In this sense, braneworld models contain most of the extra dimensional scenarios as the high string-scale limits. The only direct phenomenologically unique aspect of braneworld models is the *stringy dynamics* of the scattering that we will investigate in the most detailed in the subsequent chapters.

The ADD Scenario

The ADD scenario assumes graviton propagating freely in the bulk of $4 + n$ dimension while the SM particles are confined to the subspace of 4 dimensional spacetime. In this way, it identifies the UV cut-off scale to be the quantum gravity scale, M_D, which

could be as low as few TeVs in this "fixed-brane" scenario. By integrating out the extra dimensional degrees of freedom from the $4+n$ Einstein-Hilbert action

$$S = \int d^4x d^n y \sqrt{-\det G}\left[\frac{1}{2}M_D^{2+n}R\right] \tag{2.6}$$

to obtain the 4 dimensional effective action

$$S_{4D} = \int d^4x \sqrt{-\det G_4}\left[\frac{1}{2}M_{Pl}^2 R_4\right]. \tag{2.7}$$

We have the relationship

$$M_{Pl}^2 = V_n M_D^{2+n} \tag{2.8}$$

where V_n is the volume of the compactified extra dimensional space. The large numerical value of the Planck scale can be accounted by the large numerical value of the volume of the compactified space, and the genuine quantum gravity scale M_D could be of TeV scale. An example is when $n = 2, V \simeq (200\mu m)^n$, M_D could be about 10 TeV. The enormous mass gap between the EW scale and UV scale vanishes, and it is possible to have the quantum gravity scale to be as low as few TeVs.

The RS Scenario

For the RS scenario, the extra dimension is a curved interval (the whole bulk is AdS_5 geometry) with 2 branes as boundaries, one is our low energy universe and the other will show up at the Planck scale and hence named "Planck brane". The spacetime metric is

$$ds^2 = e^{-2ky}\eta_{\mu\nu}dx^\mu dx^\nu - dy^2 \tag{2.9}$$

where $y \in [0, \pi R]$ is the coordinate of the 5th dimension. The dependence of the warp factor multiplying to the 4d line element shows that the geometry is non-factorizable.

The quantum gravity scale M_D is related to M_{Pl} by

$$M_{Pl}^2 = \frac{M_D^3}{k}(1 - e^{-2kR\pi}). \tag{2.10}$$

The values of k and M_D are assumed to be of order of M_{Pl}, satisfying the above condition. In the simplest models with $k/M_{Pl} < 0.1, kR \simeq 10$, the effective scale at the second brane at $y = \pi R$ is of TeV scale. The graviton field is assumed to be concentrated at the $y = 0$ brane and the SM particles can be localized at the second brane with the physical scale $\Lambda \equiv M_{Pl}e^{-kR\pi} \sim 1$ TeV. Since $k \sim 10^{18}$ GeV, R becomes very small.

The bulk graviton KK states have mass $m_n = x_n \Lambda k/M_{Pl}$, where x_n are the the roots of the first-order Bessel function J_1. Effectively, while the zero-mode graviton coupling is suppressed by the Planck scale, the KK gravitons coupling is suppressed by the physical scale Λ which is of order of TeV.

The Braneworld Scenario

String theory allows the existence of the Dp-branes where the open string ends. p is the number of spatial dimensions of the brane and the world volume of the Dp-brane is a $1 + p$ dimensional spacetime. We can identify the SM particles to be open-string states naturally confined to the subspace of the Dbranes and graviton is the spin-2 closed-string state that can propagate freely in the bulk spacetime. The weakness of gravity, with respect to the gauge interactions of the SM particles, follows from a simple fact that graviton propagates in higher dimensional space than the SM particles. The quantum gravity scale and the string scale M_S again can be as low as order of TeV and rich phenomenology is within reach.

The gauge symmetry of the open-string states can be realized by the Chan-Paton

method [19]. Namely, we attach the additional degrees of freedom to the ends of the open string. These degrees of freedom can be represented by matrices due to the fact that open string has two ends. The amplitudes of the open string scattering depend only on the trace of these Chan-Paton matrices and therefore there exists the symmetry of transformation acting on these Chan-Paton matrices, i.e. the transformation which leaves the trace invariant. The symmetry group could be $U(N)$ or $SO(N)$ and remarkably it will be promoted to "local" gauge symmetry through the construction of vertex operator and 3-point amplitudes [20].

Since all of the string models provide field theory limits when $E/M_S \to 0$, it is hard to find a way to uniquely "prove" the validity of the string theory by means of the symmetries aspect and the particle spectrum. The most direct stringy effect is the stringy dynamics of the amplitudes, the existence of the string resonances (SR). We will investigate the stringy signals induced by the stringy dynamics in Chapter 4,5, and 6.

2.4 The Little Higgs models

In a class of model where Higgs is identified with the pseudo-Goldstone boson generated from the global symmetries breaking, if the symmetries are broken by two or more gauge couplings (*collective breaking*), then the Higgs mass is free from the quadratic dependence of the cut-off scale at the 1-loop level. This class of models is called the Little Higgs models (LH).

Generically, LH has a number of global symmetries that guarantee the masslessness of the Higgs. These symmetries are broken by the gauge, Yukawa and scalar couplings but the Higgs mass is still protected to be massless by the remaining global symmetries in

each breaking term. The small Higgs mass is induced at multi-loop level when there are two or more of symmetry-breaking terms involved, what-so-called "collective breaking". The Higgs now become the pseudo-Goldstone boson.

The symmetry breaking in the LH is again assumed to occur around $f = 1$ TeV and the scatterings of the theory remain perturbative until the cut-off scale $4\pi f$ at about 10 TeV. There are one-loop contributions to the Higgs mass via the extra vector-like new top quark, heavy gauge bosons, and heavy scalar that cancel the one-loop contributions from the top quark, EW gauge bosons, and the Higgs in the SM. The quartic self-coupling of the little Higgs is generated by the gauge and Yukawa interactions and the negative mass squared term is generated by the top Yukawa term. This will trigger the symmetry breaking. The signals induced by these extra particles are expected to show up around the TeV scale and we will investigate one possible channel to discover the heavy gauge bosons predicted in the LH in Chapter 3.

Chapter 3

Phenomenology of the Littlest Higgs model

The Little Higgs models [21] provide an alternative way to stabilize the light Higgs mass. In contrast to SUSY models, the Little Higgs models impose extra particles with the same statistics to cancel the leading 1-loop corrections to the Higgs mass. There is a number of Little Higgs models [22, 23] with different embedding of SM into larger group structure. The essential ingredients are

- Higgs is identified as Goldstone boson generated from spontaneous symmetry breaking of larger global symmetry realized non-linearly.
- Higgs gets mass by "collective" radiative symmetry breaking and becomes a pseudo-Goldstone boson. This mass is protected by global symmetry and stabilized up to the cut-off scale around 10 TeV or so.
- mass corrections to the Higgs from top and gauge bosons loops are also suppressed by cancellation of leading logarithmic terms with the contributions from extra

"vector-like" top quark and heavy gauge bosons.

In the explicit model of ref. [23, 24], the global $SU(5)$ symmetry with a locally gauged subgroup $[SU(2)_1 \times U(1)_1] \times [SU(2)_2 \times U(1)_2]$ is broken into $SO(5)$ with a remaining diagonally gauged $SU(2)_L \times U(1)_Y$ via a vev of order f. The 14 massless Goldstone bosons are $\mathbf{1}_0, \mathbf{3}_0$, complex $\mathbf{2}_{\pm\frac{1}{2}}$, and complex $\mathbf{3}_{\pm 1}$ with respect to the remaining $SU(2)_L \times U(1)_Y$. The hypercharge neutrals become the longitudinal components of the gauge bosons. These gauge bosons therefore have masses of the order of f. The complex triplet gets a vev $< i\phi^0 >= v'$ while the doublet gets a vev $< h^0 >= v/\sqrt{2}$.

The masses of the light and heavy gauge bosons in the Littlest Higgs model are [24]

$$M^2_{W^\pm_L} = m^2_W \left[1 - \frac{v^2}{f^2}\left(\frac{1}{6} + \frac{1}{4}(c^2 - s^2)^2\right) + 4\frac{v'^2}{v^2}\right], \tag{3.1}$$

$$M^2_{W^\pm_H} = m^2_W \left(\frac{f^2}{s^2c^2v^2} - 1\right), \tag{3.2}$$

$$M^2_{A_L} = 0, \tag{3.3}$$

$$M^2_{Z_L} = m^2_Z \left[1 - \frac{v^2}{f^2}\left(\frac{1}{6} + \frac{1}{4}(c^2 - s^2)^2 + \frac{5}{4}(c'^2 - s'^2)^2\right) + 8\frac{v'^2}{v^2}\right], \tag{3.4}$$

$$M^2_{A_H} = m^2_Z x_W \left(\frac{f^2}{5s'^2c'^2v^2} - 1 + \frac{x_H c^2_W}{4s^2c^2x_W}\right), \tag{3.5}$$

$$M^2_{Z_H} = m^2_Z \left(\frac{f^2}{s^2c^2v^2} - 1 - \frac{x_H x_W}{4s'^2c'^2c^2_W}\right), \tag{3.6}$$

where $m_W = gv/2, m_Z = gv/(2c_W)$ are the SM limits. x_H characterizes heavy bosons mixing and is given by

$$x_H = \frac{5}{2}gg'\frac{scs'c'(c^2s'^2 + s^2c'^2)}{5g^2s'^2c'^2 - g'^2s^2c^2}. \tag{3.7}$$

The couplings are related by

$$g = g_1 s = g_2 c, \;\; g' = g'_1 s' = g'_2 c', \tag{3.8}$$

$$s = \frac{g_2}{\sqrt{g_1^2 + g_2^2}}, \; s' = \frac{g_2'}{\sqrt{g_1'^2 + g_2'^2}}. \tag{3.9}$$

where g_i and g_i' $(i = 1, 2)$ are the couplings of the two copies of $SU(2)$ and $U(1)$.

3.1 WW_H production at the Linear e^+e^- Collider

Existence of the heavy $SU(2)$ gauge bosons Z_H and W_H is one of the main predictions of the Little Higgs models. The masses of Z_H and W_H should be within about a few TeV in order to solve the hierachy problem.

At an e^+e^- linear collider, if the center of mass (C.M.) energy can be set at the mass of the vector resonance, one would be able to reach a substantial production cross section and perform precision studies for the property of the particle. Above the resonance threshold, the dominant production for the heavy gauge bosons is through WW_H final state. For concreteness, we consider the Littlest Higgs model as in ref. [24]. Fixing $M_{W_H} = 1$ TeV, we plot the total cross section for WW_H production for $M_{W_H} = 1$ and 2 TeV versus C.M. energy in Fig. 3.1 by solid curves. For a fixed value of M_{W_H}, the cross section scales as $\cot^2\theta$, and the change for $\cot\theta = 1/2$ and 2 are indicated by a vertical bar. For comparison, we also include some relevant SM processes of W^+W^-, WWZ, and WWH. We see that the signal cross section for WW_H final state is large and asymptotically decreases to the level of W^+W^-.

In Fig. 3.2, we show the total cross-section versus M_{W_H} at the CLIC energies, 3 and 5 TeV, for $\cot\theta = 1$. The cross section grows when the mass increases due to the less and less severe propagator suppression $1/(s - M_{Z_H})^2$, until it is cut off due to the threshold kinematics.

Generically, the mass and coupling of W_H depends on $\cot\theta$, the mixing parameter

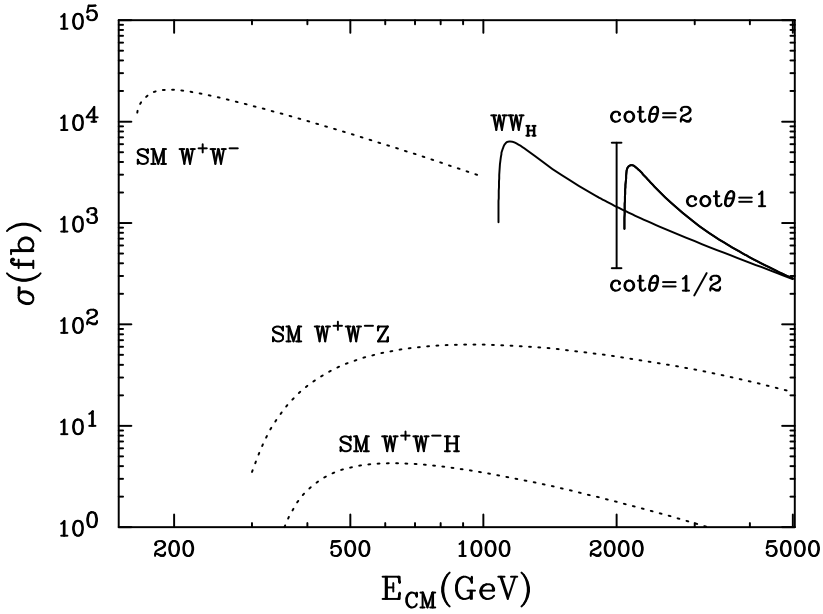

Figure 3.1: Total cross section for $e^+e^- \to WW_H$ production versus center of mass energy E_{cm} for $M_{W_H} = 1$ and 2 TeV (solid curves). Both charge states $W^\pm W_H^\mp$ have been included. Some relevant SM processes have been also included for comparison (dashed curves).

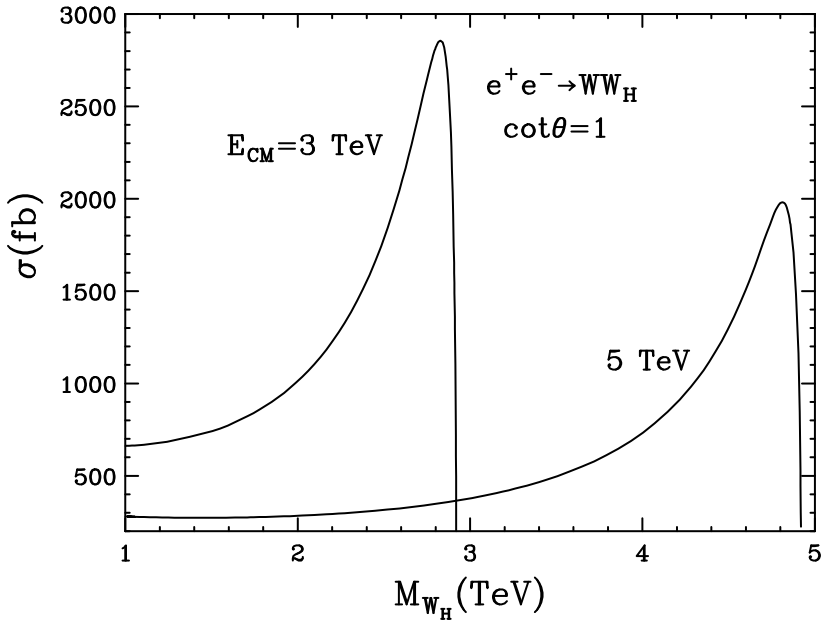

Figure 3.2: Total cross section for $e^+e^- \to WW_H$ production versus its mass M_{W_H} at the CLIC energies $E_{CM} = 3$ and 5 TeV. Both charge states $W^\pm W_H^\mp$ have been included.

between the SM and new gauge groups $SU_L(2)$ and $SU_H(2)$. Keeping the mass fixed at 1 TeV, we can explore the total cross section with respect to $\cot\theta$ as shown in Fig. 3.3.

Once W_H is produced, it can decay to SM particles, either into fermion pairs or WZ, WH. The branching fractions are given with respect to the mixing parameter $\cot\theta$ as in Fig. 3.4. The decay channels to fermions are dominant, asymptotically 1/4 for the three generations of leptons or one generation of quarks, for most of the parameter space. For small value of $\cot\theta < 0.4$, $W_H \to WH, WZ$ decay modes become more important, comparable to fermionic channels as shown in Fig. 3.4. The production rate for the signal is still quite sizable once above the kinematical threshold, and are likely above the SM backgrounds.

In summary, once above the kinematical threshold, the heavy gauge boson production

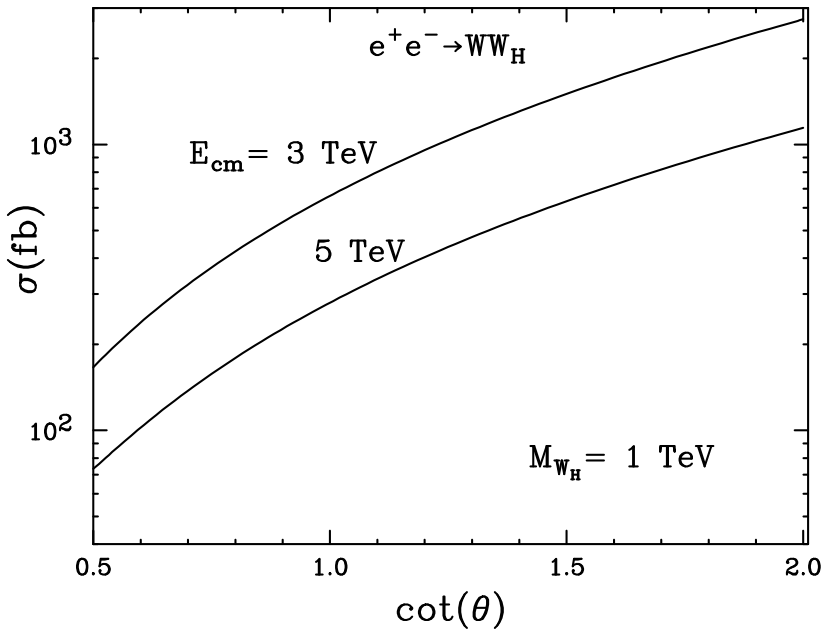

Figure 3.3: Total cross section for $e^+e^- \to WW_H$ production versus gauge coupling mixing parameter $\cot\theta$ for $M_{W_H} = 1$ TeV.

at the CLIC energies can be substantial. The threshold behavior can determine its mass accurately, and the cross section rate will measure the coupling strength $\cot\theta$.

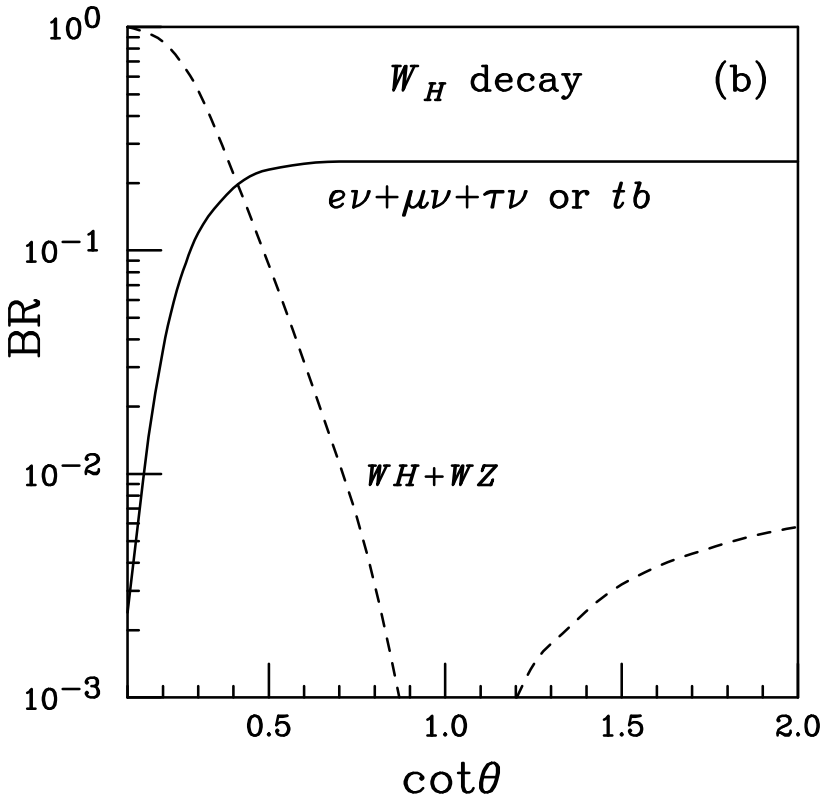

Figure 3.4: Branching fractions for W_H decay to SM particles.

Chapter 4

Low-Energy Stringy Corrections to the SM

4.1 Bounds on Four-Fermion Contact Interactions Induced by String Resonances

String theory, spoken or unspoken, is generally assumed to be the underpinning of the low scale gravity ideas [16, 17] explored theoretically and experimentally in recent years. A number of examples of ambitious "top-down" models of string realizations of low scale gravity ideas have been advanced, aiming at consistently achieving the connection to Standard Model (SM) physics from higher mass scales in certain D-brane scenarios [25]. As yet a fully realistic model like the SM has not been constructed. On the other hand, one could take a more phenomenological approach, from the "bottom up". One of the recent endeavors is to obtain the SM tree-level amplitudes at low energies [26, 27, 28] based on open-string amplitudes [29, 20]. This approach assures the correct low energy

phenomenology as given by the SM, yet captures one of the essential features of string theory, namely the string resonances, in a relatively model-independent way. The basic assumptions in this approach are that the fundamental string scale M_S is at the order of one TeV, and that the dominant contributions to the low energy processes are due to the exchange of string resonances. Earlier work on phenomenological studies dealt with QED from the M_Z scale to the first few string resonances [26], or neutrino inclusive processes far above the string scale to explore the effects from cosmic neutrinos [27, 28]. Phenomenologically, this string-amplitude approach complements the low-scale gravity calculations based on expansions in Kaluza-Klein modes [30], which are argued to be higher orders in string-coupling expansion [25, 26].

The purpose of this section is to expand this effort to model both *neutral and charged current* interactions at energies below the string scale.

Data from HERA experiments at DESY, with lepton-parton center of mass (CM) energies receiving a good fraction of the full 320 GeV, the highest energy available in laboratory experiments for deep inelastic scattering, provides one interesting testing ground for low-scale string model ideas. Similarly LEP-II, with CM energies up to 200 GeV provide another reasonably sensitive probe of the low energy limit of our string-resonance amplitudes. The full CM energy is available to excite string effects in this case. At the Tevatron, though the parton-parton collisions get typically only a modest fraction of the $1.8 - 2$ TeV available in the $p\overline{p}$ CM energy, there is still sensitivity to $0.5 - 1$ TeV scale physics.

The good agreement between all of the data from the facilities just mentioned and the SM allows bounds to be set on the mass scale of all kinds of new physics effects. For example, leptoquark states are one such effect, and perturbative string resonances can

carry the same quantum numbers as the lepto-quarks in some channels [27, 28]. At the parton level, much of the kinematical range is low enough to justify keeping the lowest order terms in an expansion in inverse string scale. This allows a direct comparison of amplitudes with the existing limits on new physics contact interactions [31, 32, 33, 34]. These observations that a comprehensive bound can be applied to a wide class of string-resonance models motivate the work we present here. We hope that exploration of the constraints imposed on the model parameters by the agreement between data and the SM will ultimately shed light on the way string theory signals could emerge as laboratory energies rise above the currently available regime.

In Section 4.1.1, we summarize the construction of neutral and charged current interactions for SM light fermions based on open-string scattering amplitudes. We then in Sec. 4.1.2 take the low-energy expansion by expanding the string amplitudes in powers of the inverse string scale evaluated at typical kinematic points to obtain the effective four-fermion contact-like interactions. We check that the approximation is good in the kinematic ranges we use. Comparing with the current limits on these interactions, we derive bounds on the string scale M_S. We conclude in Sec. 4.1.3.

4.1.1 Open String Tree Graph Amplitudes

In weakly-coupled string theory with a low string-scale, one generically expects the string amplitude corrections to the standard model processes to dominate over the graviton corrections, which enter at one loop and are parameterically suppressed by an extra factor of g^2, a gauge coupling squared [25, 26, 20]. At energies well below M_S, the stringy corrections can be systematically taken into account by the low-energy expansion of the string amplitudes in terms of s/M_S^2.

We assume that the tree-level string amplitudes represent the scattering of massless SM particles, as the zero string modes. The first attempt at exploring the low-scale string amplitudes was made to construct a string toy model of QED of electrons and photons [26]. The SM is embedded in a type IIB string theory whose 10-dimensional space has six dimensions compactified on a torus with common period $2\pi R$. There are N coincident D3-branes, on which open strings may end, that lie in the 4 extended dimensions. The extra symmetry of the massless string modes are eliminated by (unspecified) orbifold projection. The paper applies the results to Bhaba scattering and then adds several prescriptions to include some simple processes $e^+e^- \to Z^0 \to e^+e^-$ and $q\bar{q} \to g^* \to 2$ jets, where g^* represents a string resonance excitation of the gluon. However, this toy model does not attempt to be fully realistic in terms of the SM particle spectrum and their interactions.

Our construction of the tree graph amplitude follows the same pattern as that outlined in [27] and in [28]. The result is a model containing the SM on the 3-branes and no unacceptable (*i.e.,* unobserved) low energy degrees of freedom. This is accomplished by allowing the group theoretical Chan-Paton factors as free parameters. The masses of gauge bosons W and Z must be introduced by hand, since the string amplitude describes massless particle scattering and we are not consistently modeling the breaking of gauge invariance. Though all the standard model gauge couplings are assumed to unify to a single value at the string scale in this simple construction, we use the physical values of the SM electroweak couplings since we restrict ourselves here to energies below the string scale.

We begin with the general form for a four-fermion amplitude for open strings in such a braneworld framework. The parton level Mandelstam variables are denoted by $s, t,$

and u. The physical scattering process will be identified as $f_1 + f_2 \to f_3 + f_4$. The s, t and u-channels are labeled (1,2), (1,4) and (1,3), respectively. The ordered amplitude with the convention that all momenta are directed inward reads [20, 35, 36]:

$$\begin{aligned} A_{string}(s,t,u) &= ig^2 \left[t\ \overline{\psi}_1 \gamma^\mu \psi_2 \overline{\psi}_3 \gamma_\mu \psi_4 - s\ \overline{\psi}_1 \gamma^\mu \psi_4 \overline{\psi}_3 \gamma_\mu \psi_2 \right] \\ &\times \left[\frac{1}{st} S(s,t)[T(1234) + T(4321)] + (1 \leftrightarrow 4, s \leftrightarrow u) + (1 \leftrightarrow 2, t \leftrightarrow u) \right]. \end{aligned}$$

where the function $S(x, y)$ is similar to a Veneziano amplitude [37], and is defined by

$$S(x,y) = \frac{\Gamma(1-\alpha' x)\Gamma(1-\alpha' y)}{\Gamma(1-\alpha' x - \alpha' y)}, \tag{4.1}$$

where the Regge slope parameter $\alpha' = M_S^{-2}$. In the limit $M_S \gg \sqrt{s}$, $S \to 1$ and the low energy gauge theory expression for the amplitude is regained, as we show below. The factors $T(1234) + T(4321)$ and their $1 \leftrightarrow 4$ and $1 \leftrightarrow 2$ counterparts are proportional to the Chan-Paton factors [19] and involve traces over the group representation matrices, λ, of the fermions at the four vertices. For example, $T(1234) \propto Tr(\lambda^1 \lambda^2 \lambda^3 \lambda^4)$ with normalization $Tr(\lambda^a \lambda^b) = \delta^{ab}$ in the adjoint representation of $U(n)$. Typically, with our normalization, the Chan-Paton factors are in the range of -4 to 4 for a general $U(n)$ group. The above general expression serves as the basis for calculating all of the specific helicity and internal quantum number possibilities in the case that the states 3 and 4 have outgoing momenta.

Charged Current Processes

The charged current (CC) string model amplitude in the weak coupling regime receives no contribution from the graviton at one loop. In this sense it is perhaps conceptually cleaner than the neutral current (NC) case [27, 28], where the graviton exchange is contained in the one loop amplitude [26]. At energies above the string scale, the extra

power of s/M_S^2 in the graviton contribution compensates for the Yang-Mills gauge coupling suppression of the loop amplitude compared to the tree graphs; there the strong gravity dynamics and the string resonance dynamics become comparable. Though we are focusing on the low energy region, where graviton exchange is suppressed, the CC amplitude construction is simpler than that of the NC because there are fewer processes and only one gauge coupling to consider. For this reason we discuss the CC case first in some detail, and then turn to the NC case.

For definitiveness, taking all helicities for the in and out states left-handed (denoted by L), we find the string tree amplitude:

$$A^{CC}_{string}(LL) = ig^2 \left[S(s,t)\frac{s}{t}T_{1234} + S(u,t)(-\frac{s}{t} - \frac{s}{u})T_{1324} + S(s,u)\frac{s}{u}T_{1243} \right],$$

where we have further simplified notation by introducing $T_{1234} = T(1234) + T(4321)$ and so forth. The corresponding standard model electroweak (EW) tree amplitude is

$$A^{CC}_{EW} = ig^2 \frac{s}{t - M_W^2}. \tag{4.2}$$

here and henceforth, g is identified with the $SU(2)_L$ gauge coupling. We require that the charged-current in t-channel contain the W boson as its zero mode and that there is no exotic (leptoquark) zero mode in the u-channel. In order to remove the unwanted zero-mode pole, we must require

$$T_{1243} = T_{1324} \equiv T. \tag{4.3}$$

The low energy gauge theory limit should reproduce the W-pole in the t-channel in tree approximation to the string amplitude. Using Eq. (4.3) and matching the coefficient of the $1/t$ pole to the SM result of Eq. (4.2), we identify

$$T_{1234} = 1 + T \tag{4.4}$$

The tree-level result for the amplitude for $LL \to LL$ after removing the exotic zero-mode pole in the u-channel and identifying the zero-mode pole in the t-channel as the W-boson, is

$$A^{CC}_{string}(LL) = ig^2 T \frac{s}{ut} f(s,t,u) + ig^2 \frac{s}{t - M_W^2} S(s,t), \tag{4.5}$$

where

$$f(s,t,u) \equiv uS(s,t) + sS(u,t) + tS(s,u). \tag{4.6}$$

In the limit $M_S \gg \sqrt{s}$, we have

$$S(s,t) \approx 1 - \frac{\pi^2}{6} \frac{st}{M_S^4} \quad \text{and} \quad f(s,t,u) \approx -\frac{\pi^2}{2} \frac{stu}{M_S^4}. \tag{4.7}$$

The SM tree amplitude is reproduced in the limit $s/M_S^2 \to 0$. For later convenience we define $V(s,t,u)$ via Eq. (4.5) by

$$A^{CC}_{string}(LL) = ig^2 \frac{s}{t - M_W^2} V(s,t,u). \tag{4.8}$$

The above results are also applicable to right-handed anti-fermion scattering $\overline{R}\,\overline{R} \to \overline{R}\,\overline{R}$. The other helicity combinations including anti-leptons and anti-quarks can be worked out by appropriate crossing. For instance, for the scattering of a left-handed lepton and a right-handed anti-quark $L\overline{R} \to L\overline{R}$, or right-handed anti-lepton on left-handed quark $\overline{R}L \to \overline{R}L$, the $s \leftrightarrow u$ and $2 \leftrightarrow 3$ crossed amplitude applies. The amplitudes for this process read

$$\begin{aligned} A^{CC}_{string}(L\overline{R}) &= A^{CC}_{string}(\overline{R}L) = ig^2 \left[S(s,t)\frac{u^2}{st} T_{1234} + S(t,u)\frac{u}{t} T_{1324} + S(s,u)\frac{u}{s} T_{1243} \right] \\ &= A^{CC}_{string}(LL)(s \leftrightarrow u) = ig^2 \frac{u}{t - M_W^2} \overline{V}(s,t,u), \end{aligned} \tag{4.9}$$

where the generic label T is not distinguished from that in the LL case above, to avoid clutter in the notation. These expressions are the analogs of those written down for the

NC neutrino case in [27] and [28], which we expand for the full range of NC cases in the next subsection.

Neutral Current Processes

The open string perturbative amplitude construction for $2 \to 2$ NC scattering follows exactly the same pattern as described above in the charged current case. The neutral current case involves 4-fermion amplitudes as well as 2-lepton plus 2-gluon external line amplitudes [28]. We find that in the low energy realm the gluon amplitudes contribute negligibly to the constraints. Therefore, we confine ourselves to the 4-fermion construction, again identifying zero-mode poles in the t-channel with γ and Z-exchange. As before, we require that the Chan-Paton factors are constrained to cancel the exotic zero modes in the other channels. To introduce the SM factors, we adopt the device that fermion labels in the Chan-Paton factors are the guide to constructing the low energy limit. This is because the λ's of the external legs depend on the $SU(2)\otimes U(1)$ embedding in a larger (unifying) group, and the Chan-Paton traces over λ's are linked to the quantum numbers of the s, t and u-channels. The connection between the string amplitude zero mode poles and the SM poles, in keeping with this philosophy, is described next.

We consider separately the low energy matching for $2 \to 2$ amplitudes for (1) all left-handed (L) or all right-handed (R); and (2) $LR \to LR$ and $RL \to RL$.

<u>(1). $\ell_\alpha q_\alpha \to \ell_\alpha q_\alpha;\ \alpha = L, R$</u>

The string and SM electroweak tree amplitudes for the like-helicity combinations are

$$\begin{aligned} A^{NC}_{string}(\alpha\alpha) &= ig^2\left(S(s,t)\frac{s}{t}T_{1234} + S(t,u)\frac{s^2}{ut}T_{1324} + S(u,s)\frac{s}{u}T_{1243}\right) \\ A^{NC}_{EW}(\alpha\alpha) &= 2ie^2\frac{s}{t}\left(Q_qQ_\ell + \frac{t}{t-M_Z^2}\ \frac{g^\ell_\alpha g^q_\alpha}{s_W^2c_W^2}\right) \end{aligned} \tag{4.10}$$

where $Q_{q,\ell}$ are the electric charge of quark and lepton; $s_W = \sin\theta_W, c_W = \cos\theta_W$. Matching with $e = g\sin\theta_W$ gives

$$T_{1243} = T_{1324} \equiv T \tag{4.11}$$

$$T_{1234} = T + 2s_W^2\left(Q_q Q_\ell + \frac{t}{t-M_Z^2}\,\frac{g_\alpha^\ell g_\alpha^q}{s_W^2 c_W^2}\right), \tag{4.12}$$

which guarantees that there is no zero-mode exotic u-channel pole and that the SM tree amplitude is recovered in the limit $S(s,t) = S(t,u) = S(s,u) \to 1$ where $s \ll M_S^2$. Our modified string amplitude now reads

$$A_{string}^{NC}(\alpha\alpha) = ig^2 T\frac{s}{ut}f(s,t,u) + 2ig^2 s_W^2 S(s,t)\frac{s}{t}\left(Q_q Q_\ell + \frac{t}{t-M_Z^2}\,\frac{g_\alpha^\ell g_\alpha^q}{s_W^2 c_W^2}\right), \tag{4.13}$$

where $f(s,t,u)$ was defined in Eq. (4.7). Our convention for the SM neutral-current couplings is

$$g_L^f = T_{3f} - Q_f \sin^2\theta_W, \quad g_R^f = -Q_f \sin^2\theta_W. \tag{4.14}$$

We have adopted the shorthand that all parameters proportional to Chan-Paton factors are designated by the single symbol T. In fact, in our study of the low energy constraints on the models in the following section, we will make the simplifying assumption that the factors are all equal.

<u>(2). $\ell_\alpha q_\beta \to \ell_\alpha q_\beta;\ \alpha,\beta = L,R;\ \alpha \neq \beta$</u>

The string and SM electroweak tree amplitudes are

$$A_{string}^{NC}(\alpha\beta) = ig^2\left(S(s,t)\frac{u^2}{st}T_{1234} + S(t,u)\frac{u}{t}T_{1324} + S(u,s)\frac{u}{s}T_{1243}\right)$$

$$A_{EW}^{NC}(\alpha\beta) = 2ie^2\frac{u}{t}\left(Q_q Q_\ell + \frac{t}{t-M_Z^2}\,\frac{g_\alpha^\ell g_\beta^q}{s_W^2 c_W^2}\right). \tag{4.15}$$

Again, matching with $e = g \sin\theta_W$ gives

$$T_{1243} = T_{1234} \equiv T \tag{4.16}$$

$$T_{1324} = T + 2s_W^2 \left(Q_q Q_\ell + \frac{t}{t - M_Z^2} \frac{g_\alpha^\ell g_\alpha^q}{s_W^2 c_W^2} \right). \tag{4.17}$$

The final string amplitude reads

$$A_{string}^{NC}(\alpha\beta) = ig^2 T \frac{u}{st} f(s,t,u) + 2ig^2 s_W^2 S(t,u) \frac{u}{t} \left(Q_q Q_\ell + \frac{t}{t - M_Z^2} \frac{g_\alpha^\ell g_\beta^q}{s_W^2 c_W^2} \right). \tag{4.18}$$

This is $s \leftrightarrow u$ crossing from Eq. (4.13).

To obtain other amplitudes involving anti-fermions, it is a matter of simple crossing. For example, for Drell-Yan process $q\bar{q} \to \ell\bar{\ell}$, we simply have $s \leftrightarrow t$ crossing of the above formulas in Eqs. (4.13) and (4.18).

The amplitudes we have constructed are particularly convenient for comparing to the contact interaction amplitudes analyzed and constrained by data in the literature [32, 33]. We turn next to this comparison, deriving constraints on M_S in the process.

4.1.2 Linking String amplitudes to Contact Interactions

In this section, we convert constraints on contact interactions to constraints on the string scale M_S for given T values. In order to compare to data at low energies, we express string deviation from SM electroweak amplitude by $\triangle_{\alpha\beta}$ $(\alpha, \beta = L, R)$, namely

$$A_{string}(\alpha\beta) = A_{EW}(\alpha\beta) + \triangle_{\alpha\beta}. \tag{4.19}$$

Using Eq. (4.7), we find for like-helicity fermion scattering $(\alpha\alpha) = LL$ and RR

$$\triangle_{\alpha\alpha} \simeq -\frac{\pi^2}{6} \frac{st}{M_S^4} A_{EW}(\alpha\alpha) - iTg^2 \frac{\pi^2}{2} \frac{s^2}{M_S^4}, \tag{4.20}$$

where T is the generic parametrized Chan-Paton factor corresponding to the particular process. For unlike-helicity combinations in the neutral current case, $\triangle_{\alpha\beta} = \triangle_{\alpha\alpha}(s \leftrightarrow u)$,

The reduced amplitudes for contact interactions from physics beyond the SM are conventionally parameterized as [31, 32, 33, 34]

$$\triangle M^{\ell q}_{\alpha\beta} = \eta^{\ell q}_{\alpha\beta} = \epsilon \frac{4\pi}{\Lambda^2_{\ell q}}. \tag{4.21}$$

The cutoff $\Lambda_{\ell q}$ is the mass scale at which new physics sets in. It presumably corresponds to the mass of the heavy strongly interacting particles that mediate the new interaction and it is referred as the "compositeness scale". The sign factor $\epsilon = \pm 1$ allows for constructive or destructive interference between the contact interaction and the SM amplitudes. Typically, in the fit to a given class of interactions, it is designated $\Lambda_\pm$ to distinguish between fit values obtained with $\epsilon = \pm 1$.

The relations between the string contribution and the reduced amplitude parameterization can be found to be, for like-helicity fermion scattering,

$$\triangle M_{\alpha\alpha} \quad = \quad \frac{\triangle_{\alpha\alpha}}{i2s} \simeq -\frac{\pi^2}{12} g^2 \frac{s}{M_S^4}(F + 3T). \tag{4.22}$$

For unlike-helicity fermion scattering, $\triangle M_{\alpha\beta} = \triangle M_{\alpha\alpha}(s \leftrightarrow u)$. For a Drell-Yan process, which invloves with anti-fermions, we have $s \leftrightarrow t$ from Eq. (4.22). The factor F includes the information for chiral couplings and it is

$$F = \begin{cases} \frac{t}{t - M_W^2} & \text{for charged current,} \\ 2s_W^2 \left(Q_q Q_\ell + \frac{t}{t - M_Z^2} \frac{g^\ell_\alpha g^q_\beta}{s_W^2 c_W^2} \right) & \text{for neutral current } \ell q. \end{cases} \tag{4.23}$$

It is interesting to note that the leading stringy corrections to the SM amplitudes as in Eq. (4.20) enter at dimension-8, while the standard parameterization for four-fermion

contact interactions as in Eq. (4.21) is of dimension-6. Due to this additional energy-dependent suppression factor s/M_S^2, the constraints obtained from low energy data on M_S will thus be weaker than that on $\Lambda_{\ell q}$.

In certain more complicated brane-world models, for example intersecting D-branes [38], there are corrections at dimension-6 from Kaluza-Klein excitations, winding modes as well as string oscillators. They lead to stronger limit on the lower bound of the string scale, about $2-3$ TeV [38].

Validity of the Approximate Amplitudes

With the above set up, we are in position to extract bounds on the string scale from the values of parameters of contact interactions. A global fit of contact interactions to all of the data discussed above plus the low energy data from neutral current and charged current process, including atomic parity violation, is also reported in [32]. The low energy data dominate these global constraints. As noted earlier, the s/M_S^2 dependence of our string amplitudes severely suppresses stringy effects at very low energies and the low energy data are insensitive to the string scale. We will thus mainly make use of the data at highest energies available like in HERA, Tevatron and LEP-II.

Our expansion of the factors $S(x,y)$, where $x,y = s,t$ or u, should be valid if bounds on M_S are found to be well above the kinematical region covered by the data. How close can the scale be to the kinematical range of the data before the approximate expansion becomes unreliable? We address this question by computing the CC cross section $e^-p \to \nu + X$ with the full amplitudes and with the approximated amplitudes. The differential DIS cross section, in terms of the functions V in $A^{CC}_{string}(LL)$ in Eq. (4.8)

and $\overline{V}$ in $A^{CC}_{string}(L\overline{R})$ in Eq. (4.9), reads

$$\frac{d^2\sigma}{dxdQ^2} = \frac{d\sigma^{SM}}{dQ^2}[(u(x,Q^2)+c(x,Q^2))V^2 + (1-y)^2(\overline{d}(x,Q^2)+\overline{s}(x,Q^2))\overline{V}^2], \quad (4.24)$$

where $d\sigma^{SM}/dQ^2$ is the SM W-exchange Born term differential cross section. In the course of this study, we can probe as well the simple constraint on the model that follows from the measured total cross section [39, 40, 41], namely

$$\sigma(Q^2 > 200 \text{ GeV}^2) = 66.7\,^{+3.2}_{-2.9} \text{ pb},$$

at $E_{CM} = 318$ GeV, the ep C.M. energy. The ZEUS collaboration quotes the value

$$\sigma(Q^2 > 200 \text{ GeV}^2) = 69.0\,^{+1.6}_{-1.3} \text{ pb}$$

as the SM expectation using its NLO QCD fit. For example, with $T = 1$ one finds the experimental 95% CL limit

$$M_S \geq 0.45 \text{ TeV}, \quad (4.25)$$

whether one uses the full or the approximate amplitude. In general the approximate cross-sections agree with the complete calculation to 3 figures until $M_S \simeq E_{CM}$, where one finds differences of the order of a percent. For example, with $T = 1$ and $M_S = 320$ GeV, the full and approximate cross sections are 85.2 pb and 82.8 pb, while with $T = -1$ the cross sections are 62.2 pb and 62.5 pb. The approximation is evidently quite good so long as $M_S > E_{CM}$, since the lowest Regge resonance slips into the physical region when $M_S \leq E_{CM}$ and should, in principle, be represented by a resonant form with finite width. However,the vanishing of the structure functions as $x \to 1$ minimizes the impact of the nearby resonance on the DIS cross section as $M_S \to E_{CM}$ from above.

Evaluation of Lower Limits on M_S

Focusing on the chiral amplitudes A_{LL}, which enter in both the NC and CC processes, we combine Eqs. (4.21) and (4.22) to express the constraint on M_S at a given T value and Λ bound value as

$$M_S > [-\frac{\pi^2}{12}\frac{g^2 s}{\eta}(F+3T)]^{\frac{1}{4}} \text{ for DIS at HERA.} \tag{4.26}$$

For the DY process at the Tevatron and e^+e^- annihilations at LEP-II, we have $s \leftrightarrow t$ in Eq. (4.26).

In Table I we show the lower bounds on M_S that follow from the corresponding best fit values of η from the HERA NC data, the Drell-Yan data from Tevatron and the hadronic cross section from LEP-II quoted in [32]. These values follow from our NC analysis above. In the table we also use the NC data with the $SU(2)$ relation between the CC and NC amplitudes, namely

$$\triangle M_{LL}(CC) = \triangle M_{LL}^{ed} - \triangle M_{LL}^{eu},$$

to give corresponding limits on the CC amplitudes. These are not independent constraints, of course, but simply show the impact of the data in the CC sector. We also include the direct CC bound on M_S obtained in the preceding subsection from HERA data and the DY bound obtained by CDF at the Tevatron on the CC $qqe\nu$ compositeness scale [42], with the corresponding M_S bound. When translating the existing constraints on $\eta_{\alpha\beta}$ to M_S, we need to take into account the different energy-dependence as noted earlier. In computing the values of the bounds in Table I, we use the rule of thumb that the average parton energy fraction is $\langle x \rangle \simeq 1/3$, so the direct channel HERA parton CM energy squared is $s \simeq E_{CM}^2/3 \approx (0.18 \text{ TeV})^2$. At the Tevatron, where the total CM

	HERA NC		Drell-Yan		LEP	
	η (TeV^{-2})	M_S (TeV)/T	η	M_S/T	η	M_S/T
η_{LL}^{eu}	$-1.18\ ^{+0.53}_{-0.56}$	$0.34/+1$	$-0.19\ ^{+0.24}_{-0.21}$	$0.85/+1$	$-0.22\ ^{+0.086}_{-0.084}$	$0.32/0$
						$0.50/-1$
η_{LL}^{ed}	$1.53\ ^{+1.59}_{-1.35}$	$0.29/-1$	$0.88\ ^{+0.58}_{-0.73}$	$0.34/0$	$0.26\ ^{+0.095}_{-0.098}$	$0.29/0$
				$0.57/+1$		$0.48/+1$
				$0.73/-1$		
η_{CC}	$2.71\ ^{+1.67}_{-1.46}$	$0.26/-1$	$1.07\ ^{+0.62}_{-0.76}$	$0.41/0$	$0.48\ ^{+0.13}_{-0.13}$	$0.33/0$
				$0.58/+1$		$0.45/+1$
				$0.73/-1$		
	HERA σ_{CC}:	$0.45/+1$	(CDF) 0.80	$0.53/0$		
				$0.75/+1$		

Table 4.1: Lower bounds on the string scale M_S from contact interaction parameters, at a 95% CL. The Chan-Paton factor T has been taken as ± 1 as indicated.

energy was 1.8 TeV, our nominal parton CM energy squared is $s \simeq E_{CM}^2/9 = (0.6\ \text{TeV})^2$. For the momentum transfer squared we take $Q^2 = s/2$.

In the following subsections we explain the entries in the table.

HERA NC

Limits on the deviation from SM predictions for processes at HERA lead to corresponding bounds on string parameter. From Table IV of [32], the limits on $\triangle M_{LL} = \eta_{LL}^{\ell q}$, provided separately for *eeuu* and *eedd*, are given. At 2σ level (or 95% CL), we have the lower bound $\eta_{LL}^{eu} = -2.3/\text{TeV}^2$. We apply the weak isospin constraint that the *eeuu* and *eedd* amplitudes have opposite sign, which implies the upper bound $\eta_{LL}^{ed} = 4.7/\text{TeV}^2$. In order to obtain a lower bound on string scale M_S, we need the correct sign of $\triangle M$ from our string expression corresponding to each limit on value of η. Consequently, in the *eeuu* case, the gauge factor $(F + 3T) \geq 0$ is required. In the *eedd* case, the requirement is $(F + 3T) \leq 0$. With typical values $s = (0.18\ \text{TeV})^2$, $t/(t - M_Z^2) \simeq 1/2$ and $T = +1\ (-1)$, we find the bounds 0.34 (0.29) TeV as shown in the table. We should comment here that, the typical bounds on masses of leptoquark resonances at HERA are in the range $0.25 - 0.29$ TeV [41], roughly compatible with bounds from our contact interaction analysis. Slightly higher values of $|T|$ produce higher bounds on M_S. For example, with $T = -2$, the value is 0.35 TeV for *eedd*. Clearly larger absolute values of T correspond to larger bounds on M_S, limited only by the requirement that the effective coupling constants remain perturbative, consistent with our string amplitude construction. From Eq. (4.26), we see that $M_S \propto (F + 3T)^{1/4}$, or roughly proportional to $T^{1/4}$. This is also the case for DY processes at the Tevatron and e^+e^- annihilation at LEP-II.

Drell-Yan at the Tevatron

We follow the same pattern as described above, now using $s \leftrightarrow t$ of Eq. (4.22), for limits from DY processes at the Tevatron. For typical values we find the strongest bounds on string scale are $0.85, 0.73$ TeV for modest values $T = +1, -1$ for $eeuu$ and $eedd$ respectively. An independent search for deviations from the SM in the DY channel $qq\nu l$ at CDF [42], cited in [33], yields a 95% CL upper bound of $0.8/\text{TeV}^2$ on the value of η_{CC}. The corresponding limits on M_S are independent of those derived from the $eedd$ case. Searches for W' and Z' resonances at the Tevatron yield bounds similar to the larger of the bounds just quoted, namely in the range $0.75 - 0.85$ TeV [42]. As in the case of leptoquark resonance searches at HERA, the bounds on the $W'$and Z' masses at the Tevatron are roughly consistent with the contact interaction bounds we just described. Larger DY bounds rise to 0.86 TeV and 1.04 TeV when the T values are doubled to ± 2, indicating that increasing the magnitude of T has a marked effect on M_S. In Fig. 1 we show the plot of the lower bound on M_S vs. the Chan-Paton parameter T in the range $1 \leq |T| \leq 4$ for the $eeuu$ and $eedd$ cases, which give representative largest lower bounds on M_S for a given T value. In any case, it is fair to say that the resonant bounds and the contact interaction bounds are complementary ways to probe for string physics at the TeV scale.

LEP-II

The LEP-II results are from the lowest nominal energy, but have the advantage that all of the CM energy can go directly into producing new physics. For LEP-II, we use $s = (0.2 \text{ TeV})^2$ with $t \simeq -s/2$. We only consider cross-section for hadron production as stated in [31, 32]. Limits are as listed in Table I. The limits tend to be stronger than in

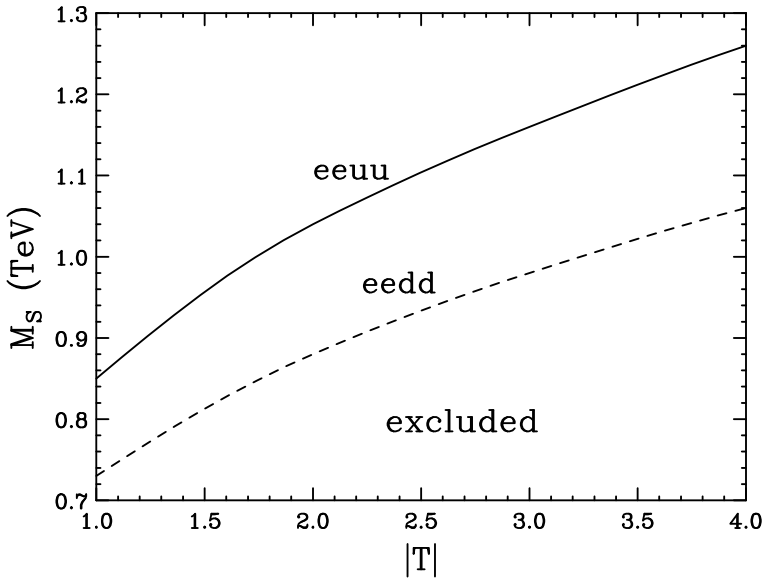

Figure 4.1: Relationship between Chan-Paton parameters and lower bounds of the string scale M_S from the DY process at the Tevatron. T is positive and negative for *eeuu* and *eedd* respectively. The region under the curves is excluded at 95% CL.

the DIS at HERA case, since the values of $\eta's$ and their uncertainties are significantly smaller and the CM energy is slightly larger than the characteristic value used in our HERA analysis. A consistent but somewhat weaker limit is given in Ref. [26] with $M_S \geq 0.41$ TeV.

4.1.3 Summary and Conclusions

Combining the low energy limit of string amplitudes for NC and CC processes, we find that bounds on the string scale can be obtained that complement and extend previous analyses. In particular, we extend previous models to cover all neutral current phenomena and, for the first time, offer a model of charged current amplitudes in a string resonance framework. The essence of the approach we adopt is that of Ref. [27]. The low

energy limit of each string amplitude reproduces the corresponding SM amplitude. This leaves only a limited number of Chan-Paton factors unspecified, and these are treated as free parameters whose values are related by requiring consistency with the perturbative construction of the string amplitudes. In the absence of new physics signals, they are constrained by the agreement between the SM and the data for a given string scale. More generally, the parameter space consists of the string scale M_S and a limited number of free dimensionless parameters denoted generically by T. We refer to this as a "bottom up" approach to probing the string aspect of braneworld.

We have focused in this paper on the match between the low energy limit of the open-string four-fermion amplitudes at typical kinematical region and the constraints on contact interaction parameters determined by data from HERA, Tevatron and LEP-II. The bounds on the string mass scale are comparable in every case to those found in specific models or from leptoquark and W' and Z' searches at HERA and Tevatron. This is no surprise, since the accelerator energy and the precision of the measurements dictate the accessible scale in searches for new physics. It is also no surprise that the highest energy data provide the highest values of the lower bound on new physics. The Drell-Yan processes at the Tevatron lead to our strongest constraints, namely

$$M_S \geq \begin{cases} 0.9 \text{ TeV} & \text{for } |T| = 1, \\ \\ 1.3 \text{ TeV} & \text{for } |T| = 4, \end{cases} \tag{4.27}$$

as shown in Fig. 1 for the *eeuu* case.

The relationship between string scale M_S and Quantum Gravity scale M is model-dependent [25, 26]. However, $M_S < M$ quite generally, so the bound on M_S applies to M as well. In one simple case of D-brane scenario, the string scale and the quantum

gravity scale in the weakly coupled string sector are related by [26]

$$\frac{M}{M_S} = \frac{k}{g^{1/2}} \tag{4.28}$$

where the model-dependent factor k is of order 1. Taking the value $k = 1$ and the $SU(2)$ gauge coupling at the weak scale for illustration, we obtain from Eqs. (4.27) and (4.28) a conservative bound on the gravity scale

$$M \geq \begin{cases} 1.1 \text{ TeV} & \text{for } |T| = 1, \\ \\ 1.6 \text{ TeV} & \text{for } |T| = 4 \end{cases} \tag{4.29}$$

from the Drell-Yan analysis of the Tevatron data. This estimate of the range of values of the scale of gravity in large extra dimensions is competitive with the current accelerator search values and the value from the specific model of Ref. [26]. But again we advise caution because of the model dependence of our estimate.

We conclude that a TeV string scale can measurably modify weak current amplitudes even well below the string scale. The corresponding limits on this scale and the scale of gravity are quite interesting and worth further exploration. Including these considerations in the interpretation of future data will add an extra dimension, or more, to the search for new physics at the TeV scale.

4.2 TeV-Scale Stringy Signals at Linear e^+e^- Collider

In this section, we will investigate the low-energy effects induced by the TeV-scale string resonances in the EW tree-level e^+e^- scattering at $E_{cm} = 500$ GeV. Using the same

matching technique, the stringy extended amplitudes are

$$A(\ell_\alpha \bar{\ell}_\beta \to q_\alpha \bar{q}_\beta) \;=\; ig_L^2 \left(\frac{t}{s} F_{\alpha\alpha} S(s,t) + T \frac{t}{us} f(s,t,u) \right) \tag{4.30}$$

where $\alpha, \beta = L, R$, the helicity of the fermion and antifermion. For $\ell_\alpha \bar{\ell}_\beta \to q_\beta \bar{q}_\alpha$, the amplitude is $t \leftrightarrow u$ and $F_{\alpha\alpha} \to F_{\alpha\beta}$ of the above. Using the low-energy approximation

$$S(s,t) \;\simeq\; 1 - \frac{\pi^2}{6}(\frac{st}{M_S^4}) \tag{4.31}$$

$$f(s,t,u) \;\simeq\; -\frac{\pi^2}{2}(\frac{stu}{M_S^4}), \tag{4.32}$$

the above amplitude becomes

$$A(\ell_\alpha \bar{\ell}_\beta \to q_\alpha \bar{q}_\beta) \;\simeq\; ig_L^2 \left(\frac{t}{s} F_{\alpha\alpha} - \frac{\pi^2}{6}(F_{\alpha\alpha} + 3T) \frac{t^2}{M_S^4} \right). \tag{4.33}$$

Again, for $\ell_\alpha \bar{\ell}_\beta \to q_\beta \bar{q}_\alpha$, the amplitude is $t \leftrightarrow u$ and $F_{\alpha\alpha} \to F_{\alpha\beta}$ of the above. From these approximated formula, the angular distributions and the angular Left-Right asymmetry can be computed as in Figure 4.2-4.7.

As we will see in the following section, the low-energy stringy corrections in the processes *involving two vector bosons* are only from spin-2 states due to Yang's theorem and therefore the similarity between the stringy corrections and the Kaluza-Klein (KK) graviton exchange [57] in the low-energy limit is guaranteed. For the 4-fermion cases, the higher-spin stringy corrections contain both spin-1 and spin-2 as we can see from the angular decomposition of t^2 in Eqn. (4.33) into the Wigner functions $d^1_{1,-1}(\cos\theta = 1 + 2t/s)$ and $d^2_{1,-1}(\cos\theta)$.

In the coincident-branes scenario, the KK contributions are argued to be suppressed by the string coupling [26] and therefore we expect to see the stringy low-energy effects before the KK's.

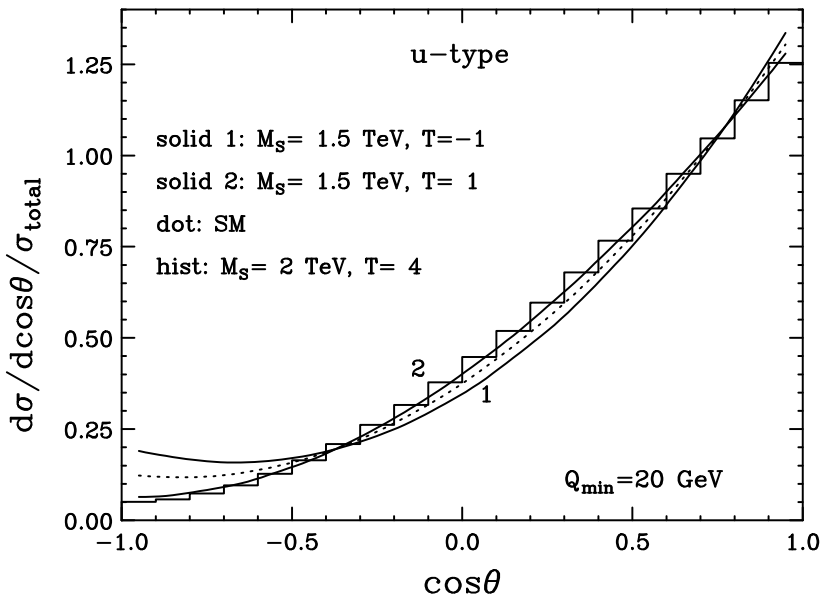

Figure 4.2: Normalized angular distribution for u-type quark final states

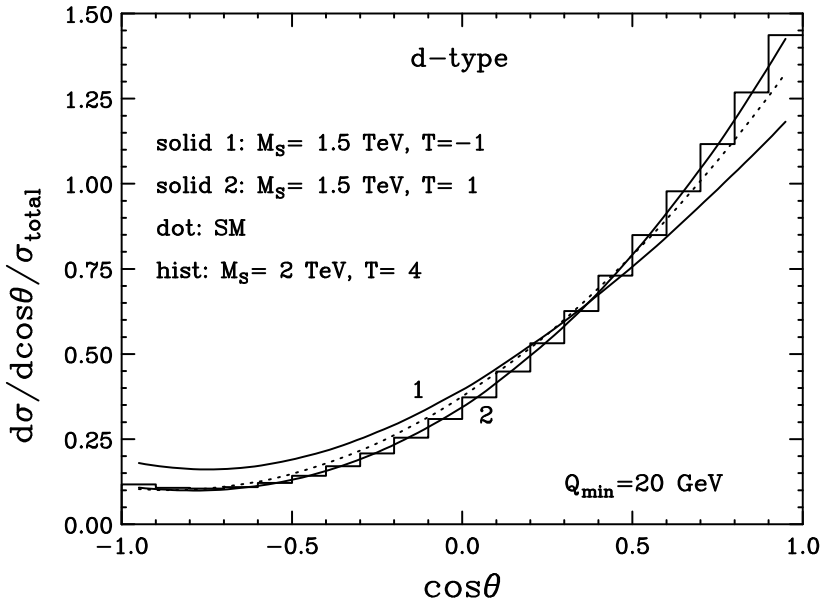

Figure 4.3: Normalized angular distribution for d-type quark final states

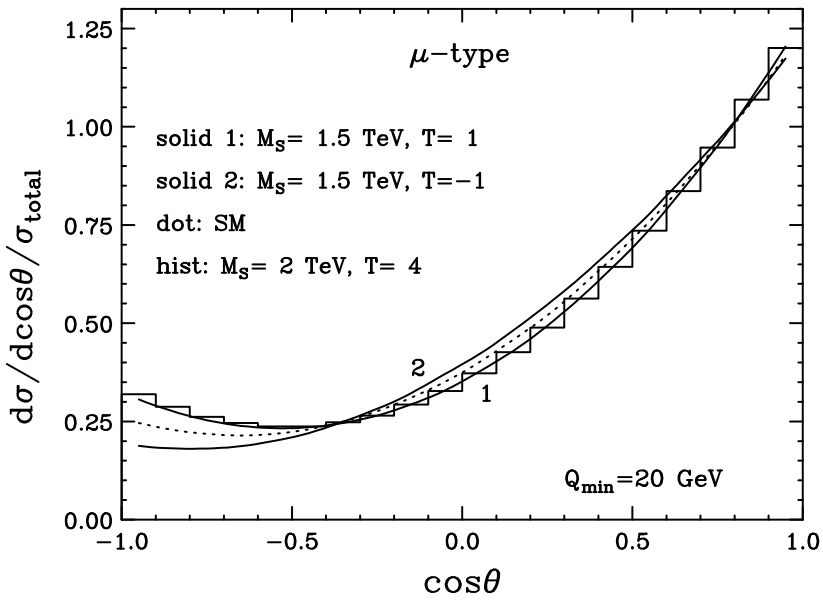

Figure 4.4: Normalized angular distribution for μ-type quark final states

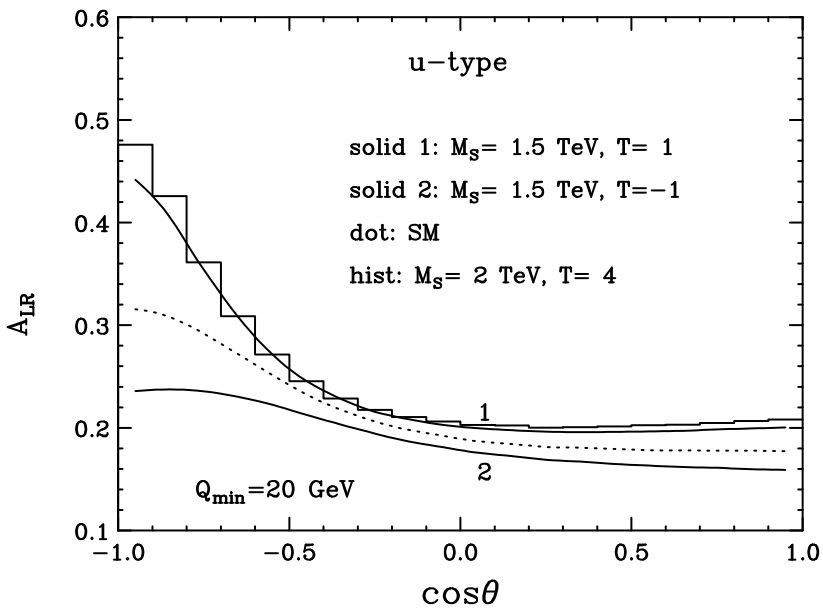

Figure 4.5: Angular Left-Right Asymmetry for u-type quark final states

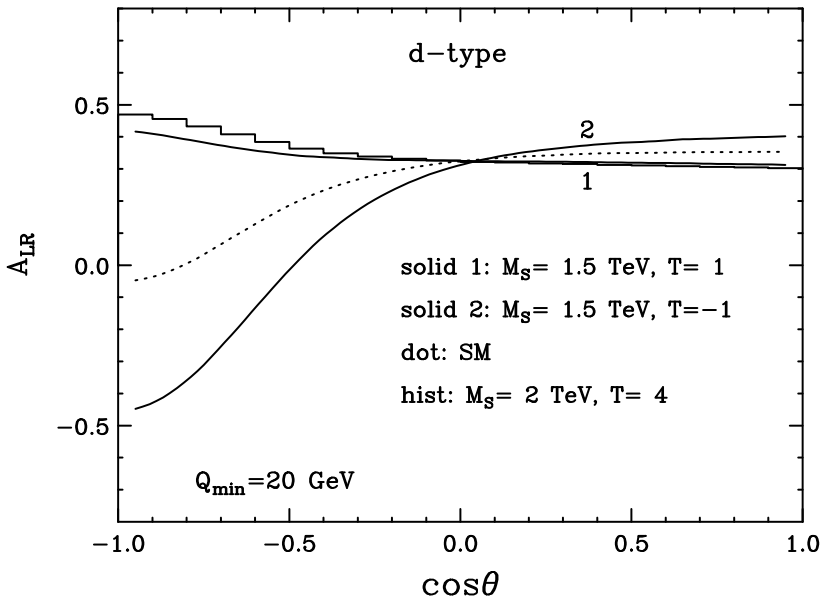

Figure 4.6: Angular Left-Right Asymmetry for d-type quark final states

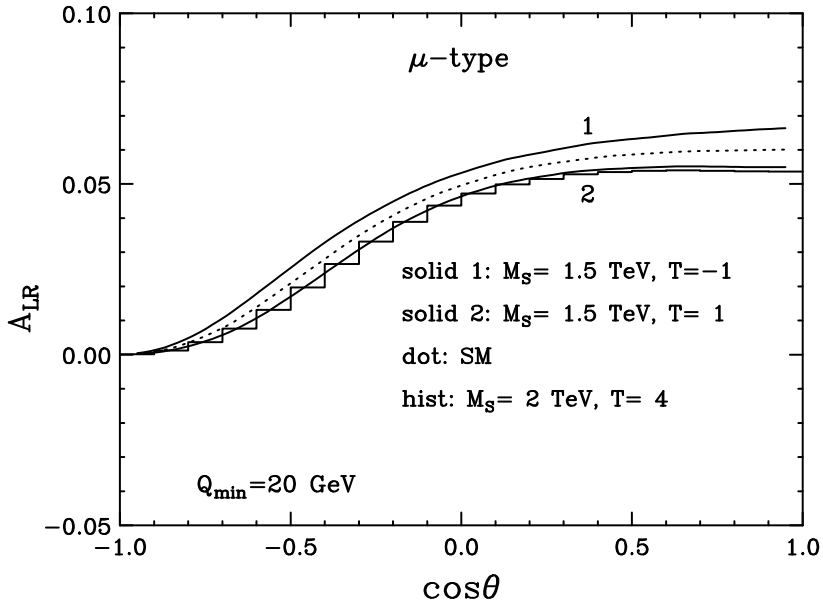

Figure 4.7: Angular Left-Right Asymmetry for μ-type quark final states

4.3 Similarity between Kaluza-Klein and Open-String Low-Energy Amplitudes

Scatterings in TeV-scale string scenarios have been proved to be phenomenologically viable. In these models [16, 26, 27, 81, 78, 17], gravity is naturally weakened due to freedom to propagate into extra dimensional direction in the bulk while standard model particles are identified as open string whose ends are confined to D-branes, usually assumed to be 3 dimensional. Since string theory requires ten dimensional spacetime and we have experimental limit on size of extra dimension $R < 200\ \mu$m[61], compactification is an inevitable. Boundary conditions of compactified dimensions discretize momenta perpendicular to brane and give rise to discrete spectrum of Kaluza-Klein(KK) excitations. Each standard model particle can be assigned to have a corresponding KK tower of states with the same 4 dimensional quantum numbers and masses roughly proportional to the inverse of size of the compactified radii of extra dimensions. Parallel to the brane, i.e. our matter universe, scattering of standard model particles is calculated as the open-string scattering amplitude[26, 27, 28, 81] with string coupling g_s identified as g_{YM}^2. As we approach higher energy, stringy behaviour of open-string scattering become visible, specifically contribution from string resonances(SR) become significant. We can calculate deviations from typical standard model amplitudes and put constraints on string scale, M_S, using experimental data from particle accelerators[26, 81].

In conventional Kaluza-Klein models where only graviton has KK modes being decomposed into spin-2,1, and 0[62], there are corrections to standard model amplitudes due to the exchange of graviton and KK excitations. Each mode of the KK contribution is suppressed by the Planck mass, M_{Pl}. These KK-states interact only weakly $\sim 1/M_{Pl}^2$

with particles on the brane. However, eventhough each KK exchange is suppressed by the Planck mass, when we sum over the tower of states from $1/R$ to M_D, the total contribution adds up to $\sim 1/M_D^4$ which could be in the range of the TeV-scale without being ruled out by previous experiments. This opens up possibility that there is an unobserved tower of KK-states with mass $\sim 1/R$ spanned in low energy ranging from less than 1 eV upto some cut off scale M_D.

In this section, we will show that in certain processes; such as diphoton production, there is remarkable similarity between amplitudes from SR and KK exchanges in both the angular distribution and the energy dependence aspects. Since SR amplitudes are calculated from the scattering of open strings on the brane while the KK amplitudes are extra-dimensional corrections from the bulk components of gravitons, their similarity is therefore something of curious nature. It also suggests that we might as well find two copies of similar contributions in the form of dimension-8 operator in future colliders for diphoton production processes.

4.3.1 Open-string amplitudes for diphoton production processes

Since all the relevant diphoton processes of KK model in ADD scenario have been calculated in ref. [63], we will calculate only open-string amplitudes for diphoton production. One of the processes which is of importance in an open-string model is scattering of two photons into two photons(4-photon scattering). There are two reasons for special interest in this process. First, the amplitude vanishes at the tree-level in standard QED; it is a 1-loop effect and thus is very weak. Secondly, since photon is identified with the $U(1)$ sector of any open-string models, its Chan-Paton matrix is always diagonal

and unique. Therefore the Chan-Paton factors(trace of four Chan-Paton matrices) can never be zero. This results in a universal form for the non-vanishing 4-photon scattering amplitude in open-string models with only one undetermined parameter, the string scale M_S. Constraints on the string scale from 4-photon scattering is therefore a definite and universal condition applicable to every model in braneworld scenario.

We will consider 4 possible initial 2-particle states that give diphoton final state, namely, $\gamma\gamma, q\bar{q}, gg$ and $\ell\bar{\ell}$.

4-photon scattering

The open-string tree-level amplitudes for 4-photon scattering can be expressed generically [26, 47, 49](see also Appendix) for each helicity combination as:

(1). $\gamma_\alpha\gamma_\alpha \to \gamma_\alpha\gamma_\alpha;\ \alpha = L, R$

$$A_{string} = ig^2 T \frac{s}{ut} f(s,t,u) \tag{4.34}$$

where $T \equiv T_{1234} = T_{1324} = T_{1243}$ are Chan-Paton factors and $f(s,t,u) \equiv uS(s,t) + sS(t,u) + tS(u,s)$; is (s,t,u)-symmetric function which vanishes in the low energy limit.

(2). $\gamma_\alpha\gamma_\beta \to \gamma_\alpha\gamma_\beta;\ \alpha, \beta = L, R;\ \alpha \neq \beta$

$$A_{string} = ig^2 T \frac{t}{us} f(s,t,u) \tag{4.35}$$

where $T \equiv T_{1234} = T_{1324} = T_{1243}$ are again Chan-Paton factors. For $\gamma_\alpha\gamma_\beta \to \gamma_\beta\gamma_\alpha(\alpha \neq \beta)$, we simply exchange $t \leftrightarrow u$ in the second case. Note that Chan-Paton factors for all helicity combinations are the same because the trace of a product of diagonal matrices does not depend on the ordering. Due to its Abelian nature, the massless photon is always represented by diagonal commuting(with respect to each other) matrices. In the low

energy approximation ($s,t,u \ll M_S^2; S(s,t) \approx 1 - \pi^2 st/6M_S^4, f(s,t,u) \approx -\pi^2 stu/2M_S^4$), these amplitudes give

$$\bar{\Sigma}|A_{string}|^2 = \frac{1}{8}(\pi^2 T g^2)^2 \frac{s^4+t^4+u^4}{M_S^8} \tag{4.36}$$

We will identify the coupling g with the QED coupling, e, since photon is associated with QED by definition.

Diphoton Production at the Tevatron

There are contributions from quark-antiquark and gluon-gluon initial states. First we consider quark-antiquark amplitudes:

(1). $q_\alpha \bar{q}_\beta \to \gamma_\alpha \gamma_\beta;\ \alpha,\beta = L,R;\ \alpha \neq \beta = L,R$

$$A_{string} = ig^2 \left[T_{1234} \frac{\sqrt{ut}}{s} + T_{1324}\sqrt{\frac{t}{u}} + T_{1243}\frac{t}{s}\sqrt{\frac{t}{u}} \right] \tag{4.37}$$

$$A_{QED} = 2ie^2 Q_q^2 \sqrt{\frac{t}{u}} \tag{4.38}$$

Matching with $g = e$ gives;

$$T_{1234} = T_{1243} \equiv T \tag{4.39}$$

$$T_{1324} = T + 2Q_q^2 \tag{4.40}$$

$$A_{string} = ie^2 T \frac{1}{s}\sqrt{\frac{t}{u}} f(s,t,u) + 2ie^2 Q_q^2 \sqrt{\frac{t}{u}} S(t,u) \tag{4.41}$$

(2). $q_\alpha \bar{q}_\beta \to \gamma_\beta \gamma_\alpha;\ \alpha,\beta = L,R;\ \alpha \neq \beta = L,R$

This is just $t \leftrightarrow u$ of the first case. Note that because two photons are Abelian to each other, Chan-Paton parameters, T, in both cases are exactly the same. With the same low-energy approximation as in 4-photon case, writing $A_{string} = A_{QED} + A_{cor}$, we have

$$\bar{\Sigma}|A_{string}|^2 = \frac{1}{3}(\frac{1}{4})\left(\Sigma|A_{QED}|^2 - 2\Sigma|A_{QED}||A_{cor}| + \Sigma|A_{cor}|^2\right) \tag{4.42}$$

where

$$\Sigma|A_{cor}|^2 = \frac{e^4}{4}(\frac{\pi^4}{9})(Q_q^2 + \frac{3}{2}T)^2(\frac{s^4}{M_S^8})(1-\cos^4\theta) \tag{4.43}$$

$$-2\Sigma|A_{QED}||A_{cor}| = -4e^4(\frac{\pi^2}{3})(Q_q^2 + \frac{3}{2}T)Q_q^2(\frac{s^2}{M_S^4})(1+\cos^2\theta) \tag{4.44}$$

$$\Sigma|A_{QED}|^2 = 16e^4Q_q^4(\frac{1+\cos^2\theta}{1-\cos^2\theta}) \tag{4.45}$$

with $u/s = -\frac{1}{2}(1+\cos\theta), t/s = -\frac{1}{2}(1-\cos\theta)$. We have also assume that all T's are color-blind and they are the same for every pair of quark-antiquark.

Now we turn to $gg \to \gamma\gamma$. Since the final state is color-neutral, the initial gluons must be a color singlet and therefore they must have opposite helicity.

(1). $g_\alpha g_\beta \to \gamma_\alpha\gamma_\beta$ with $\alpha, \beta = L, R, \alpha \neq \beta$.

$$A_{string} = ig^2T\frac{t}{us}f(s,t,u) \tag{4.46}$$

(2). $g_\alpha g_\beta \to \gamma_\beta\gamma_\alpha$ with $\alpha, \beta = L, R, \alpha \neq \beta$.

$$A_{string} = ig^2T\frac{u}{ts}f(s,t,u)(t \leftrightarrow u \text{ of above}) \tag{4.47}$$

We assume that Chan-Paton factors are independent of the helicity of initial gluons i.e. $tr(t_g^Lt_g^L) = tr(t_g^Lt_g^R) = tr(t_g^Rt_g^R)$. This is equivalent to the statement that the interaction is non-chiral. In this non-chiral case, all Chan-Paton factors are the same T. These amplitudes then give

$$\bar{\Sigma}|A_{string}|^2 = \frac{g^4\pi^4T^2}{64}(\frac{s^4}{M_S^8})\frac{1}{8}(1+6\cos^2\theta+\cos^4\theta) \tag{4.48}$$

The question of which coupling g should be identified with now arises. In standard model, the interaction is achieved by tree-level graviton exchange($\sim 1/M_{Pl}^2$) and through gauge interactions at one-loop level($\sim \alpha\alpha_s$). However, we are modelling stringy corrections to QED coupling and therefore we set $g = e$. Strange as it looks from the viewpoint of field theory considering there is no corresponding vertices to begin with, this is allowed in a string theoretic framework if $T \neq 0$. Scattering amplitude of this kind could be of the same order of magnitude as the 4-photon scattering. According to our expressions above, they are $1/M_S^4$-suppressed in low energy limit and they become larger as we approach M_S. At the Tevatron, these contributions from $gg \to \gamma\gamma$ would be of negligible size due to the low luminosity of gluons in the parton distribution functions of proton and antiproton [81].

Scattering of Dilepton into Diphoton

This is the same as $q\bar{q}$ initial state with $Q_q^2 = 1$. We will start off our comparison between open-string and Kaluza-Klein expressions by focussing on the electron-positron initial state. We can see the similarity between open-string, Eq. (4.43-4.44), and Kaluza-Klein cross-section formula, Eq. (9) of ref. [63]. By making the identification

$$\frac{M_D^4}{F} = \frac{M_S^4}{-\frac{\pi^2}{3}\alpha(Q_q^2 + \frac{3T}{2})} \tag{4.49}$$

$$= \frac{\Lambda_+^4}{2\alpha} \tag{4.50}$$

where $F = \log(M_D^2/s), 2/(n-2)$ for $n = 2, n > 2$ when n is the number of extra dimensions. M_D is mass cutoff in Kaluza-Klein model[62], and Λ_+ is the Drell's QED cutoff. Following statistical analysis of Cheung's [63], for example, at OPAL($\sqrt{s} = 189$

GeV), $\Lambda_+ > 345$ GeV, we have

$$M_S \;>\; 0.33 - 0.59 \text{ TeV for } T = (-1) - (-4). \tag{4.51}$$

Note that the same data gives $M_D > 0.98$ TeV for $n = 4$(number of extra dimensions). Considering the fact that M_D is related to the quantum gravity scale which is larger than string scale, M_S, generically, this result is consistent. The similarity between open-string and Kaluza-Klein amplitudes in this case is nevertheless not surprising as the first correction to the $e^+e^- \to \gamma\gamma$ is generated by a unique dimension-8 operator [26]. We therefore expect the same similarity in $q\bar{q} \to \gamma\gamma$ between Kaluza-Klein and open-string amplitudes and we will see that this is the case.

4.3.2 Comparison between open-string and Kaluza-Klein amplitudes

Exactly the same identification, Eq. (4.49) works in $q\bar{q} \to \gamma\gamma$ scattering. To translate the statistical analysis of Cheung's[63], we assume $Q_q^2 \approx 1/2$ to be the same for all quarks. For Tevatron Run II, $n = 4(M_D > 1.43$ TeV)

$$M_S \;\simeq\; (0.40 - 0.61)M_D \text{ for } T = (-1) - (-4) \tag{4.52}$$

$$M_S \;>\; 0.57 - 0.87 \text{ TeV for } T = (-1) - (-4) \tag{4.53}$$

This limit is consistent with the limit from dilepton production in [81].

Next we turn to the 4-boson cases, namely $gg \to \gamma\gamma$ and $\gamma\gamma \to \gamma\gamma$. In $gg \to \gamma\gamma$, Eq. (10) of ref. [63] has exactly the same energy-dependence and angular distribution as Eq. (4.48) for the open-string case, the correspondence is

$$\frac{F}{M_D^4} \;=\; \pm\frac{\frac{\pi^2}{2}T\alpha}{M_S^4} \tag{4.54}$$

For the 4-photon scattering, comparing Eq. (6.18) with Eq. (5) of [63], we have the correspondence

$$\frac{F}{M_D^4} = \pm\frac{\frac{\pi^2}{4}T\alpha}{M_S^4} \tag{4.55}$$

The scattering of 2 photons into 2 photons is forbidden at tree-level of QED. The first non-zero QED-contribution comes from one-loop fermion scattering. In open-string models, however, the tree-level QED-strength string-amplitudes are generically non-zero. Assignment of a diagonal matrix to the photon is unique and the trace of the product of four matrices is non-vanishing in any $U(n)$ and therefore the amplitude does exists at tree-level. The low value of these tree-level amplitudes, Eq. (4.34-4.35), is a result of s, t, u symmetry in open-string amplitude.

In this aspect, 4-photon scattering is special; any open-string model gives a non-zero tree-level($\simeq \alpha$) amplitude for the process and the cross-section increases with energy. Moreover, the background from α^2-terms in QED is reduced as energy increases (Fig. 1 of [63]) in the energy range we can probe in current and future colliders. Limits on lower bound of string scale M_S obtained from 4-photon scattering would be universal for every open-string model and it would be used as the standard normalization for the value of Chan-Paton parameters.

4.3.3 Understanding string-KK Similarity in Diphoton production

The open-string amplitudes we use are the formula for scattering of 4 particles through gauge bosons exchange extended to string scattering by Veneziano extension(i.e. multiplying the corresponding channel by $S(s,t), S(t,u)$ and $S(u,s)$). For massless external

particles, the amplitudes are factorized into three distinct helicity combinations. Each one approaches different field-theory limits in low energy corresponding to $1/s, 1/t$ and $1/u$ gauge-boson propagators[49]. In other words, the 0th resonance of the formula corresponds to gauge-boson(spin-1) exchange in field theory expansion. String correction comes in as exchange of higher spin states as we see from

$$S(s,t) \simeq 1 - \frac{\pi^2}{6}(\frac{st}{M_S^4}) \tag{4.56}$$

where string correction is the 2nd term in the expression. Additional power of t in the numerator of the correction term brings an additional spin state to the intermediate state. In this case, there is spin-2 exchange in addition to the spin-1(gauge boson) exchange due to the correction term. Notably, $S(t,u)$ brings in 1 and 2 additional spins since $u = -s - t$ and $ut = -st - t^2$ and we will end up with spin-1,2 and 3 exchange in the amplitude containing single $S(t,u)$ term.

From the above general argument, we analyze the diphoton production processes. To illustrate important point, we first consider the 4-photon scattering. As we see from Eq. (4.34-4.35), at low energy, the first-order amplitudes are proportional to $s/t, s/u$ and $u/s, u/t$(they add up to zero in each helicity case at the leading order before string corrections) and therefore appear to have spin-1 exchange contributions. However Yang's theorem[64] implies that these contributions actually are spin-0 components of gauge boson exchange as we can see easily from explicitly writing down tree-level Feynman diagrams. Therefore the string corrections add spin exchange up to spin-2 for each helicity combination, proportional to s^2, t^2 and u^2 respectively. After the corrections, Yang's theorem again prevents spin-1 exchange after the string corrections and we are left with only spin-2 exchange(since the original spin-0 scattering vanishes without string corrections).

The same argument applies to other processes with diphoton final state, they start with only spin-0 exchange before string corrections and end up with spin-2 exchange and original SM-exchange(processes such as $q\bar{q}, e^+e^- \to \gamma\gamma$ have non-vanishing SM part that remains) after string corrections. Low-energy open-string corrections of amplitudes for diphoton production thus are spin-2 exchange in nature. On the other hand, KK corrections in conventional KK model[62] are naturally spin-2 exchange. It was shown by Feynman, Kraichnan, and Weinberg[65] that Lorentz-invariant CPT-preserved spin-2 exchange interaction is unique and similarity between open-string and Kaluza-Klein in diphoton production is a manifestation of this. The only difference between them is the strengths of couplings. Gravitational(KK) is much weaker than SR-extended QED interaction due to different spaces of propagation. Summation over KK tower amplifies KK contribution to somewhat the same scale as SR contribution. In some regions of parameter space, we therefore expect to have two copies of dimension-8 operators correcting standard model amplitudes. The scale could be as low as 1 TeV due to previous estimations[26, 81] and our current results.

4.3.4 Conclusions

Tree-level open-string scattering amplitudes of various diphoton production processes have been calculated with unspecified Chan-Paton parameters. With the assumption of nonchiral interaction, we found remarkably similar forms(for both energy dependence and angular distribution) between low energy open-string scattering amplitudes and diphoton production amplitudes via graviton exchange in Kaluza-Klein model regardless of the fact that one is confined to D3brane and the other propagates freely in the bulk. Applying the low energy constraints on mass scale of one model to another is therefore

allowed and we extract some constraints on string scale M_S from constraints on M_D in KK model. We found an agreement(somewhat weaker) with other constraints on M_S from the 4-fermion processes[81], about $0.6 - 0.9$ TeV. Also we emphasize that the 4-photon interaction is unique and universal in every open-string model as well as it is phenomenologically clean from SM background.

Caution thus has to be made when doing new physics analysis on diphoton production. There could be two copies of exactly the same form of corrections to SM amplitudes, one from SR(low E) and one from KK(tower of states). In some cases of low-scale string scenario with large compatified extra dimension, the SR corrections to SM amplitudes will be dominant and they will show up first since KK-graviton exchange is more suppressed by higher power of coupling[26]. KK-graviton exchange will also show up as smaller contributions with exactly the same angular distribution and energy dependence at a somewhat higher scale($M_D > M_S$). However, it is also possible that the string scenario is of much higher scale or not valid at all, in which case we might find only one copy of corrections to SM diphoton amplitudes coming from conventional field theoretic KK exchange. In the intermediate kinematic region(100 GeV $< E < M_S, M_D$), we need cross-check from other channels like the 4-fermion scattering to distinguish between signals from SR and signals from KK models. As we go to higher energy($E > M_S$), since we can investigate the resonances directly, the detailed energy and angular distributions at the resonances will determine whether it is SR or KK exchange with more certainty[66].

Chapter 5

TeV-Scale String Resonances at Hadron Colliders

String theory [43] remains to be the leading candidate to incorporate gravity into a unified quantum framework of the elementary particle interactions. The string scale (M_S) is naturally close to the quantum gravity scale $M_{\rm Pl} \approx 10^{19}$ GeV, or to a grand unification (GUT) scale $M_{GUT} \approx 10^{17}$ GeV [44]. It has been argued recently that the fundamental string scale can be much lower [45]. With the existence of large effective volume of extra dimensions beyond four, the fundamental quantum gravity scale may be as low as a TeV. This is thought to have provided an alternative approach to the hierarchy problem [16, 17], namely the large gap between the electroweak scale $\mathcal{O}(100$ GeV) and the Planck scale of $M_{\rm Pl}$. What is extremely interesting is that these scenarios would lead to very rich phenomenology at low energies in particle physics [25, 30, 26] and astroparticle physics [46, 27, 28] that may be observable in the next generation of experiments.

One generic feature of string models is the appearance of string resonances (SR) in scattering of particles in the energy region above the string scale. The scattering amplitudes are of the form of the Veneziano amplitudes [43, 47, 26], which may develop simple poles. In the s-channel, the poles occur at $\sqrt{s} = \sqrt{n}M_S$ $(n = 1, 2, \ ...)$ with degeneracy for different angular momentum states. It has been argued [25, 26] that the scattering involving gravitons (closed strings) is perturbatively suppressed by higher power of string coupling with respect to the open-string scatterings which therefore are the dominant phenomena at energies near and above the string scale.

In this section, we consider the possibility of producing the string resonances of a TeV-scale mass and studying their properties at colliders. We adopt the simplest open-string model in the D-brane scenario [47, 26]. It is assumed that all standard model (SM) particles are identified as open strings confined to a D3-brane universe, while a graviton is a closed string propagating freely in the bulk. For a given string realization of the SM, one should be able to calculate the open-string scattering amplitudes, in particular the Chan-Paton factors [19] that are determined by the group structure of the particle representations and their interactions. Unfortunately, there is no fully satisfactory construction of the SM from string theory and we are thus led to parameterize our ignorance. We demand that our stringy amplitudes reproduce the SM amplitudes at low energies. The zero-modes of the scattering amplitudes are all identified as the massless SM particles and no new exotic states of the zero-modes are present. By taking Chan-Paton factors to be free parameters, a non-trivial stringy extension of the SM amplitudes to a higher energy region is accomplished by a unique matching between stringy amplitudes and those of the SM at low energies.

In fact, this scheme has been exploited in some earlier works. These include possible low-energy effects from the string amplitudes on four-fermion interactions [81], and searching for signals in cosmic neutrino interactions [27, 28]. In this paper, we explore the search and detailed study of their properties for these string resonances at hadron colliders such as the Fermilab Tevatron and the CERN Large Hadron Collider (LHC). In the string models, we expect a series of resonances with a predicted mass relation $\sqrt{n}M_S$ $(n = 1, 2, \ ...)$. Moreover, the angular distributions of the SR signals in parton-parton c.m. frame present distinctive shapes in dileptonic and diphotonic channels due to the angular momentum decomposition. Rather small forward-backward asymmetry is another feature of the model. These are all very unique and remarkably specific in contrast to signals from other sources of new physics. It is found that the LHC experiments may be sensitive to a string scale of $M_S \sim 8$ TeV.

The rest of the section is organized as follows. We first construct tree-level open-string scattering amplitudes for the dileptonic and diphotonic production processes in Sec. 5.0.5, which reproduce the SM amplitudes at low energies and extend to include string resonances. In Sec. 5.0.6, string resonance approximation is discussed and each string resonance is expanded into partial waves to see their angular momentum states. Using the Z' constraints at the Tevatron, lower bounds on the string scale are obtained in Sec. IV. The analysis at the LHC is carried out in Sec. V. We summarize in Sec. VI our results and emphasize the generic features and profound implications of the amplitude construction. The complete expressions for the scattering amplitudes and the decay widths are given in two appendices.

5.0.5 Construction of open-string amplitudes

The 4-point tree-level open-string amplitudes can be expressed generically [43, 47, 26]

$$A_{string} = S(s,t)\ A_{1234}\ T_{1234} + S(t,u)\ A_{1324}\ T_{1324} + S(u,s)\ A_{1243}\ T_{1243} \tag{5.1}$$

where (1, 2, 3, 4) represents external massless particles with incoming momenta. A_{ijkl} are kinematic parts for $SU(N)$ amplitudes [49], which are given in Appendix A. The Mandelstam variables at parton level are denoted by s, t and u. For physical process ($12 \to 34$), the s, t and u-channels are labeled by (1,2), (1,4) and (1,3), respectively. T_{ijkl} are the Chan-Paton factors and in the usual construction,

$$T_{1234} = tr(\lambda_1\lambda_2\lambda_3\lambda_4) + tr(\lambda_4\lambda_3\lambda_2\lambda_1). \tag{5.2}$$

Following Ref. [49], we adopt the normalization of $tr(\lambda_a\lambda_b) = \delta_{ab}$. Since a complete string model construction for the electroweak interaction of the standard model is unavailable, we will assume that these Chan-Paton factors are free parameters and T_{ijkl} is typically in range of -4 to 4. $S(s,t)$ is essentially the Veneziano amplitude

$$S(s,t) \quad = \quad \frac{\Gamma(1-\alpha' s)\Gamma(1-\alpha' t)}{\Gamma(1-\alpha' s-\alpha' t)} \tag{5.3}$$

where the Regge slope $\alpha' = M_S^{-2}$, and the amplitude approaches unity as either s/M_S^2 or $t/M_S^2 \to 0$.

Of special interests for this article are the $2 \to 2$ processes that may lead to clear experimental signatures at the Tevatron and LHC. We thus concentrate on two clean channels: the Drell-Yan (DY) dilepton production ($\ell\bar{\ell}$) and the diphoton production ($\gamma\gamma$), from $q\bar{q}$ annihilation and possibly gluon-gluon fusion. In this section, we explicitly construct the string amplitudes for these production processes.

Dilepton Production

At hadron colliders, the $2 \to 2$ dilepton production processes are $q\bar{q}, gg \to \ell\bar{\ell}$. The tree-level process for $gg \to \ell\bar{\ell}$ is absent in the SM. In the massless limit of the fermions, we label their helicities by the chirality $\alpha, \beta = L, R$. For the process with initial state $q\bar{q}$, we have two cases depending on the helicity combination of the final state leptons. The non-vanishing amplitudes are those for $\alpha \neq \beta$. The external particle ordering is $(12 \to 34)$.

(A1). $q\bar{q}$ annihilation $q_\alpha \bar{q}_\beta \to \ell_\alpha \bar{\ell}_\beta$:

With the notation as in Appendix A, this process belongs to a type of $f^\pm f^\mp f^\mp f^\pm$, with $\pm$ denoting the helicity of the particle with respect to incoming momentum. Our construction thus leads to the physical amplitude

$$A_{string}(q_\alpha \bar{q}_\beta \to \ell_\alpha \bar{\ell}_\beta) = ig^2 \left[T_{1234} S(s,t) \frac{t}{s} + T_{1324} S(t,u) \frac{t}{u} + T_{1243} S(u,s) \frac{t^2}{us} \right]. \tag{5.4}$$

The corresponding standard model amplitude is via the electroweak interaction,

$$A_{SM} \;=\; ig_L^2 \frac{t}{s} F_{\alpha\alpha}, \tag{5.5}$$

where the photon and Z contributions are given by

$$F_{\alpha\beta} = 2Q_\ell Q_q x_{\rm w} + \frac{s}{s - m_Z^2} \frac{2 g_\alpha^\ell g_\beta^q}{1 - x_{\rm w}}. \tag{5.6}$$

Here $x_{\rm w} = \sin^2\theta_W$ and the $SU(2)_L$ coupling $g_L = e/\sin\theta_W$. The neutral current couplings are $g_L^f = T_{3f} - Q_f x_{\rm w},\ g_R^f = -Q_f x_{\rm w}$.

The crucial assumption for our approach is to demand the string expression Eq. (6.15) to reproduce the standard model amplitude in the low-energy limit when $s/M_S^2 \to 0$. This can be achieved by identifying the string coupling with the gauge coupling $g = g_L$,

and matching the Chan-Paton factors T_{ijkl} as

$$T_{1243} = T_{1324} \equiv T; \quad T_{1234} = T + F_{\alpha\alpha}. \tag{5.7}$$

We then obtain the full result

$$A_{string}(q_\alpha \bar{q}_\beta \to \ell_\alpha \bar{\ell}_\beta) = i g_L^2 S(s,t) \frac{t}{s} F_{\alpha\alpha} + i g_L^2 T \frac{t}{us} f(s,t,u), \tag{5.8}$$

$$f(s,t,u) = uS(s,t) + sS(t,u) + tS(u,s). \tag{5.9}$$

For simplicity, we will take the Chan-Paton parameter T to be positive and $0 \leq T \leq 4$. Taking T to be negative will not change our numerical results appreciably.

A few interesting features are worthwhile commenting. First, we see that the string amplitude Eq. (6.18) consists of two terms: one proportional to the SM result multiplied by a Veneziano amplitude $S(s,t)$; the other purely with string origin proportional to an unknown Chan-Paton parameter T. In the low-energy limit $s \ll M_S^2$, $f(s,t,u) \to s + t + u = 0$, reproducing the SM result regardless of T. This implies that T cannot be determined unless one specifies the detailed embedding of the SM to some more generalized group structure in a string setup. The seemingly disturbing fact is that one of the Chan-Paton factors T_{1234} must be made dependent upon the Z-pole, rather than pure gauge couplings. This reflects our ignorance of treating the electroweak symmetry breaking in our approach.

As for the other helicity combination $q_\alpha \bar{q}_\beta \to \ell_\beta \bar{\ell}_\alpha$, it belongs to the class of $f^\pm f^\mp f^\pm f^\mp$. We apply the same methods as stated above and find the crossing relation $t \leftrightarrow u$ and an index interchange in the F factor,

$$A_{string}(q_\alpha \bar{q}_\beta \to \ell_\beta \bar{\ell}_\alpha) = i g_L^2 S(s,u) \frac{u}{s} F_{\beta\alpha} + i g_L^2 T \frac{u}{ts} f(s,t,u). \tag{5.10}$$

with $T \equiv T_{1234} = T_{1324}$.

(A2). Gluon fusion $g_\alpha g_\beta \to \ell_\alpha \bar{\ell}_\beta$:

In our open-string model, there is the possibility of dilepton production via two initial state gluons. This amplitude vanishes at tree-level in the standard model, but could be non-zero in the open-string model if the gluons and leptons belong to some larger gauge group in which the Chan-Paton trace is non-vanishing. The amplitude belongs to a type of $g^\pm g^\mp f^\mp f^\pm$ according to Appendix A. With $T \equiv T_{1234} = T_{1324} = T_{1243}$, the result reads

$$A_{string}(g_\alpha g_\beta \to \ell_\alpha \bar{\ell}_\beta) = i g_L^2 T \frac{1}{s}\sqrt{\frac{t}{u}}\, f(s,t,u), \tag{5.11}$$

where T may be different for each helicity combination of external particles. In fact, there exists an intrinsic ambiguity for the string coupling identification since there are both strong interaction and electroweak interaction involved simultaneously. Coupling identification for this subprocess would not be determined without an explicit string model construction. This problem is beyond the scope of this article. To be conservative, we have identified the string coupling with the weak coupling g_L.

For $g_\alpha g_\beta \to \ell_\beta \bar{\ell}_\alpha$, we have $t \leftrightarrow u$ of the above expression.

Diphoton Production

Another clean signal in addition to dilepton production at hadron colliders is the diphoton final state. We therefore construct the string amplitudes for diphoton processes in this section. We again label the helicities by α, β, and as in the dileptonic processses, the non-vanishing amplitudes are those with $\alpha \neq \beta$.

(B1). $q\bar{q}$ annihilation $q_\alpha \bar{q}_\beta \to \gamma_\alpha \gamma_\beta$:

Using the kinematic amplitudes for fermions and gauge bosons $f^\mp f^\pm g^\pm g^\mp$ as given in Appendix A and the matching techniques between the string and SM amplitudes

described in the previous section, we obtain the following open-string amplitudes for $T \equiv T_{1234} = T_{1243}$,

$$A_{string}(q_\alpha \bar{q}_\beta \to \gamma_\alpha \gamma_\beta) = 2ie^2 Q_q^2 \sqrt{\frac{t}{u}} S(t,u) + ie^2 T \frac{1}{s} \sqrt{\frac{t}{u}}\ f(s,t,u), \tag{5.12}$$

which correctly reproduce SM amplitudes at low energies, given by the first term. For the other helicity combination $\gamma_\beta \gamma_\alpha$, the amplitude can be obtained by $t \leftrightarrow u$.

(B2). Gluon fusion $g_\alpha g_\beta \to \gamma_\alpha \gamma_\beta$:

Identifying this process with $g^\pm g^\mp g^\mp g^\pm$, one has

$$A_{string}(g_\alpha g_\beta \to \gamma_\alpha \gamma_\beta) = ie^2 T \frac{t}{us} f(s,t,u). \tag{5.13}$$

with $T \equiv T_{1234} = T_{1324} = T_{1243}$. Note that this amplitude is of purely stringy origin. There exists the same ambiguity for the string coupling identification as in $gg \to \ell\bar{\ell}$. To be conservative, we have matched the string coupling with the electromagnetic interactions.

For the other helicity combination $\gamma_\beta \gamma_\alpha$, the amplitude can be obtained by $t \leftrightarrow u$.

5.0.6 String Resonances and Partial Waves Expansion

The factor $\Gamma(1 - s/M_S^2)$ in the Veneziano amplitude develops simple poles at $s = nM_S^2$ $(n = 1, 2, 3...)$, implying resonant states with masses $\sqrt{n} M_S$. At energies near the string scale, string resonances thus become dominating. One can perform a resonant expansion,

$$S(s,t) \approx \sum_{n=1}^{\infty} \frac{t(\frac{t}{M_S^2} + 1)...(\frac{t}{M_S^2} + n - 1)}{(n-1)!(s - nM_S^2)}. \tag{5.14}$$

Thus, by neglecting $S(t,u)$ which does not contain s-channel poles,

$$f(s,t,u) = uS(s,t) + sS(t,u) + tS(u,s)$$

$$\approx \; 2 \sum_{n=\text{odd}}^{\infty} \frac{ut(\frac{t}{M_S^2}+1)...(\frac{t}{M_S^2}+n-1)}{(n-1)!(s-nM_S^2)}. \tag{5.15}$$

It is a remarkable result that this purely stringy function $f(s,t,u)$ has only odd-n SRs due to the crossing symmetry between t and u. It represents the stringy effects of spin-excitations along the string worldsheet, which are suppressed at low energy. These are the generic features of stringy effects we wish to explore at the high energy experiments.

String Resonances in Dileptonic and Diphotonic Amplitudes

The open-string amplitude construction for Drell-Yan processes predicts the existence of exotic intermediate states such as leptoquarks in the u-channel and higher spin bosonic excitations in the s-channel as string resonances. Due to the limited c.m. energy accessible at collider experiments, we need to keep only the first few resonances. Applying the general results of Eqs. (5.14) and (6.32) to the dilepton string amplitudes, we obtain the amplitude formula for the first two resonances, with θ defined as angle between initial quark and final anti-lepton in the parton c.m. frame,

$$A_{SR}(q_\alpha \bar{q}_\beta) \approx \begin{cases} ig_L^2 \frac{(1-\cos\theta)^2}{4} \left[\frac{s}{s-M_S^2}(F_{\alpha\alpha}+2T) + \frac{s}{s-2M_S^2} F_{\alpha\alpha}\cos\theta \right] & \text{for } \ell_\alpha \bar{\ell}_\beta \\ \\ ig_L^2 \frac{(1+\cos\theta)^2}{4} \left[\frac{s}{s-M_S^2}(F_{\beta\alpha}+2T) - \frac{s}{s-2M_S^2} F_{\beta\alpha}\cos\theta \right] & \text{for } \ell_\beta \bar{\ell}_\alpha. \end{cases}$$

The full amplitude then will appear as a sum

$$A \approx A_{SM} + A_{SR}. \tag{5.16}$$

A few remarks on the amplitudes are in order. Firstly, even we set free Chan-Paton parameter T to zero, there are still contributions from string resonances. This can be seen from the Veneziano factor multiplying to the SM term in the string formula.

Significant differences from the standard model cross sections can be expected if the string scale is accessible at future colliders. Second, the amplitude for the first (odd-n) string resonance depends on the Chan-Paton parameter T, while the second (even-n) resonance does not. The even resonances are completely determined by the gauge factors F in the standard model.

In the string model, there is a possible contribution from gluon fusion to lepton pairs, as seen in Eq. (5.11). Near the string resonance, we have

$$A_{SR}(g_\alpha g_\beta) \approx i g_L^2 T \, \frac{s}{s - M_S^2} \, \frac{1 \mp \cos\theta}{2} \sin\theta, \tag{5.17}$$

where the sign " $-$ " corresponds to $g_\alpha g_\beta \to \ell_\alpha \bar{\ell}_\beta$, and " $+$ " to $\ell_\beta \bar{\ell}_\alpha$ with $\alpha \neq \beta$. There are only odd-n string resonances from this gluon contribution. This is generic for any processes if the standard model amplitude vanishes at tree-level. It is always proportional to the function $f(s,t,u)$ which vanishes in the low energy limit, which only has odd-n resonances. As a comparison, for processes with the non-vanishing amplitudes in standard model at tree-level, their open-string amplitude will most likely contain both odd- and even-n SRs.

The only exception is when the stringy correction piece multiplying to the standard model amplitude is $S(t,u)$ which does not contain SR pole in the s-channel. This occurs naturally when the zero-mode (SM) tree-level exchange is in t or u but not in the s channel. We can see from the list in Appendix A that A_{1324}, to be multiplied with $S(t,u)$ in the full amplitude expression, never contain s-channel pole. This is consistent with the physical picture that SR is the spin excitation of the zero-mode intermediate state. If the zero-mode (SM) intermediate state does not exist, then there will not exist SR interacting with the same gauge charges. An example of this kind of processes is $q\bar{q} \to \gamma\gamma$ which we can see from Eq. (5.12). For diphoton production, there are thus

only odd-n string resonances. The first SR ($n = 1$) for both processes are

$$A_{SR}(q_\alpha \bar{q}_\beta \to \gamma_\alpha \gamma_\beta) = ie^2 T \frac{s}{s - M_S^2} \frac{1 - \cos\theta}{2} \sin\theta, \tag{5.18}$$

$$A_{SR}(g_\alpha g_\beta \to \gamma_\alpha \gamma_\beta) = 2ie^2 T \frac{s}{s - M_S^2} \frac{(1 - \cos\theta)^2}{4}. \tag{5.19}$$

The expressions for opposite helicity combinations ($\gamma_\beta \gamma_\alpha$) are given by $\theta \to \pi - \theta$. Observe that SR coupling is proportional to T which is completely undetermined. We will include these $n = 1$ resonances and ignore those of $n = 3$ in our LHC analysis for the diphoton signals.

Partial Waves Expansion of String Resonances

There is degeneracy of states with different angular momenta at each SR as can be seen from the dependence on different powers of t for each n in Eq. (5.14). Generically, any amplitude $A(s, t)$ can be expanded in terms of the Wigner functions $d^j_{mm'}(\cos\theta)$ [15] as

$$A(s, t) = 16\pi \sum_{j=M}^{\infty} (2j + 1) a_j(s) d^j_{mm'}(\cos\theta) \tag{5.20}$$

where $M = \max(|m|, |m'|)$, and $a_j(s)$ are the partial wave amplitudes corresponding to a definite angular momentum state j.

For our purpose, we expand the SR amplitudes for each mass eigenstate of a given n by the Wigner functions as in Table 5.1.

It becomes clear that the different angular momentum states will lead to very distinctive angular distributions of the final state leptons for the SR signals and may serve as important indicators in exploring the resonance properties. To regularize the poles, the decay widths have been included. The coefficients α^j_n, decay widths Γ^j_n, and the relevant Wigner functions are given in Appendix B.

5.0.7 Bounds on the String Scale from the Tevatron

At the Fermilab Tevatron, the clean channels of dileptons and diphotons have been actively searched for. The CDF collaboration has been searching for a Z' gauge boson in the dilepton channel and a lower bound $M_{Z'} > 690$ GeV had been set based on their Run I data [50] for a neutral gauge boson with SM-like couplings. Similar results were obtained by the D0 collaboration [51]. The non-existence of a signal put an upper bound on the production cross section and can thus be translated to stringent constraints on the string scale.

Using CTEQ5L parton distribution functions [52] , we estimate the total cross-sections for the string resonance signatures at various string scales with $T = 1 - 4$. Since there is degeneracy of state with different angular momenta at the same mass, we use partial wave expansion to split each SR pole. We regulate the resonance pole by including the decay width of each angular momentum state separately. The detailed treatment for the width calculation is given in Appendix B. For instance, for $M_S = 1$ TeV, $n = 1$ and $T = 1$, the widths of SR in the Drell-Yan process are 240 (48) GeV for $j = 1$ (2), while the width of SR in $gg \to \ell\bar{\ell}$ is 19 GeV with the only $j = 2$ state. When we compare with Tevatron data on their Z' search, we need only the first SR, the lightest state (including the angular momentum degeneracy).

In Figure 5.1, we present the total cross section for the DY process ($\ell = e, \mu$) via the SR versus its mass M_S, for different values of the Chan-Paton parameter $T = 0 - 4$ as shown by the solid curves. Both contributions from $q\bar{q}$ and gg are taken into account. To extract the lower bound on the string scale, we have simulated the experimental acceptance cuts on the invariant mass of the lepton pair, transverse momentum of the

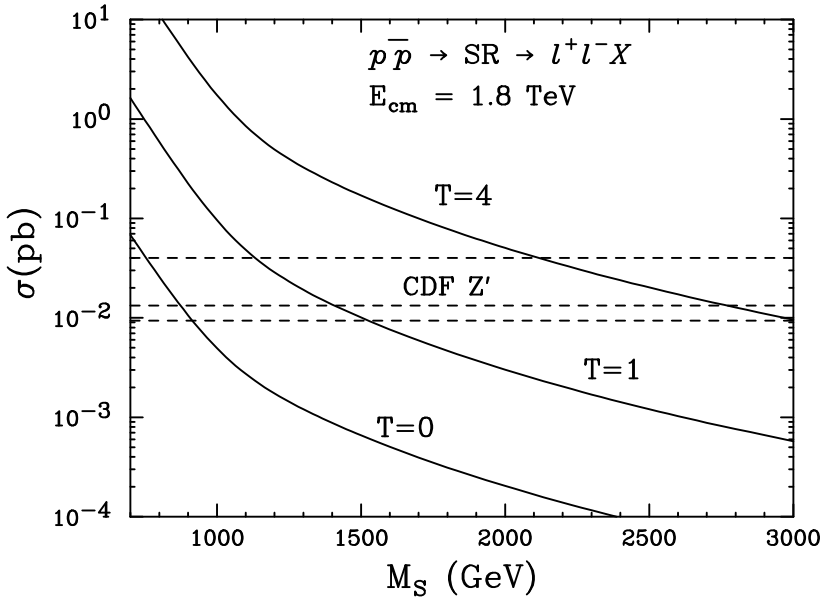

Figure 5.1: Total cross section for the DY process ($\ell = e, \mu$) via the SR versus its mass M_S, for different values of $T = 0 - 4$ (the solid curves). Detector acceptance cuts of Eq. (5.21) have been imposed. The horizontal dashed lines show the 95% C.L. upper bound on $\sigma(Z')B(Z' \to \ell\ell)$ for integrated luminosities 110 pb^{-1}, 1 fb^{-1} and 2 fb^{-1}, respectively.

leptons, and their rapidity to be

$$M(\ell\ell) > 50 \text{ GeV}, \quad p_T(\ell) > 18 \text{ GeV}, \quad |y_\ell| < 2.4. \tag{5.21}$$

We extrapolate CDF result [50] of 110 pb^{-1} on the Z' mass bound at 95% C.L. through dilepton production to a higher mass scale to obtain an upper bound on the production cross section, as shown by the horizontal dashed lines, corresponding to different integrated luminosities, 110 pb^{-1}, 1 fb^{-1} and 2 fb^{-1}, respectively. The intersections between the top horizontal line from the extrapolated data and the curves calculated for string resonances are located at $1.1 - 2.1$ TeV for $T = 1 - 4$, and thus yield the current

lower bound on M_S. This gives a stronger bound for the string scale than that based on a contact interaction analysis [81]. A bound obtained from the diphoton final state is weaker than that from the DY process, and we will not present it here.

In the near future with an integrated luminosity of 2 fb^{-1} at the Tevatron, one should be able to extend the search to $M_S \sim 1.5 - 3$ TeV for $T = 1 - 4$, as indicated in Fig. 5.1. It is interesting to note that even for $T = 0$, one still has some sensitivity at the Tevatron, reaching $M_S \sim 1$ TeV.

5.0.8 String Resonances at the LHC

At the LHC, operating at $E_{cm} = 14$ TeV with an expected luminosity of 300 fb^{-1}, could produce a sufficiently large number of events induced by SRs with masses of several TeV. We will first present various aspects of dilepton and diphoton SR-induced signals in comparison with the expected SM backgrounds. Then we will proceed to set the lower bound on the string scale if we do not see any SR-induced signals at the LHC. For illustration, we take a fixed string scale of $M_S = 2$ TeV and $T = 1$. All of the processes are calculated with the minimal acceptance cuts on the final state particles of leptons and photons

$$p_T > 20 \text{ GeV}, \quad |y| < 2.4. \tag{5.22}$$

To be more realistic in generating the resonant structure, we smear the particle energies according the electromagnetic calorimeter response with a Gaussian distribution

$$\frac{\Delta E}{E} = \frac{5\%}{\sqrt{E/\text{GeV}}} \oplus 1\%. \tag{5.23}$$

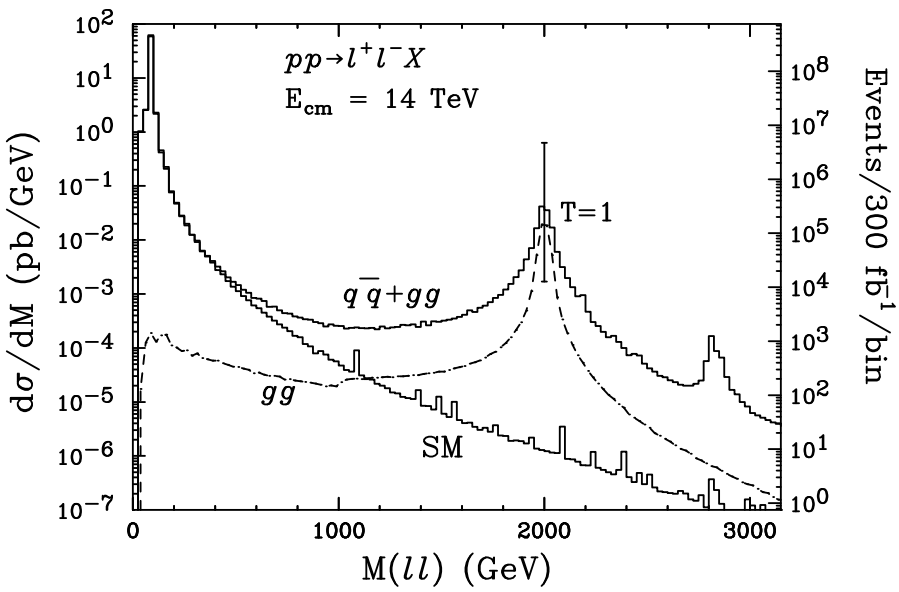

Figure 5.2: Invariant mass distributions for DY dilepton production at the LHC, for the continuum SM expectation and the SR contributions with $M_S = 2$ TeV and $T = 1$: $q\bar{q} + gg$ (top curve) and gg only (dashed). The vertical bar at the $n = 1$ SR peak indicates the enhancement for $T = 4$.

The resonance signals

In Figure 5.2, we present the invariant mass distributions of the DY dileptons for the SM background expectation and the string resonances, including both $q\bar{q}$ and gg contributions as labeled. At low energies, the stringy amplitudes reproduce SM results as expected. At higher energies, the resonant structure in the invariant mass distribution can be very pronounced. The dilepton processes have both even- and odd-n SRs, with masses M_S, $\sqrt{2}M_S$ for $n = 1, 2$. Recall that the second SR is independent of the Chan-Paton parameter T, in contrast to the first SR which is dependent on T. To illustrate this effect, we have also depicted the peak height for the choice of $T = 4$. Therefore, the number of events around the first SR (the cross section) will determine the Chan-Paton parameter T, while the number of events around the second SR will be predicted essentially by the SM couplings. Moreover, the mass of the second string resonance is remarkably predicted to be $\sqrt{2}M_S$, fixed with respect to the first resonance. These essential aspects of SR signals allow us to distinguish this unique model from other new physics. The scale on the right-hand side gives the number of events per bin for an integrated luminosity of 300 fb^{-1}.

The differential cross-sections for diphoton production are shown in Fig. 5.3 for the SM background and the string resonant contribution. The diphoton processes have only odd-n SRs and thus the peak is at M_S for $n = 1$. The contribution from $gg \to \gamma\gamma$ is again separately shown for comparison (dashed curve). Although it would just double the diphoton signals at the peak of SR by including the gg channel, we have pointed out earlier that the string coupling identification to e is ambiguous.

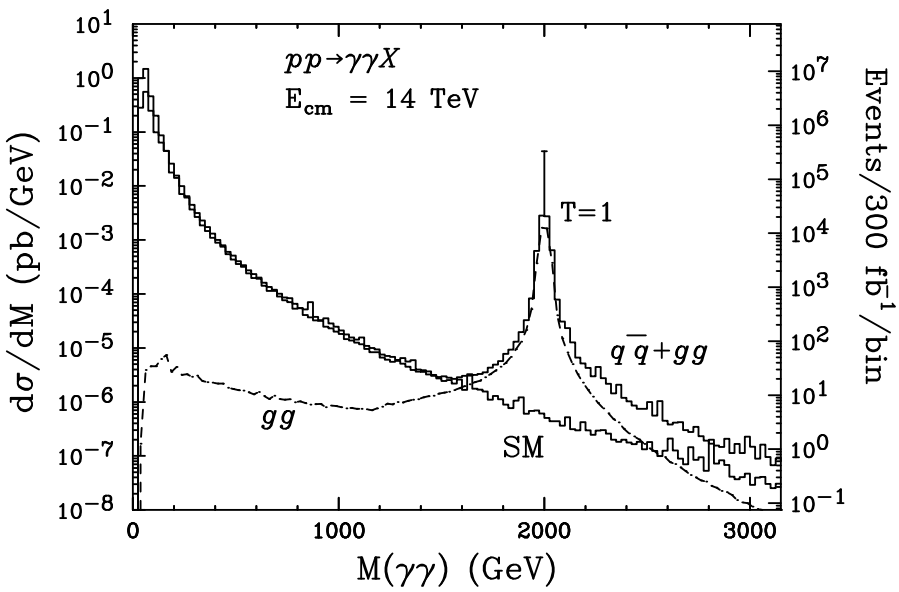

Figure 5.3: Invariant mass distributions for diphoton production at the LHC, for the continuum SM expectation and the SR contributions with $M_S = 2$ TeV and $T = 1$: $q\bar{q} + gg$ (top curve) and gg only (dashed). The vertical bar at the $n = 1$ SR peak indicates the enhancement for $T = 4$.

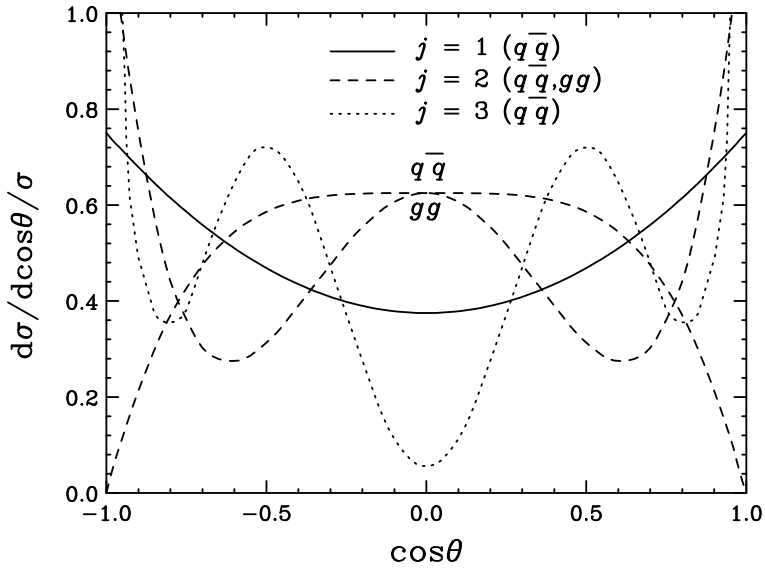

Figure 5.4: Normalized theoretical angular distributions of string resonances with spin 1, 2, and 3 in the DY channel $pp \to \ell^+\ell^- X$.

Angular distributions

As already seen from Table 5.1, there are interesting mass-degeneracies with different angular momentum states. This will lead to distinctive angular distributions when the pair invariant mass is close to the string resonance. It is thus tempting to explore how this unique aspect could be studied.

We first tabulate the angular dependence for the processes with given n, j values in Table 5.2. As always, the angle θ is defined in the $\ell\bar{\ell}$ or $\gamma\gamma$ rest frame with respect to the beam direction. It is indeed interesting to see the drastic differences of the angular distributions for different processes. For instance, there is a degeneracy of spin 1 and 2 at the first SR in dileptonic processes. Spin-2 contributions to dileptonic processes have two possible sources with totally different angular distributions. One is from SR of $q\bar{q}$ initial state and another is from SR of gg one as illustrated in Fig. 5.4 by the

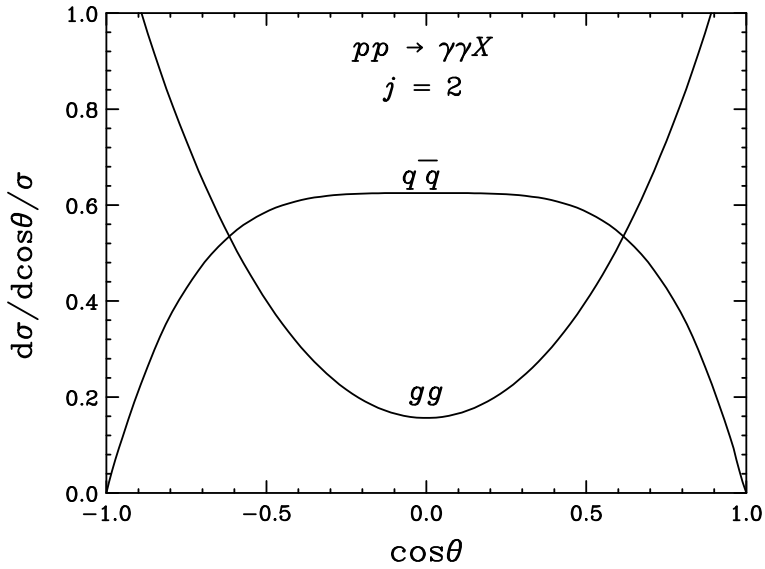

Figure 5.5: Normalized theoretical angular distributions of string resonances with only spin-2 in $pp \to \gamma\gamma X$.

dashed curves. Here, the contribution of spin-2 SR from $q\bar{q}$ is one-ninth of the spin-1 contribution of the same process while the contribution from gg is directly proportional to the Chan-Paton parameter T. These two contributions of spin-2 exchange could change the angular distribution significantly from the conventional "Z'" exchange that we would encounter in many extensions of the SM [53, 54, 55]. It is obvious that this unique angular distribution is also distinguishable from new-physics models with only spin-2 exchange such as Kaluza-Klein graviton [56]. For diphoton processes, there is only spin-2 SR from both $q\bar{q}$ and gg initial states, as shown in Fig. 5.5.

In Figure 5.6, the predicted angular distributions (normalized to unity) of dileptonic signals are presented with the choice of $T = 1$ for both $q\bar{q}$ and gg initial states, for two different mass eigenstates $n = 1, 2$. The events are selected not only by imposing the acceptance cuts of Eq. (5.22), but also by choosing the invariant mass around the

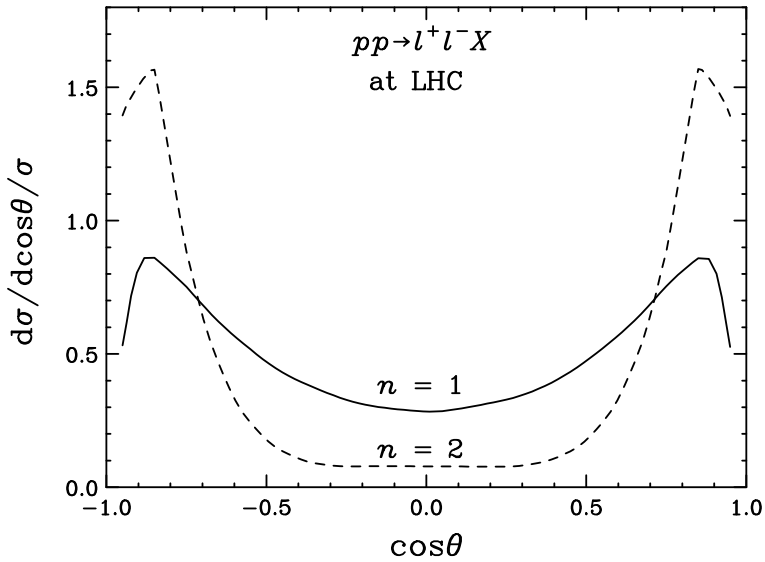

Figure 5.6: Normalized angular distributions for $n = 1$ (solid) and $n = 2$ (dashed) string resonances in the DY channel $pp \to \ell^+\ell^- X$ with appropriate cuts of Eq. (5.22).

resonance mass

$$\sqrt{n}M_S - 2\Gamma_n < M < \sqrt{n}M_S + 2\Gamma_n. \tag{5.24}$$

We see from the figure that the distribution for $n = 1$ is less pronounced near $\cos\theta \sim \pm 1$ than that for $n = 2$. The eventual drop is due to the acceptance cuts. One could imagine to fit the observed distributions in Fig. 5.6 by the combination of the functions listed in Table 5.2 to test the model prediction. Similar distribution for the $\gamma\gamma$ final state is shown in Fig. 5.7, where the total contribution of $q\bar{q} + gg$ (the solid curve) and that for $q\bar{q}$ only (the dashed curve) are compared at $T = 1$ for both processes.

The Forward-Backward asymmetry

For parton-level subprocess $q\bar{q} \to \ell\bar{\ell}$, forward-backward asymmetry is defined as

$$A_{FB}^{q\ell} = \frac{N_F - N_B}{N_F + N_B} \tag{5.25}$$

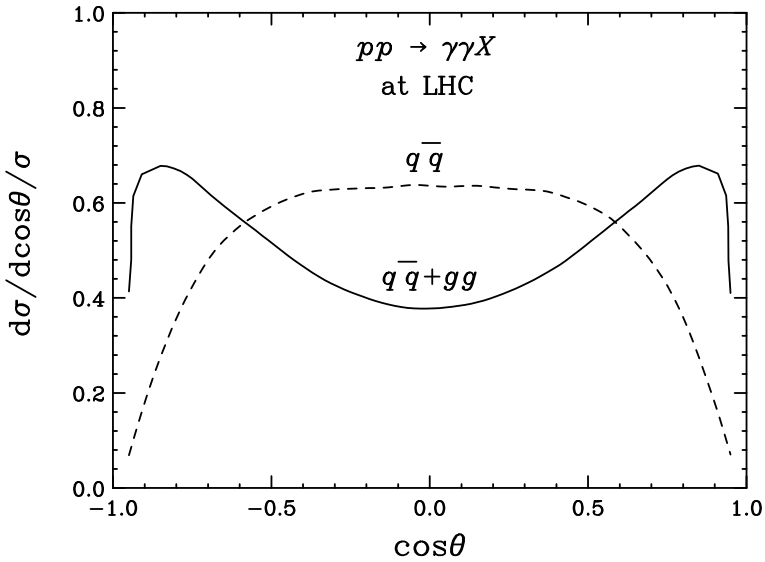

Figure 5.7: Normalized angular distributions for $n = 1$ string resonance in the diphoton channel $pp \to \gamma\gamma X$ with appropriate cuts of Eq. (5.22). The solid curve represents the total contribution of $q\bar{q} + gg$ and the dashed curve is for $q\bar{q}$ only.

where $N_{F(B)}$ is the number of events with final lepton moving into the forward (backward) direction. At pp colliders, the annihilation process is from the valence quarks and the sea antiquarks. Therefore, the produced intermediate resonant state will most likely move along the direction of the initial valence quark due to its higher fraction of momentum [54]. With respect to one particular boost direction of the final dilepton, we can consequently extract information of the forward-backward asymmetry of the subprocess.

In our open-string model, the asymmetry is given, for $s \gg m_Z^2$, by

$$A_{FB}^{q\ell} = \left(\frac{30}{32}\right) \frac{(G_{LL}^q)^2 + (G_{RR}^q)^2 - (G_{LR}^q)^2 - (G_{RL}^q)^2}{(G_{LL}^q)^2 + (G_{RR}^q)^2 + (G_{LR}^q)^2 + (G_{RL}^q)^2} \tag{5.26}$$

$$= \begin{cases} -0.176\ (-0.039) & \text{for } q = u, T = 1\ (4) \\ \\ 0.140\ (0.037) & \text{for } q = d, T = 1\ (4) \end{cases} \tag{5.27}$$

where $G^q_{\alpha\beta} = F_{\alpha\beta} + 2T$, the interaction factor of the fermions defined in Sec. 5.0.5. This asymmetry is inherited from the SM part, $F_{\alpha\beta}$, in the amplitudes. The value of $A^{q\ell}_{FB}$ for SM with $s \gg m_Z^2$ is 0.61 (0.64) for u (d) quark. The asymmetry is diluted by the symmetric SR contribution since typically $T > F_{\alpha\beta}$. The forward-backward asymmetry is hardly visible when $T = 4$. This also can be viewed as another feature to distinguish the SR from the other states like Z' which normally yields larger asymmetry [54].

The reach on the string scale

For the unfortunate possibility that we do not detect any signals with SR properties, the absence of signals implies certain bound on the string scale M_S and Chan-Paton parameters T. We present the sensitivity reach at 95% C.L. in Fig. 5.8 as a function of the integrated luminosity at the LHC. The results are obtained by assuming the Gaussian statistics and by demanding $S/\sqrt{S+B} > 3$, where the signal rate is estimated in the dilepton-mass window $[M_S - 2\Gamma_1, M_S + 2\Gamma_1]$ at the first SR. The lower bound on the string scale could reach $M_S > 8.2 - 10$ TeV for $T = 1 - 4$ at a luminosity of 300 fb^{-1}.

5.0.9 Summary and Conclusions

We have constructed tree-level open-string amplitudes for dilepton and diphoton processes. The massless SM particles are identified as the stringy zero-modes. For a given $2 \to 2$ scattering process, by demanding the open-string amplitudes reproduce the SM

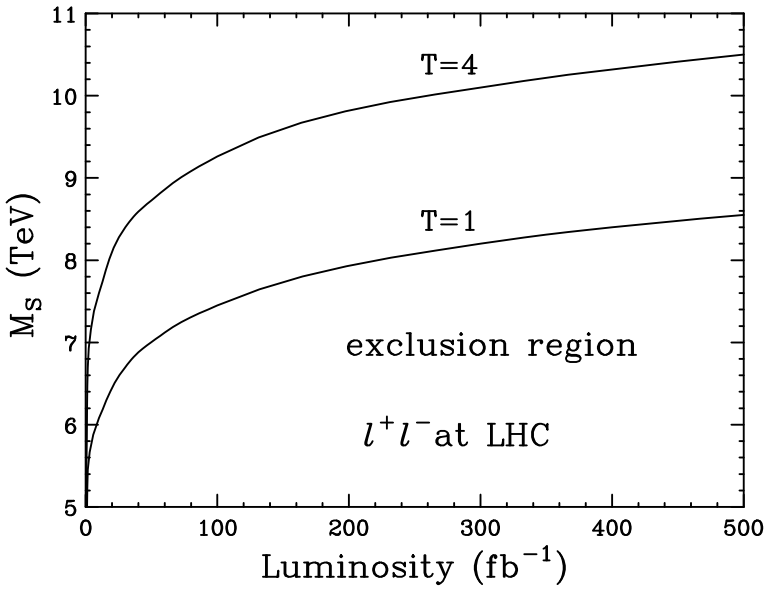

Figure 5.8: Sensitivity reach at 95% C.L. of M_S at various luminosities at the LHC.

ones at low energies, the amplitudes can be casted into a generic form

$$A_{string} \sim A_{SM}(s,t,u) \cdot S(s,t,u) + Tf(s,t,u) \cdot g(s,t,u), \tag{5.28}$$

where A_{SM} is the SM amplitude, $S(s,t,u) = S(s,t), S(s,u)$ or $S(t,u)$ the Veneziano amplitudes, T the undetermined Chan-Paton parameter, $f(s,t,u)$ a kinematical function given in Eq. (5.9), and $g(s,t,u)$ some process-dependent kinematical function. The amplitudes have the following general features:

- By construction, they reproduce the standard model amplitudes at low energies $s \ll M_S^2$, since $S(s,t) \to 1$ and $f(s,t,u) \to 0$, and thus fixing the string couplings with respect to the SM gauge couplings.

- The Veneziano amplitude $S(s,t)$ and $f(s,t,u)$ develop stringy resonances at energies $\sqrt{s} = \sqrt{n}M_S$ $(n = 1, 2, ...)$.

- $S(s,t)$ leads to both even- and odd-n resonances, while $f(s,t,u)$ yields only odd-n SRs. Thus, the even-n resonances are completely fixed by the SM interactions, independent of the unknown factor T.

- For the standard model processes that either vanish at tree-level (such as $gg \to \gamma\gamma$), or do not contain s-channel exchange (such as $q\bar{q} \to \gamma\gamma$), there will be no SRs which couple with SM charges as in the first term of Eq. (5.28). Yet, there can still be SR contributions from purely stringy effects, directly proportional to T, given in the second term of the equation.

We would like to emphasize the profound implication of our amplitude construction and the generic structure of Eq. (5.28). The basic assumption of this work is to take the tree-level open-string scattering amplitudes of Eq. (6.11) as the description of leading new physics beyond the SM near the TeV threshold. As long as one accepts this approach and demands the amplitudes to reproduce the SM counterparts at low energies, Eq. (5.28) would be the natural consequence. There are essentially only two unknown parameters: the string scale M_S and the Chan-Paton parameter T. This construction should be generic for any leading-order $2 \to 2$ processes of massless SM particle scattering, and thus be applicable for further phenomenological studies.

We have calculated numerically the total cross-section of DY through the first string resonance and compared with the CDF data for Z' production. We establish the current lower bound of the string scale at about $1.1 - 2.1$ TeV which is stronger than limits from the contact-interaction analysis [81]. The bound from Tevatron can be improved to $1.5 - 3$ TeV with an integrated luminosity of 2 fb^{-1}.

At the CERN LHC, with the high luminosity expected and much larger center-of-mass energy, SR-induced signals for $M_S \lesssim 8$ TeV can be substantial and a large number

of events is predicted around the SR in dilepton and diphoton processes regardless of the value of the Chan-Paton parameters T. The second string resonance with a mass $\sqrt{2}M_S$ may be observed in the dilepton channel as well. Distinctive angular distributions and the forward-backward asymmetry may serve as indicators to distinguish the SR from other new physics. For a larger value of M_S, SR signals become weaker and we may establish the sensitivity on the lower bound of the string scale for $T = 1 - 4$ to be $M_S > 8.2 - 10$ TeV at 95% C.L. with a luminosity of 300 fb^{-1}.

5.0.10 Appendix

kinematic table

Consider a tree-level scattering of four massless gauge bosons in $SU(N)$ gauge theory, with all momenta incoming. The only non-vanishing amplitudes are those with two positive and two negative helicities. There are six of them, each as a sum of three terms of independent permutations. The general formula for one permutation is given in Ref. [49] as

$$A_{1234} = ig^2 \frac{\langle IJ\rangle^4}{\langle 12\rangle\langle 23\rangle\langle 34\rangle\langle 41\rangle}, \tag{5.29}$$

where I, J label the two gauge bosons with negative helicities. Obviously, the above amplitude is invariant if I, J are for the positive helicity gauge bosons. $\langle pq\rangle$ is the spinor product defined by

$$\langle pq\rangle \equiv \overline{\Psi_-(p)}\Psi_+(q) \tag{5.30}$$

and $|\langle pq\rangle|^2 = 2p \cdot q$. The order of $\langle XY\rangle$ in the denominator is cyclic of 1234. For processes involving fermions, the supersymmetric relation of Eq. (4.9) in [49] can been

applied. The expressions for four fermions ($ffff$) are exactly the same as those for four gauge bosons ($gggg$) for each corresponding helicity and particle permutation. The amplitudes for processes with two bosons and two fermions vanish when the two fermions (or bosons) have the same helicity. A useful list of the amplitudes relevant to our scattering amplitude construction in the text is given as follows, where the superscripts indicate the helicities with respect to the incoming momenta.

$$g^{\pm}g^{\mp}g^{\mp}g^{\pm}/f^{\pm}f^{\mp}f^{\mp}f^{\pm} : A_{1234} = ig^2\frac{\langle 14\rangle^2}{\langle 12\rangle^2}, \qquad A_{1324} = ig^2\frac{\langle 14\rangle^2}{\langle 13\rangle^2}, A_{1243} = ig^2\frac{\langle 14\rangle^4}{\langle 12\rangle^2\langle 13\rangle^2}$$

$$g^{\pm}g^{\mp}g^{\pm}g^{\mp}/f^{\pm}f^{\mp}f^{\pm}f^{\mp} : A_{1234} = ig^2\frac{\langle 13\rangle^4}{\langle 12\rangle^2\langle 14\rangle^2}, A_{1324} = ig^2\frac{\langle 13\rangle^2}{\langle 14\rangle^2}, A_{1243} = ig^2\frac{\langle 13\rangle^2}{\langle 12\rangle^2}$$

$$g^{\pm}g^{\mp}f^{\mp}f^{\pm}/f^{\mp}f^{\pm}g^{\pm}g^{\mp} : A_{1234} = ig^2\frac{\langle 13\rangle\langle 14\rangle}{\langle 12\rangle^2}, \quad A_{1324} = ig^2\frac{\langle 14\rangle}{\langle 13\rangle}, \; A_{1243} = ig^2\frac{\langle 14\rangle^3}{\langle 13\rangle\langle 12\rangle^2}$$

Expressions for other helicity combinations can be achieved by properly crossing two particle momenta, or by cyclic permutation under which Eq. (5.29) is invariant. In doing so, some identities may be useful:

- $A_{ijkl} = A_{lkji}; \quad A_{ijkl} = A_{ilkj};$
- invariant under the sign change ($++ \leftrightarrow --$).

calculation of decay widths

The partial decay width of SR with a mass $m = \sqrt{n}M_S$ and angular momentum j to a final state $\ell\bar{\ell}$ can be written generically as

$$\Gamma_n^j = \frac{1}{2m}\frac{1}{2j+1}\int dPS_2 |A(X_n^j \to \ell\bar{\ell})|^2. \tag{5.31}$$

The two-body phase space element is $dPS_2 = d\Omega/8$, and the decay matrix element squared can be related to the scattering amplitude by

$$|A(X_n^j \to \ell_3\bar{\ell}_4)|^2 = (s-m^2)|A_n^j(\ell_1\bar{\ell}_2 \to \ell_3\bar{\ell}_4)| \quad \text{with } p_1 = p_3,\ p_2 = p_4. \tag{5.32}$$

With the help of partial wave expansion in terms of the Wigner functions $d^j_{mm'}$ as discussed in Sec. 5.0.6, we have

$$A_n^j(\ell_\alpha\bar{\ell}_\beta \to \ell_\alpha\bar{\ell}_\beta) = ig^2 G_{\alpha\alpha}\frac{s\ \alpha_n^j\ d^j_{1,-1}}{s-m^2}. \tag{5.33}$$

where

$$G = \begin{cases} F + 2T & \text{for odd } n, \\ F & \text{for even } n, \end{cases} \tag{5.34}$$

with F and T given in text. The coefficient α_n^j satisfies normalization condition $\sum_{j=1}^{n+1}|\alpha_n^j| = 1$. The final expression for decay width of the SR is therefore

$$\Gamma_n^j = \frac{g^2}{16\pi}\frac{\sqrt{n}M_S}{2j+1}\ G_{\alpha\alpha}\ |\alpha_n^j| \tag{5.35}$$

This expression can be easily generalized to other elastic processes. As for the case of diphoton production, the gauge coupling factor $G = T$ after absorbing the 1/2 factor for identical particles, and the coupling $g^2/16\pi = \alpha/4$, instead of $\alpha/4x_{\rm w}$ as in the dilepton case. It should also be noted that even we do have a non-vanishing SM part in the

$q\bar{q}\gamma\gamma$ channel, there is no corresponding contribution from an SR and consequently to the width of diphoton processes.

For completeness, in Table 5.3 we provide the expansion coefficients in Eq. (5.33), and the relevant Wigner functions are

$$d^1_{1,-1} = \frac{1-\cos\theta}{2} \tag{5.36}$$

$$d^2_{1,-1} = \frac{1-\cos\theta}{2}(2\cos\theta+1) \tag{5.37}$$

$$d^3_{1,-1} = \frac{1}{4}\left(\frac{1-\cos\theta}{2}\right)(15\cos^2\theta+10\cos\theta-1) \tag{5.38}$$

$$d^2_{2,-1} = -\sin\theta\left(\frac{1-\cos\theta}{2}\right) \tag{5.39}$$

$$d^2_{2,-2} = \left(\frac{1-\cos\theta}{2}\right)^2 \tag{5.40}$$

with $d^j_{1,1}(x) = (-1)^{j-1}d^j_{1,-1}(-x)$ and $d^2_{2,m}(x) = d^2_{2,-m}(-x)(m=1,2)$.

Numerically, the total widths for each processes when $T=1$ are

$$\Gamma^{1,2}_1(q\bar{q}\ell\bar{\ell}) = 240,\ 48\ \text{GeV}\left(\frac{M_S}{\text{TeV}}\right), \tag{5.41}$$

$$\Gamma^{1,2,3}_2(q\bar{q}\ell\bar{\ell}) = 46,\ 26,\ 5.8\ \text{GeV}\left(\frac{M_S}{\text{TeV}}\right), \tag{5.42}$$

$$\Gamma^2_1(gg\ell\bar{\ell}) = 19\ \text{GeV}\left(\frac{M_S}{\text{TeV}}\right), \tag{5.43}$$

$$\Gamma^2_1(q\bar{q}\gamma\gamma) = 3.9\ \text{GeV}\left(\frac{M_S}{\text{TeV}}\right), \tag{5.44}$$

$$\Gamma^2_1(gg\gamma\gamma) = 3.5\ \text{GeV}\left(\frac{M_S}{\text{TeV}}\right). \tag{5.45}$$

where we have included all necessary decay modes into related final states for each resonance. For instance, the width $\Gamma(q\bar{q}\ell\bar{\ell})$ includes the partial decay widths of SR into charged leptons, neutrinos, and quarks. Partial decay modes into massive bosons such as the Higgs and $W^\pm, Z$ are not included.

Table 5.1:

<u>DY dilepton pairs</u>	
$A_{SR}^{n=1}(q_\alpha \bar{q}_\beta \to \ell_\alpha \bar{\ell}_\beta)$	$ig_L^2(F_{\alpha\alpha}+2T)\sum_{j=1}^{2}\frac{s\ \alpha_1^j\ d_{1,-1}^j}{s-M_S^2+i\Gamma_1^j M_S}$
$A_{SR}^{n=1}(q_\alpha \bar{q}_\beta \to \ell_\beta \bar{\ell}_\alpha)$	$ig_L^2(F_{\beta\alpha}+2T)\sum_{j=1}^{2}\frac{s\ \alpha_1^j\ d_{1,1}^j}{s-M_S^2+i\Gamma_1^j M_S}$
$A_{SR}^{n=2}(q_\alpha \bar{q}_\beta \to \ell_\alpha \bar{\ell}_\beta)$	$ig_L^2\ F_{\alpha\alpha}\sum_{j=1}^{3}\frac{s\ \alpha_1^j\ d_{1,-1}^j}{s-2M_S^2+i\Gamma_2^j\sqrt{2}M_S}$
$A_{SR}^{n=2}(q_\alpha \bar{q}_\beta \to \ell_\beta \bar{\ell}_\alpha)$	$ig_L^2\ F_{\beta\alpha}\sum_{j=1}^{3}\frac{s\ \alpha_1^j\ d_{1,1}^j}{s-2M_S^2+i\Gamma_2^j\sqrt{2}M_S}$
$A_{SR}^{n=1}(g_\alpha g_\beta \to \ell_\alpha \bar{\ell}_\beta,\ \ell_\beta \bar{\ell}_\alpha)$	$ig_L^2 T\frac{s\ d_{2,\mp 1}^2}{s-M_S^2+i\Gamma_1 M_S}$
<u>Diphoton final state</u>	
$A_{SR}^{n=1}(q_\alpha \bar{q}_\beta \to \gamma_\alpha \gamma_\beta,\ \gamma_\beta \gamma_\alpha)$	$ie^2 T\ \frac{s\ d_{2,\mp 1}^2}{s-M_S^2+i\Gamma_1 M_S}$
$A_{SR}^{n=1}(g_\alpha g_\beta \to \gamma_\alpha \gamma_\beta,\ \gamma_\beta \gamma_\alpha)$	$2ie^2 T\ \frac{s\ d_{2,\mp 2}^2}{s-M_S^2+i\Gamma_1 M_S}$

Table 5.2:

process		angular dependence	
$\underline{q\bar{q} \to \ell\bar{\ell}}$			
$n = 1,$	$j = 1$	$(d^1_{1,-1})^2 + (d^1_{1,1})^2 \propto$	$1 + \cos^2\theta$
	$j = 2$	$(d^2_{1,-1})^2 + (d^2_{1,1})^2 \propto$	$1 - 3\cos^2\theta + 4\cos^4\theta$
$n = 2,$	$j = 1$	$(d^1_{1,-1})^2 + (d^1_{1,1})^2 \propto$	$1 + \cos^2\theta$
	$j = 2$	$(d^2_{1,-1})^2 + (d^2_{1,1})^2 \propto$	$1 - 3\cos^2\theta + 4\cos^4\theta$
	$j = 3$	$(d^3_{1,-1})^2 + (d^3_{1,1})^2 \propto$	$1 + 111\cos^2\theta$
			$-305\cos^4\theta + 225\cos^6\theta$
$\underline{gg \to \ell\bar{\ell}}$			
$n = 1,$	$j = 2$	$(d^2_{2,-1})^2 + (d^2_{2,1})^2 \propto$	$1 - \cos^4\theta$
$\underline{q\bar{q} \to \gamma\gamma}$			
$n = 1,$	$j = 2$	$(d^2_{2,-1})^2 + (d^2_{2,1})^2 \propto$	$1 - \cos^4\theta$
$\underline{gg \to \gamma\gamma}$			
$n = 1,$	$j = 2$	$(d^2_{2,-2})^2 + (d^2_{2,2})^2 \propto$	$1 + 6\cos^2\theta + \cos^4\theta$

	n	$j=1$	2	3
$q\bar{q}\ell\bar{\ell}$	1	$3/4$	$\mp 1/4$	0
	2	$-9/20$	$\pm 5/12$	$-2/15$
$q\bar{q}\gamma\gamma$	1	0	-1	0
	2	0	0	0
$gg\ell\bar{\ell}$	1	0	-1	0
	2	0	0	0
$gg\gamma\gamma$	1	0	1	0
	2	0	0	0

Table 5.3: Coefficients α_n^j of partial wave expansion in each processes. Upper (lower) sign in $q\bar{q}\ell\bar{\ell}$ corresponds to scattering of quark into lepton with like (opposite) helicity.

Chapter 6

Stringy Interaction and Low-Energy Effects in Braneworld Models

6.1 Stringy Gauge "Singlet" Interaction

One embedding of $U(1)_{em}$ into $U(2)$ in coincident-branes model was investigated by Cullen, Perelstein, and Peskin [26]. All tree-level QED amplitudes for e^+, e^-, and γ are reproduced with the identification

$$t^+ = \begin{pmatrix} 0 & 1 \\ 0 & 0 \end{pmatrix}, \quad t^- = \begin{pmatrix} 0 & 0 \\ 1 & 0 \end{pmatrix}, \quad t^3 = \frac{1}{\sqrt{2}} \begin{pmatrix} 1 & 0 \\ 0 & -1 \end{pmatrix}. \tag{6.1}$$

where t^-, t^+, and t^3 is the Chan-Paton matrix of e_L^-, e_L^+, and A_μ respectively. The choice satisfies the 3-point relations

$$[t^\pm, t^3] \propto \mp t^\pm, \quad [t^+, t^-] \propto t^3 \tag{6.2}$$

and therefore is reproducing the 3-point QED vertex in the field theory limit (where $E/M_S \ll 1$). Remarkably, this choice of Chan-Paton matrices lead to the non-vanishing

tree-level open-string scattering $\gamma\gamma \to \gamma\gamma$[26, 67], e.g.

$$A(\gamma_R\gamma_R \to \gamma_R\gamma_R) \;=\; ie^2\frac{s}{ut}f(s,t,u) \tag{6.3}$$

This is due to the non-vanishing trace, $tr(t^3t^3t^3t^3)$, appearing in the $2 \to 2$ tree-level open-string formula. This "stringy" interaction becomes vanishing at low energy, $E/M_S \ll 1$, due to the on-shell condition $s+t+u=0$. Interestingly, while stringy 3-point correlation ($\propto tr([t^3,t^3]t^3)$) between three photons vanishes in this choice of Chan-Paton matrices, the stringy 4-point (and more generically $n(>3)$-point) correlation is not zero at higher energies. This is the first example of the gauge "singlet" (uncharged) interaction induced by stringy dynamics which becomes non-negligible at higher energies.

When we embed the low-energy group into the larger group, the states which are represented by diagonal Chan-Paton matrices (more generically anything that commutes with the matrices assigned to the gauge boson states) always appear as "uncharged" or "singlet" under the low-energy group (it could be confusing for fundamental $U(1)$ where everything is singlet, in such case, we embed $U(1)$ into larger group, e.g. 2×2 matrix as mentioned above and below where everything is represented by non-singlet). This is due to the fact that the 3-point amplitude is vanishing. Those states, even *appear as* singlets with respect to the low-energy group, could actually be part of other representations at higher energies. In this sense, the quotation of "singlet" is meant to be interpreted as states appearing to be uncharged under low-energy group but actually are part of non-trivial representations at higher energies.

Any diagonal matrices commuting with this t^3 represent the uncharged QED "singlet" particle with vanishing 3-point QED vertex. These "singlet" components of the particles, however, can have the stringy interaction mentioned above as we can see from

the following assignment

$$t^+ = \begin{pmatrix} \epsilon & 1 \\ 0 & \epsilon \end{pmatrix}, \quad t^- = \begin{pmatrix} \epsilon & 0 \\ 1 & \epsilon \end{pmatrix}, \quad t^3 = \frac{1}{\sqrt{2}} \begin{pmatrix} 1 & 0 \\ 0 & -1 \end{pmatrix}. \tag{6.4}$$

where we have added diagonal components to the fermions. This choice of Chan-Paton matrices give the following set of amplitudes

$$A(e^-_\alpha e^+_\beta \to e^-_\alpha e^+_\beta) = 2ie^2 S(s,u)\frac{t^2}{us} + 4ie^2\frac{t}{us}f(s,t,u)(\epsilon^4 + 2\epsilon^2) \tag{6.5}$$

$$A(e^-_\alpha e^+_\beta \to e^-_\beta e^+_\alpha) = 2ie^2 S(s,u)\frac{u}{s} + 4ie^2\frac{u}{ts}f(s,t,u)(\epsilon^4 + 2\epsilon^2) \tag{6.6}$$

$$A(e^-_\alpha e^+_\beta \to \gamma_\alpha\gamma_\beta) = -2ie^2 S(t,u)\sqrt{\frac{t}{u}} + ie^2\frac{1}{s}\sqrt{\frac{t}{u}}f(s,t,u)(2\epsilon^2 + 1) \tag{6.7}$$

Remarkably, the amplitudes are in the form we encountered in the parametrised approach with the undetermined Chan-Paton parameters T identified as $4(\epsilon^4 + 2\epsilon^2)$ and $2\epsilon^2 + 1$. They reproduce the SM amplitudes at low energies and the T can be related to ϵ. It is important to note that in the limit $\epsilon \to 0$, the only remaining stringy gauge "singlet" interaction is in $e^-e^+ \to \gamma\gamma$ process, characterized by the $f(s,t,u)$ term. In this limit, the amplitudes are identical to those of ref. [26] as expected.

We might worry about the fact that this new assignment involves non-traceless matrices and consequently do not satisfy the first relation in Eqn. (6.2). Nevertheless, since we never directly observe the 3-particle process containing only the QED vertex, this is not required phenomenologically as long as we can reproduce all of the observable $2 \to 2$ processes at low energies correctly.

Another more generic traceless $U(2)$ assignment is

$$t^+ = \frac{1}{1+\epsilon^2}\begin{pmatrix} -\epsilon & 1 \\ -\epsilon^2 & \epsilon \end{pmatrix}, \quad t^- = \frac{1}{1+\epsilon^2}\begin{pmatrix} -\epsilon & -\epsilon^2 \\ 1 & \epsilon \end{pmatrix}, \tag{6.8}$$

$$t^3 = (\frac{1}{\sqrt{2}})\frac{1-\epsilon^2}{1+\epsilon^2}\begin{pmatrix} 1 & \frac{2\epsilon}{1-\epsilon^2} \\ \frac{2\epsilon}{1-\epsilon^2} & -1 \end{pmatrix}. \tag{6.9}$$

This choice satisfies *both* relations in Eqn. (6.2). Interestingly, the QED amplitudes from this assignment turns out to be independent of the parameter ϵ, and they are identical to those of the Eqn. (6.1) as in ref. [26](i.e. Eqn. (6.5)-(6.7) with $\epsilon = 0$). For the traceless class of matrix assignment that satisfy Eqn. (6.2), there is the *parameterisation invariance* of the trace of the Chan-Paton matrices and the amplitudes are invariant. In this choice of Chan-Paton matrices, the Chan-Paton parameter T vanish in the 4-fermion cases while remain non-vanishing in the processes involving photons.

This parameterisation invariance is nothing but the parametric realization of the symmetry $SO(2) \subset SU(2)$ acting on the Chan-Paton matrices as we can see that the transformation $t \to U^\dagger t U$ for $UU^\dagger = 1$ leaves the trace of the product of t's invariant and thus the amplitudes. If we start with the choice of t's from Eqn. (6.1) and set

$$U = \begin{pmatrix} \cos\epsilon & \sin\epsilon \\ -\sin\epsilon & \cos\epsilon \end{pmatrix} \tag{6.10}$$

then with $\cos\epsilon \simeq 1, \sin\epsilon \simeq \epsilon$, the choice of Eqn. (6.8-6.9) is derived upto the normalizing factors.

Another possibility to realize the stringy interaction for all SM particles is to extend SM group to $SM \times U(1)$, containing extra $U(1)$ underwhich the SM particles are uncharged ("singlet"). In this way, all of the scattering involving SM particles will naturally contain the purely stringy gauge "singlet" interaction proportional to $f(s,t,u)$. It is also reasonable to assume the SM-singlet right-handed (sterile) neutrino, N_R, to have the same kind of purely stringy scattering as investigated in ref. [27, 28]. Additionally, ref. [68] considers $U(1)$ gaugino stringy scattering in the same fashion.

In coincident-branes model that we are considering, the low-energy approximation of the stringy interaction is of dimension 8, $\sim (E^4/M_S^4)$. There is a number of interesting phenomenological consequences from this stringy gauge interaction. One possibility is to obtain the bound on the string scale M_S and the Chan-Paton parameter T from the experimental constraints on the rare processes such as proton decay and flavour-changing-neutral-current (FCNC) by considering the process being induced by the stringy (gauge "singlet") interaction [69].

The limit on the lower bound of the string scale from proton decay could be as high as 10^5 TeV for $T = 1$ (see the next section). The bound on M_S is proportional to $T^{1/4}$ and thus is not sensitive to the value of T (the bound becomes about 10^4 TeV when $T = 10^{-4}$ and not significantly different for $T > 1$).

6.2 Remarks on Limits on the String Scale in Braneworld Scenario

Proton decay has been an important issue which provides stringent test to various GUT models. Conventional $SU(5)$ GUT, even being the simplest model, was ruled out by severe experimental limit on proton lifetime as well as its original SUSY version[70, 71](SGUT). This is due to the dimension 5 proton decay in the $SU(5)$ SGUT model. However, in models with extra dimensions, there are new ways to prevent proton decay e.g. by assuming nontrivial boundary condition on extra-dimensional components of fields[72, 73]. Proton decay through dangerous dimension 5 operator could also be suppressed by the use of appropriate discrete symmetries[74]. The leading contribution of proton decay is then of dimension 6 contact form being suppressed by the square

of the mass scale. With these developments, SGUT $SU(5)$ can be modified to survive experimental limit on proton lifetime.

For SGUT $SU(5)$ in intersecting-branes models, symmetry is more naturally broken by discrete Wilson lines[75]. This is different from symmetry breaking mechanism in conventional 4-dimensional GUT. We achieve gauge couplings unification by extra dimensional unification and it does not correspond, in general, to 4 dimensional GUT. Threshold corrections in RGE in extra dimensional models contains extra contribution from massive Kaluza-Klein states. This brings in dependence on geometrical factors, $L(Q)$, as well as volume of compactified manifold, V_Q. They play the role of M_{GUT} in the running of gauge couplings[76]. In this sense, M_{GUT} does not have any meaning in extra-dimensional unification but a parameter to keep track of unification expressed in 4 dimensional GUT language.

In this section, we will first discuss results from ref. [77] on tree-level amplitudes in SUSY $SU(5)$ intersecting-branes model and the possibility of getting limit on the upper bound of the string scale in this D6-D6 model and proceed to discuss generic properties of quantum part of amplitudes in braneworld scenario in relation to number of twisted fields we introduce into the models. Then we consider IR-correction to quantum part of amplitudes from classical-solutions contribution of the path integral, i.e. instanton contribution. Quantum and classical contributions are discussed separately in order to emphasize unique characteristics of each one of them. Phenomenology of braneworld scenario involves combination of effects from both local quantum behaviour and global classical contributions determined by compactification. In this way we can discuss some possibilities that give purely stringy low energy amplitudes which do not have field theory correspondence. One example of such processes could be proton decay as discussed in

ref. [77]. Finally for comparison to "top-down" approach, we calculate proton decay in "bottom-up" coincident branes model using certain choices of Chan-Paton factors to kinematically suppress the amplitude[28]. Estimated limit on lower bound of the string scale in this case is remarkably high.

6.2.1 IR-amplitudes in Intersecting-branes Models

Generically, branes with any dimensionalities can intersect or be coincident. There are a number of semi-realistic models of intersecting-branes with equal dimensionality[78] and therefore we will focus more on this case. For completeness, we will also comment on IR behaviour of intersecting-branes with different dimensionalities such as D3-D7 configuration. Finally we show that in certain situations, IR limit of string amplitudes in intersecting-branes scenario can be purely stringy with no standard model correspondence and they are automatically suppressed by the string scale.

Intersecting-branes with Equal Dimensionality and Proton Decay

As in ref.[77], we will consider dimension-6 channel of proton decay assuming dimension-5 channel is suppressed by some means such as discrete symmetries[74]. In intersecting-branes model with particular $SU(5)$-group structure, leading contribution to proton decay is purely stringy [77]. This is a dimension-6 operator proportional to string coupling g_s and $\alpha' = 1/M_S^2$. The formula for quantum amplitude of processes such as $p \to \pi^0 e_L^+$ from ref. [77] is

$$A(1,2,3,4) \;=\; i\pi \frac{g_s}{M_S^2} I(\theta_1,\theta_2,\theta_3)\bar{u_1}\gamma^\mu u_2 \bar{u_3}\gamma_\mu u_4 T_{1234} \tag{6.11}$$

where

$$I(\theta_1,\theta_2,\theta_3) = \int_0^1 \frac{dx}{x^{1+\alpha' s}(1-x)^{1+\alpha' t}} \prod_{i=1}^{3} \frac{\sqrt{\sin \pi\theta_i}}{[F(\theta_i, 1-\theta_i; 1; x) F(\theta_i, 1-\theta_i; 1; 1-x)]^{1/2}}, \tag{6.12}$$

θ_i are $SU(3)$ parameters relating 3 complex coordinates representing transverse directions to $1+3$ dimensional intersection region and T_{1234} is corresponding Chan-Paton factor in $SU(5)$. $F(x) \equiv F(\theta, 1-\theta; 1, x)$ is hypergeometric function. Dependence on $F(x)$ comes from correlation function of four bosonic twisted fields

$$< \sigma_+(0)\sigma_-(x)\sigma_+(1)\sigma_-(\infty) > \quad \sim \quad \sqrt{\sin \pi\theta} \frac{[x(1-x)]^{-2\Delta_\sigma}}{[F(x)F(1-x)]^{1/2}} \tag{6.13}$$

with $\Delta_\sigma = \theta(1-\theta)/2$. As $x \to 0$,

$$F(x) \to 1, \; F(1-x) \to \frac{1}{\pi} \sin \pi\theta \ln(\frac{\delta}{x}) \tag{6.14}$$

where δ is some function of θ given in ref.[82]. This asymptotic behaviour determines convergency of x-integration in the s-channel limit.

In this setup, there is relationship between string parameters $(g_s, M_S, L(Q))$ and field theory GUT parameters (α_{GUT}, M_{GUT}) as in Eq. (50) of [77],

$$g_s \quad = \quad \frac{\alpha_{GUT} L(Q) M_S^3}{(2\pi)^3 M_{GUT}^3} \tag{6.15}$$

where $L(Q) = 4q \sin^2(5\pi w/q)$, Ray-Singer torsion, contains information on geometry of the compactified 3-manifold $Q = S^3/Z_q$[77, 76]. This relationship relates g_s to M_S through numerical values of 4 dimensional α_{GUT}, M_{GUT}. Substitute this into Eq. (6.11), we have

$$A_{string} \quad = \quad i \frac{\alpha_{GUT} M_S}{2(2\pi)^2 M_{GUT}^3} (L(Q) I T_{1234}) \bar{u_1} \gamma^\mu u_2 \bar{u_3} \gamma_\mu u_4 \tag{6.16}$$

$I(s, t \to 0)$ is in $[7, 11.5]$ range, $L(Q)$ ranges from less than 1 to about order of 10. With minimal choice that produces standard model gauges, $L(Q) = 8$[77]. Using numerical values of 4-dimensional $SU(5)$ SGUT(i.e. unification condition), $\alpha_{GUT} \simeq 0.04, M_{GUT} \simeq 2 \times 10^{16}$ GeV leading to proton lifetime $\tau_{GUT} \simeq 1.6 \times 10^{36}$ years[71], and experimental limit on proton lifetime, $\tau > 4.4 \times 10^{33}$ years[79], we have inequality

$$\frac{\tau_{string}}{\tau_{GUT}} = \left|\frac{A_{GUT}}{A_{string}}\right|^2 > \left(\frac{4.4}{1.6}\right) \times 10^{-3} \tag{6.17}$$

leading to

$$M_S < 118 M_{GUT} \simeq 2.4 \times 10^{18} \text{ GeV} \tag{6.18}$$

where we have approximated $I \simeq 10$.

There is also constraint from perturbative condition, $g_s < 1$, using again Eq. (6.15) with same set of numerical values, we have $M_S < 9.2 M_{GUT} \simeq 1.8 \times 10^{17}$ GeV. Grand unification and perturbative conditions together put limit on upper bound of string scale above which perturbative viewpoint breaks down. Any SGUT(with D6-D6 configuration) string theories with larger M_S would have to interact strongly and we need to consider proton decay in dual pictures. The value of the upper bound of string scale, (6.18), is outside the perturbative constraint and therefore it is unfortunately inconclusive. However, it is interesting that this upper limit on string scale does exist only in this D6-D6 model, if we have sufficiently more severe bound on proton decay in the future experiments, it would lead inevitably to limit on the upper bound of the string scale.

An important aspect of this low-energy amplitude is the fact that it does not contain any $1/s$(Mandelstam's variable) pole like in conventional field theory amplitudes. Rather it is proportional to g_s/M_S^2, we interpret this as a purely stringy effect which appears as contact interaction in field theory. The advantage is it can suppress proton decay

amplitude to be of the order of the string scale and therefore smallness is explained without the need of massive bosons exchange of the order of SGUT scale. Remarkably, experimental limit on proton lifetime results in limit on UPPER bound of string scale in contrast to conventional SGUT cases where limit on lower bound of X, Y bosons is derived. Grand unification requirement in SGUT $SU(5)$ D6-D6 model relates string coupling to string scale and as a consequence, put limit on upper bound of the string scale.

This result can be understood to be originated from difference between "top-down" and "bottom-up" approaches to string theory. In top-down approach, we start with string parameters (g_s, M_S) and geometrical details of compactification and we try to derive low energy parameters such as $g_{YM}, g1, g2, g3$, Yukawa coupling, mixing angles and so on. With unification assumption, g_s is tied to M_S and geometrical factors and not a free parameter in the model. Experimental constraint from proton decay then results in upper bound on M_S. On the contrary, focussing mainly on kinematic extension of field-theory amplitudes to contain string resonances effect, bottom-up[80, 26, 27, 28, 81] approach simply fixes $g_s = g_{YM}^2$. Without assuming unification, there is no particular relationship between g_s and M_S. This, in a traditional way, finally provides lower bound on the string scale when subject to experimental constraints[26, 81].

On the other hand, there seems to be disadvantage considering the need to have $1/s$ IR-divergence in order to reproduce field theory results at low energy[81]. We need the correct IR limit of string amplitudes which contain the 0th mode pole as gauge boson exchange. Intersecting-branes amplitudes actually provide $1/s$ pole in IR limit when we consider only one complex coordinate and one twisted field contribution together with classical contribution from two branes wrapping the same torus T^2[82, 83]. Difference

from the present case is due to differing number of twisted fields in the quantum part of the amplitude and the classical contribution of string winding modes which we will see later. There are 3 sets of twisted-field(from 3 complex coordinates) correlation function, Eq. (6.13), in the D6-D6 intersecting-branes model we are considering and they provide kinematic IR-regularisation to the amplitude[77]. We can find critical number of twisted-field correlation functions above which IR divergence will be regularised by considering low energy expression for kinematic part of quantum amplitude containing ℓ twisted fields

$$\int_0^a \frac{dx}{x}(-\ln x)^{-\ell/2} = \frac{2-\ell}{2}(-\ln x)^{1-\ell/2}|_0^a \text{ for } \ell \neq 2 \tag{6.19}$$

$$= -\infty \text{ for } \ell = 2 \tag{6.20}$$

where $a \ \epsilon \ (0,1)$ is some small number, ℓ is number of correlation functions of twisted fields. This is the same as Eq. (22) in [77] when generalised to ℓ twisted fields. The integration converges when $\ell \geq 3$ and therefore critical number of twisted fields is 3. At least 3 twisted fields are required to regulate IR behaviour and this implies that we need to twist boundary condition of string in 3 complex coordinates of the model. This is the case with D6-D6 setup.

Using analytic continuation from negative s to $s \geq 0$ like in usual Veneziano amplitude, we get some information on how the poles look like at $s = 0$ and consequently at $s = nM_S^2$.

$$\int_0^a dx \frac{(-\ln x)^{-\ell/2}}{x^{\alpha' s+1}} = \int_{-\ln a}^{\infty} du \ u^{-\ell/2} e^{\alpha' s u} \tag{6.21}$$

$$= \frac{\Gamma(1-\frac{\ell}{2}, -\alpha' s \ln a)}{s^{1-\ell/2}} (\alpha')^{\ell/2-1} \tag{6.22}$$

where incomplete Gamma function $\Gamma(x,y) \equiv \int_y^\infty e^{-u} u^{x-1} du$. Notably for $\ell = 2$, it gives $\sim (\ln s)$ pole as $s \to 0$. At $\ell = 0$, we have normal gauge boson exchange $1/s$ pole. For

$\ell > 0$, twisted fields modify pole by power of $\ell/2$. At $\ell \geq 3$, amplitude is regulated. Behaviour of all other poles at $s = nM_S^2$ for each value of ℓ are given by analytic continuation from pole at $s = 0$ we have here.

In Dp-Dp intersecting-branes($3 < p < 6$) with 1+3 dimensional intersection region, we need to change boundary condition of interbrane-attached string in $p-3$ complex dimensions. Therefore we need to introduce $p-3$ twisted fields into each vertex operator(NS sector). Since the number of twisted fields is always less than 3, the amplitudes have IR divergences(not necessarily corresponding to gauge boson exchange) given by Eq. (6.22). In D5-D5, since $\ell = 5-3 = 2$, quantum amplitude gives $(\ln s)$ divergence. In D4-D4, $\ell = 1$ and we thus have fractional pole $1/s^{1/2}$. In these models, we do not have purely stringy amplitudes, g_s/M_S^2, as leading order as in D6-D6 case. However, from Eq. (6.22), there are string resonance terms analytically continued from $s = 0$ region. At low energy, these terms $g_s \alpha'^{\ell/2}/(s - nM_S^2)^{1-\ell/2} \simeq g_s/nM_S^2$. Therefore there could be g_s/M_S^2 contact term in the amplitude regardless of the number of twisted fields $3 > \ell > 0$.

Another curious aspect of amplitudes in SGUT intersecting-branes models is the factor $\alpha_{GUT}^{-1/3}$ enhancement comparing to 4 dimensional GUT amplitudes[77]. We will see that this is the effect from compactification and it depends on how we achieve 1+3 world from 10 dimensional space. Consider the parameters relation, Eq. (6.15) could be generalized to Dp-Dp case,

$$g_s \sim \alpha_{GUT} \left(\frac{M_S^{p-3}}{M_{GUT}^{p-3}} \right) \tag{6.23}$$

ignoring geometry factor. This leads to

$$\frac{g_s}{M_S^2} \sim g_s^{1+2/(3-p)} \left(\frac{\alpha_{GUT}^{2/(p-3)}}{M_{GUT}^2} \right) \tag{6.24}$$

which has enhancement factor $\alpha_{GUT}^{(5-p)/(p-3)}$ comparing to 4 dimensional GUT amplitude $\sim \alpha_{GUT}/M_{GUT}^2$. Interestingly, this factor disappears at $p = 5$ along with dependence of amplitude on g_s. Since low energy limit of purely stringy part of tree-level amplitudes always appear as g_s/M_s^2 contact interaction form, we can conclude that stringy effect always appears with this enhancement(or dehancement) factor $\alpha_{GUT}^{(5-p)/(p-3)}$. We can interpret the factor as a result from certain choice of compactification which gives our 1+3 dimensional matter universe. Projected onto 4 dimensional field theory, fractional power of coupling α_{GUT} could as well be interpreted as "non-perturbative" characteristic of the amplitudes. Observe also that coincident-branes limit $p = 3$ gives conventional "bottom-up" $g_s \sim \alpha_{GUT}$ identification and relationship between g_s and M_S remarkably disappears. There is consistency between top-down and bottom-up approaches.

Intersecting-branes with Different Dimensionalities

We can obtain $1 + 3$ intersection region from other combinations of intersecting-branes with differing dimensionalities. An example of D3-D7 system has been calculated [38] and there is IR pole in the amplitude coming from instanton contributions cancelling effect of twisted fields as we will see later in section C. Here we will focus only on quantum part of the amplitude and according to previous argument, we will show that IR behaviour is finite.

Using again correlation function of four bosonic twisted fields, Eq. (6.13), we reach at the same Eq. (6.20) as a check for IR behaviour of the amplitude. Since there are $\ell = 4$ twisted fields in a vertex operator in order to change four boundary conditions of D7 to D3 which is larger than critical number of twisted fields (namely 3), therefore quantum part of four-fermion amplitude is finite and thus proportional to g_s/M_S^2 in low

energy limit(from Eq. (6.22)).

6.2.2 Classical Contributions to String Amplitudes

In path integral calculation of string scattering amplitude, the action is divided into quantum and classical contributions and they are factorized from one another. Physically, quantum part depends only on local behaviour of quantum theory while classical part contains information of global geometry which constrains classical solutions of the system. While classical contribution of path integral of field on sphere is constant and can be absorbed into string coupling(since there is no winding modes), classical contribution of field on nontrivial compactified manifold like torus contains various topological contributions from winding states. We need these information to be manifest in order to extract correct low energy behaviour of string scattering amplitude.

The simplest nontrivial case in which classical contribution has been calculated is T^2 torus with two branes wrapping specified by wrapping numbers (n_1, m_1) and (n_2, m_2)[82, 83]. Following ref.[83], the classical contribution of the path integral is

$$\sum_{r_1,r_2} \exp -\frac{\sin(\pi\theta)}{2\pi\alpha'} \left[\frac{F(1-x)}{F(x)}(r_1 L_1)^2 + \frac{F(x)}{F(1-x)}(r_2 L_2)^2 \right] \tag{6.25}$$

In the $x \to 0$ limit(s-channel limit), the exponential contribution from L_1 lattice is zero except the zero mode, $r_1 = 0$ while the contribution from L_2 lattice becomes constant for each r_2. With respect to one r_2 winding state, the contribution is just constant and low energy behaviour is thus governed totally by quantum part of the amplitude. This would be the case if the winding states summation $\sum_{r_2}$ is somehow truncated at finite terms.

However, we can use Poisson resummation to make some low energy behaviour manifest which can be seen explicitly in the Poisson resummation formula.

$$\sum_n \exp(-\pi a n^2) \quad = \quad \sqrt{\frac{1}{a}} \sum_m \exp(-\frac{\pi}{a} m^2) \tag{6.26}$$

The pole at $a = 0$ arises on the left-handed side as an infinite sum of various instantons but not being manifest in each term. The right-handed side manifests this pole as the volume factor in the upfront. This pole becomes visible at low energy in this new "vacuum" choice after the Poisson resummation. This resummation leads to

$$\sum_{r_1, m_2} \sqrt{\frac{2\pi^2 \alpha' F(1-x)}{L_2^2 \sin(\pi\theta) F(x)}} \exp - \frac{F(1-x)}{F(x)} \left[\frac{\sin(\pi\theta)}{2\pi\alpha'} (r_1 L_1)^2 + \frac{2\pi^3 \alpha'}{\sin(\pi\theta)} (\frac{m_2}{L_2})^2 \right] \tag{6.27}$$

for classical partition function. The exponential of $F(1-x)/F(x)$ reduces to power of x as $x \to 0$.

$$\exp - \frac{F(1-x)}{F(x)} [...] \quad \sim \quad \left(\frac{\delta}{x} \right)^{-[...] \sin(\pi\theta)/\pi} \tag{6.28}$$

This power of $1/x$ shift the $1/s$ pole as we can see from

$$[...] \frac{\sin(\pi\theta)}{\pi} \quad = \quad r_1^2 \left(\frac{M_S^2}{M_1^2} \right) + \alpha' (m_2 M_2)^2 \tag{6.29}$$

where $M_1^2 = 2\pi^2 / L_1^2 \sin^2(\pi\theta)$, $M_2^2 = 2\pi^2 / L_2^2$ are corresponding KK masses. With respect to L_2, the resonances appear at $s = (m_2 M_2)^2$. With respect to L_1, the resonances appear at $s = r_1^2 M_S^4 / M_1^2$. These are the usual KK and winding corrections which are not unexpected. We can see that in the instanton-decoupled limit $M_S \gg M_c (M_c = 1/L_1$ or $1/L_2)$, the $r_1 \neq 0$ contribution is very suppressed since the poles are at very high energies while the contribution from M_2 resonances are at low energies and thus non-negligible. We can see that even each r_2 winding state contribution is suppressed, the infinite sum of their contributions become significant at low energies. This is made manifest by Poisson resummation.

Next we turn to the factor $\sqrt{F(1-x)/F(x)}$ in front of the exponential in Eq. (6.27), this is the leading order contribution to x-integration of the amplitude and consequently the part that modifies effect of twisted fields to low energy physics. Using approximation in Eq. (6.14), the factor gives $(-\ln(x))^{1/2}$ as $x \to 0$. This will modify the power of $-\ln(x)$ in Eq. (6.21) to $(-\ln(x))^{(1-\ell)/2}$. In other words, when there is one T^2, we replace ℓ by $\ell - 1$, when there is two tori, $T^2 \times T^2$, we replace by $\ell - 2$ and so on. We see that this piece results in fractional power of $1/s$, exotic kinematic effect which does not exist in field theory or KK models. In D6-D6 model, we can assume two branes wrapping compactified space $T^2 \times T^2 \times T^2$[83]. In this case, effects of twisted fields are completely compensated by these factors from classical contribution and we thus recover $1/s$ pole at low energy. Therefore, around the resonances, since $x \simeq 0$ is dominant in the x-integration, the Veneziano form of the amplitude is naturally recovered in this choice of compactification. Note that this is not necessary and there are possibilities for exotic IR behaviour, i.e. g_s/M_S^2 contact form or fractional power of $1/s$(Eq. (6.22)), of total amplitudes in other choices of compactification.

The rule is if we have two intersecting branes wrapping same n T^2 tori, we replace ℓ by $\ell - n$ in Eq. (6.22) to get leading order behaviour of $1/s$ pole. Complete cancellation occurs when $\ell = n$ and we always retrieve $1/s$ gauge boson exchange contribution. In cases where $\ell - n > 2$, we have IR finite amplitude and it is suppressed automatically by the string scale M_S and effectively decouple at low energy. In model construction, instead of arbitrary intersection and compactification choices(modulo previously known conditions such as SUSY preservation or GUT which are a matter of preferences), we also have to consider this kinematic aspect of string amplitudes. For low energy phenomenology purpose, since we do not observe exotic fractional powers of $1/s$, therefore

they should be eliminated by appropriate choices of compactification corresponding to number of twisted fields we have when we setup branes intersection. At higher energy, there is no reasons(so far) to prevent these terms, they are part of stringy effects unique in intersecting-branes models.

Note also that after Poisson resummation, since the $1/s$ pole is recovered together with the factor of M_2/M_S for each T^2(from Eq. (6.27)), the argument on the limit of the upper bound on the string scale from proton decay is no longer valid in this choice of compactification.

On the other hand, instead of interpreting low energy physics in terms of field theoretic resonances(i.e. $x \to 0, 1$ limits corresponding to s, t-channel exchanges), it is pointed out in ref. [82, 84, 85] that there exists purely stringy contribution(instanton contribution) when contribution around saddle point of classical action is dominant in the x-integration. However caution has to be made that this is the case only when quantum part of the amplitude is regulated(no singularity along x-integration). If there is IR divergence from quantum part, it means the contribution from pole at $x = 0(1)$ is dominant and saddle-point approximation ceases to be valid. In the case that the quantum part is regulated, we can conclude from the previous section that leading order must be of contact form, g_s/M_S^2, now multiplying with exponential suppression from area of the worldsheet instanton. As expected, even in this saddle-point approximation, the instanton effect is multiplied by g_s/M_S^2 and thus suppressed by the string scale.

6.2.3 Limit on lower bound of string scale in bottom-up approach from proton decay

In "bottom-up" coincident-branes model[26, 27, 81], we do not have effect of twisted fields in the picture, all fermions and gauge fields are identified with open string living on the same stack of branes with unspecified number of branes. Assuming some unification group which have leptons and quarks in the same multiplet(in order to induce proton decay), we can identify each particle with appropriate Chan-Paton matrix. Tree-level amplitude for 4 fermions is generically[26, 81, 47]

$$A_{string} = ig_s \left[A(s,t)S(s,t)T_{1234} + A(t,u)S(t,u)T_{1324} + A(u,s)S(u,s)T_{1243}\right] \tag{6.30}$$

where $A(x,y)$ is kinematic part of $SU(n)$ amplitude[49, 26],

$$S(x,y) = \frac{\Gamma(1-\alpha' x)\Gamma(1-\alpha' y)}{\Gamma(1-\alpha' x-\alpha' y)}, \tag{6.31}$$

the usual part of Veneziano amplitude with the 0th pole excluded(put into $A(x,y)$ part explicitly). Chan-Paton factors $T_{ijkl} = tr(t^i t^j t^k t^l + reverse)$(t's are Chan-Paton matrices) contains information of gauge group, mixing and so on of external particles. To be more specific, we consider $u_L d_R \to \bar{u}_R e_L^+$ process of proton decay like in intersecting-branes case. Proton decay amplitude is extremely small(if not 0) and therefore we match string amplitude with 0 at low energy. Following ref. [81]

$$\begin{aligned} A_{string}(f_L f_R \to f_R f_L) &= ig_s \left[\frac{u^2}{st}T_{1234}S(s,t) + \frac{u}{t}T_{1324}S(t,u) + \frac{u}{s}T_{1243}S(u,s)\right] \\ &\simeq 0 \end{aligned} \tag{6.32}$$

where s,t,u are conventional Mandelstam variables. At low energy, $S(x,y) \to 1$ and since $s+t+u=0$, this leads to constraints on Chan-Paton factors, $T_{1234} = T_{1324} =$

$T_{1243} \equiv T$. Plug back into Eq. (6.32), retrieving the next non-vanishing term from $S(x,y) \simeq 1 - \frac{\pi^2}{6}\frac{xy}{M_S^4}$,

$$A_{string} = -ig_s T\frac{\pi^2}{2}(\frac{u^2}{M_S^4}) \tag{6.33}$$

Like in intersecting-branes case, we compare with A_{GUT} and use experimental limit on proton decay while setting $T = 1$(if $T = 0$, there is no tree-level stringy proton decay and no limit on the string scale could be derived),

$$\frac{\tau_{string}}{\tau_{GUT}} = \left|\frac{A_{GUT}}{A_{string}}\right|^2 = (\frac{4}{\pi^4})\frac{1}{u^2}(\frac{M_S^4}{M_{GUT}^2})^2 > \left(\frac{4.4}{1.6}\right) \times 10^{-3} \tag{6.34}$$

where we have identified $g_s = 4\pi\alpha_{GUT}$. At $E_{CM} \simeq 1$ GeV, $u \simeq 0.5$ GeV^2, this gives

$$M_S > 8.5 \times 10^7 \text{ GeV} \sim 10^5 \text{ TeV} \tag{6.35}$$

a remarkably strong limit on string scale. Observe that this kind of kinematic suppression makes use of worldsheet duality(i.e. s, t duality of Veneziano amplitude) to eliminate the contact interaction term g_s/M_S^2(dimension-6 operator), leaving only dimension-8 operator, u^2/M_S^4, as leading-order stringy correction which results in stringent limit on M_S. This limit, however, ignores the conventional spontaneous symmetry breaking mechanism which suppresses proton decay by making the X and Y GUT bosons very massive. It actually reflects the limit of proton decay from "purely stringy" effect which could exist if $T \neq 0$ in some specific embedding of the fermions in some unspecified open-string representation at higher energies.

6.2.4 Conclusions

First we have discussed the possibility of getting limit on the upper bound of the string scale in D6-D6 intersecting-branes $SU(5)$ SGUT setup as in ref. [77] from the experimental constraint on the proton decay. The quantum part of the four-fermion tree-level

amplitude in this case is of the contact form with g_s/M_S^2 dependence due to the number of twisted-field correlations. We commented on how different number of twisted-field correlations in different Dp-Dp setup could lead to different IR behaviour of the quantum part of the amplitude.

Then we discussed appearance of the enhancement(or dehancement) factor $\alpha_{GUT}^{(5-p)/(p-3)}$ in Dp-Dp setup when we compare stringy contact term g_s/M_S^2 to the α_{GUT}/M_{GUT}^2 factor in 4 dimensional GUT amplitude. This non-integer power of α_{GUT} is natural from the viewpoint that we "project" the extra-dimensional unification onto conventional 4 dimensional GUT RGE.

In non-trivial compactification such as T^2, there are classical winding states contribution to the amplitude. We explicitly demonstrated how Poisson resummation of the instanton contributions makes the classical instanton contribution to $x \to 0$ region manifest. In intersecting-branes scenario, there are contributions from both quantum and classical part to the $x \to 0$ region in the stringy amplitude, and we need both to obtain the usual gauge boson $1/s$ pole at low energies.

Finally we estimated the lower bound on the string scale in "bottom-up" coincident-branes approach using constraint on proton decay. The limit is derived solely from purely stringy(of another kind of purely stringy effect from the dimension 6 mentioned above) contribution when appropriate choice of Chan-Paton factors is chosen. Comparing to other constraints on the string scale in the "bottom-up" approach [81], this lower bound is remarkably strong, about 10^5 TeV.

Bibliography

[1] V. D. Barger and R. J. N. Phillips, *Collider Physics*, Addison-Wesley (1991).

[2] Particle Data Group (2004).

[3] M. E. Peskin and D. V. Schroeder, *An Introduction to Quantum Field Theory*, Addison-Wesley (1995).

[4] Scott Willenbrock, TASI-04 Lecture Notes on the Standard Model [hep-ph/0410370].

[5] Martin Schmaltz, hep-ph/0210415.

[6] L.J. Hall, J. Lykken, and S. Weinberg, Phys. Rev. **D27**, 2359 (1983).

[7] S.K. Soni and H.A. Weldon, Phys. Lett. **126B**, 215 (1983); Y. Kawamura, H. Murayama, and M. Yamaguchi, Phys. Rev. **D51**, 1337 (1995).

[8] M. Dine and A.E. Nelson, Phys. Rev. **D48**, 1277 (1993); M. Dine, A.E. Nelson, and Y. Shirman, Phys. Rev. **D51**, 1362 (1995); M. Dine *et al.*, Phys. Rev. bf D53, 2658 (1996).

[9] G.F. Giudice, and R. Rattazzi, Phys. Reports **322**, 419 (1999).

[10] L. Randall and R. Sundrum, Nucl. Phys. **B557**, 79 (1999).

[11] Z. Chacko, M.A. Luty, and E. Ponton, JHEP **0007**, 036 (2000); D.E. Kaplan, G.D. Kribs, and M. Schmaltz, Phys. Rev. **D62**, 035010 (2000); Z. Chacko *et al.*, JHEP **0001**, 003 (2000).

[12] M. Quiros, TASI-02 *Lecture Notes*, hep-ph/0302189.

[13] R. Barbieri, L.J. Hall, and Y. Nomura, Phys. Rev. **D66**, 045025 (2002); Nucl. Phys. **B624**, 63 (2002).

[14] J. Scherk and J.H. Schwarz, Phys. Lett. **82B**, 60 (1979); Nucl. Phys. **B153**, 61 (1979).

[15] K. Hagiwara *et al.*, Particle Data Group, Phys. Lett. **B592**, 1 (2004).

[16] N. Arkani-Hamed, S. Dimopoulos, and G.R. Dvali, Phys. Lett. **B429**, 263 (1998); I. Antoniadis *et al.*, Phys. Lett. **B436**, 257 (1998).

[17] L. Randall and R. Sundrum, Phys. Rev. Lett. **83**, 3370 (1999).

[18] T. Appelquist, H.C. Cheng, and B.A. Dobrescu, Phys. Rev. **D64**, 035002 (2001).

[19] J. E. Paton and H. M. Chan, Nucl. Phys. **B10**, 516 (1969).

[20] J. Polchinski, *String Theory, Vols. I and II*, Cambridge University Press (1998).

[21] N. Arkani-Hamed, A. G. Cohen, and H. Georgi, Phys. Lett. B **513**, 232 (2001) [hep-ph/0105239], N. Arkani-Hamed, A. G. Cohen, T. Gregoire, and J. G. Wacker, JHEP **0208**, 020 (2002) [hep-ph/0202089].

[22] N. Arkani-Hamed, A. G. Cohen, E. Katz, A. E. Nelson, T. Gregoire, and J. G. Wacker, JHEP **0208**, 021 (2002) [hep-ph/0206020], I. Low, W. Skiba, and D. Smith, Phys. Rev. **D66**, 072001 (2002) [hep-ph/0207243].

[23] N. Arkani-Hamed, A. G. Cohen, E. Katz, and A. E. Nelson, JHEP **0207**, 034 (2002) [hep-ph/0206021].

[24] T. Han, H. Logan, B. McElrath, L.T. Wang, Phys. Rev. **D67** 095004 (2003), [hep-ph/0301040].

[25] A. Antoniadis, N. Arkani-Hamed, S. Dimopoulos, and G. Dvali, Phys. Lett. **B436**, 257 (1998). G. Shiu and S.H. Tye, Phys. Rev. **D58**, 106007 (1998); L.E. Ibanez, R. Rabadan, and A.M. Uranga, Nucl. Phys. **B542**, 112 (1999); I. Antoniadis, C. Bachas, and E. Dudas, Nucl. Phys. **B560**, 93 (1999); K. Benakli, Phys. Rev. **D60**, 104002 (1999); E. Dudas and J. Mourad, Nucl. Phys. **B575**, 3 (2000); E. Accomando, I. Antoniadis, and K. Benakli, Nucl. Phys. **B579**, 3 (2000); L.E. Ibanez, F. Marchesano, and R. Rabadan, JHEP **0111**, 002 (2001); G. Aldazabal, S. Franco, L.E. Ibanez, R. Rabadan, and A.M. Uranga, JHEP **0102**, 047 (2001); M. Cvetic, G. Shiu, and A.M. Uranga, Phys. Rev. Lett. **87**, 201801 (2001); I. Klebanov and E. Witten, Nucl. Phys. **B664**, 3 (2003).

[26] S. Cullen, M. Perelstein and M. Peskin, Phys. Rev. **D62**, 055012 (2000).

[27] F. Cornet, J. Illana, and M. Masip, Phys. Rev. Lett. **86**, 4235 (2001).

[28] J. Friess, T. Han, and D. Hooper, Phys. Lett. **B547**, 31 (2002).

[29] M.R. Garousi and R.C. Myers, Nucl. Phys. **B475**, 193 (1996); A. Hashimoto and I.R. Klebanov, Nucl. Phys. Proc. Suppl. **55B**, 118 (1997).

[30] G. Giudice, R. Rattazzi, and J. Wells, Nucl. Phys. **B544**, 3 (1999); T. Han, J.D. Lykken, and R. Zhang, Phys. Rev. **D59**, 105006 (1999); E.A. Mirabelli, M. Perelstein and M.E. Peskin, Phys. Rev. Lett. **82**, 2236 (1999); J. Hewett, Phys. Rev.

Lett. **82**, 4765 (1999); T. Rizzo, Phys. Rev. **D59**, 115010 (1999); H. Davoudiasl, J.L. Hewett, and T.G. Rizzo, Phys. Rev. Lett. **84**, 2080 (2000); H. Davoudiasl, J.L. Hewett, and T.G. Rizzo, Phys. Rev. **D63**, 075004 (2001).

[31] V. Barger, K. Cheung, K. Hagiwara, and D. Zeppenfeld, Phys. Rev. D **57**, 391 (1998).

[32] K. Cheung, Phys. Lett. **B517**, 167 (2001).

[33] K. Hagiwara *et al.*, PDG, Phys. Rev. **D66**, 010001 (2002).

[34] E. Eichten, Kenneth D. Lane, and Michael E. Peskin, Phys. Rev. Lett. **50**, 811 (1983).

[35] D. Friedan, E. Martinec, and S. Shenker, Phys. Lett. **B160**, 55 (1985); D. Friedan, E. Martinec, and S. Shenker, Nucl. Phys. **B271**, 93 (1986); J. Cohn, D. Friedan, Z. Qiu, and S. Shenker, Nucl. Phys. **B278**, 577 (1986).

[36] J. Schwartz, Phys. Rept. **89**, 223 (1982).

[37] G. Veneziano, Nuovo Cim. **57A**, 190 (1968); Phys. Rept. **C9**, 199 (1974).

[38] I. Antoniadis, K. Benakli, and A. Laugier, JHEP **0105**, 044 (2001).

[39] The ZEUS Collaboration, The European Physical Journal **12**, 411 (2000); Erratum: The European Physical Journal **C27**, 305 (2001).

[40] The ZEUS Collaboration, S. Chekanov *et al.*, Phys. Lett. **B539**, 197 (2002); Erratum: Phys. Lett. **B552**, 308 (2003).

[41] The ZEUS Collaboration, DESY-03-041, March 2003, [hep-ex/0304008].

[42] The CDF Collaboration, T. Affolder *et al.*, Phys. Rev. Lett. **87**, 231803 (2001).

[43] For a pedagogical text, see, *e.g.*, J. Polchinski, *String Theory, Vols. I and II*, Cambridge University Press (1998).

[44] K. R. Dienes, Phys. Rept. **287**, 447 (1997) [hep-th/9602045].

[45] I. Antoniadis, Phys. Lett. **B246**, 377 (1990); J. D. Lykken, Phys. Rev. D **54**, 3693 (1996) [hep-th/9603133].

[46] S. Cullen and M. Perelstein, Phys. Rev. Lett. **83**, 268 (1999) [hep-ph/9903422]; V. D. Barger, T. Han, C. Kao and R. J. Zhang, Phys. Lett. B **461**, 34 (1999) [hep-ph/9905474]; C. Tyler, A. Olinto, and G. Sigl, Phys. Rev. **D63**, 055001 (2001) [hep-ph/0002257]; C. Hanhart, D.R. Phillips, S. Reddy, and M.J. Savage, Nucl. Phys. **B595**, 335 (2001) [nucl-th/0007016]; J. L. Feng and A. D. Shapere, Phys. Rev. Lett. **88**, 021303 (2002) [hep-ph/0109106]; A. Ringwald and H. Tu, Phys. Lett. **B529**, 1 (2002) [hep-ph/0201139]; S. Hannestad and G.G. Raffelt, Phys. Rev. Lett. **88**, 071301 (2002) [hep-ph/0110067].

[47] A. Hashimoto and I.R. Klebanov, Phys. Lett. **B381**, 437 (1996) [hep-th/9604065]; Nucl. Phys. Proc. Suppl. **55B**, 118 (1997) [hep-th/9611214].

[48] P. Burikham, T. Han, F. Hussain and D. McKay, Phys. Rev. **D69**, 095001 (2004) [hep-ph/0309132]; P. Burikham, JHEP **0407**, 053 (2004) [hep-ph/0407271].

[49] M.L. Mangano and S.J. Parke, Phys. Rep. **200**, 301 (1991).

[50] F. Abe *et al.* (CDF collaboration), Phys. Rev. Lett. **B79**, 2192 (1997).

[51] V.M. Abazov *et al.* (D0 Collaboration), Phys. Rev. Lett. **B87**, 061802 (2001).

[52] H. Lai *et al.*, CTEQ collaboration, Eur. Phys. J. **C12**, 375 (2000) [hep-ph/9903282].

[53] For comprehensive reviews on Z' properties and theoretical models, see *e.g.*, J. Hewett and T. Rizzo, Phys. Rept. **183**, 193 (1989); M. Cvetic and P. Langacker, Mod. Phys. Lett. **A11**, 1247 (1996). For a comparative study of Z' at different colliders, see, S. Godfrey, Phys. Rev. **D51**, 1402 (1995) [hep-ph/9411237]. For a recent review, see, A. Leike, Phys. Rept. **317**, 143 (1999) [hep-ph/9805494].

[54] P. Langacker, R.W. Robinett, and J.L. Rosner, Phys. Rev. **D30**, 1470 (1984); M. Dittmar, Phys. Rev. **D55** 161 (1997) [hep-ex/9606002].

[55] M. Carena, A. Daleo, B.A. Dobrescu, T.M.P. Tait, Phys. Rev. **D70**, 093009 (2004) [hep-ph/0408098].

[56] B.C. Allanach, K. Odagiri, M.A. Parker, B.R. Webber, JHEP **0009**, 019 (2000) [hep-ph/0006114].

[57] J. Hewett, Phys. Rev. Lett. **82**, 4765 (1999) [hep-ph/9811356].

[58] P. Burikham, T. Han, F. Hussain, and D. McKay, *Phys. Rev.* **D69**, 095001 (2004), [hep-ph/0309132].

[59] G. Shiu and S.H. Tye, *Phys. Rev.* **D58**, 106007 (1998); L.E. Ibanez, R. Rabadan, and A.M. Uranga, *Nucl. Phys.* **B542**, 112 (1999); I. Antoniadis, C. Bachas, and E. Dudas, *Nucl. Phys.* **B560**, 93 (1999); K. Benakli, *Phys. Rev.* **D60**, 104002 (1999); E. Accomando, I. Antoniadis, and K. Benakli, *Nucl. Phys.* **B579**, 3 (2000).

[60] L. Randall and R. Sundrum, *Phys. Rev. Lett.* **83**, 3370 (1999), [hep-ph/9905221].

[61] Adelberger E. G., for the Eöt-Wash Collaboration, [hep-ex/0202008].

[62] Tao Han, Joseph D. Lykken, and Ren-Jie Zhang, *Phys. Rev.* **D59**, 105006 (1999), [hep-ph/9811350].

[63] Kingman Cheung, *Phys. Rev.* **D61**, 015005 (2000), [hep-ph/9904266].

[64] C. N. Yang, *Phys. Rev.* **77**, 242 (1950).

[65] R. P. Feynman, *Feynman Lectures on Gravitation*(Addison-Wesley) (1995); R. H. Kraichnan, *Phys. Rev.* **98**, 1118 (1955); S. Weinberg, *Gravitation and Cosmology*(Wiley, New York) (1972).

[66] Piyabut Burikham, Terrance Figy, Tao Han, Phys. Rev. **D71**, 016005 (2005) [hep-ph/0411094].

[67] P. Burikham, JHEP **0407**, 053 (2004) [hep-ph/0407271].

[68] I. Antoniadis, M. Tuckmantel, Nucl. Phys. **B697**, 3 (2004) [hep-th/0406010].

[69] Piyabut Burikham, JHEP **0502**, 030 (2005) [hep-th/0502102].

[70] P. Langacker, Phys. Rep. **72C**, 185(1981).

[71] J. Hisano, hep-ph/0004266.

[72] L. J. Hall and Y. Nomura, Phys. Rev. **D65**, 125012 (2002) [hep-ph/0111068].

[73] K. R. Dienes, E. Dudas, and T. Gherghetta, Nucl. Phys. **B537**, 47 (1999) [hep-ph/9806292].

[74] E. Witten, hep-ph/0201018.

[75] P. Candelas, G. Horowitz, A. Strominger, and E. Witten, Nucl. Phys. **B258**, 46(1985).

[76] T. Friedmann and E. Witten, Adv. Theor. Math. Phys. **7**, 577 (2003) [hep-th/0211269].

[77] I. Klebanov and E. Witten, Nucl. Phys. **B664**, 3 (2003) [hep-th/0304079].

[78] G. Shiu and S.H. Tye, Phys. Rev. **D58**, 106007 (1998) [hep-th/9805157]; L.E. Ibanez, R. Rabadan, and A.M. Uranga, Nucl. Phys. **B542**, 112 (1999) [hep-th/9808139]; I. Antoniadis, C. Bachas, and E. Dudas, Nucl. Phys. **B560**, 93 (1999) [hep-th/9906039]; K. Benakli, Phys. Rev. **D60**, 104002 (1999) [hep-ph/9809582]; E. Accomando, I. Antoniadis and K. Benakli, Nucl. Phys. **B579**, 3 (2000) [hep-ph/9912287]; M. Axenides, E. Floratos, and C. Kokorelis, JHEP **0310**, 006 (2003) [hep-th/0307255].

[79] K. S. Ganezer, Int. J. Mod. Phys. **A16**, 855 (2001).

[80] S. Kachru and E. Silverstein, Phys. Rev. Lett. **80**, 4855 (1998) [hep-th/9802183].

[81] P. Burikham, T. Han, F. Hussain, and D. McKay, Phys. Rev. **D69**, 095001 (2004) [hep-ph/0309132]; Piyabut Burikham, Terrance Figy, Tao Han, Phys. Rev. **D71**, 016005 (2005) [hep-ph/0411094].

[82] S. A. Abel and A. W. Owen, Nucl. Phys. **B663**, 197 (2003) [hep-th/0303124].

[83] M. Cvetič and I. Papadimitriou, Phys. Rev. **D68**, 046001 (2003); Erratum-ibid. **D70**, 029903 (2004) [hep-th/0303083].

[84] S. A. Abel, M. Masip, and J. Santiago, JHEP **0304**, 057 (2003) [hep-ph/0303087].

[85] S. A. Abel, O. Lebedev, and J. Santiago, Nucl. Phys. **B696**, 141 (2004) [hep-ph/0312157].